To the Graduate Council:

I am submitting herewith a dissertation written by Aarthi Sundararajan entitled “Regulation of B cell response to respiratory viruses”. I have examined the final electronic copy of this dissertation for form and content and recommend that it be accepted in partial fulfillment of the requirements for the degree of Doctor of philosophy, with a major in Microbiology.

Thandi Onami, Major Professor

We have read this dissertation and recommend its acceptance:

Mark Y.Sangster, Timothy E. Sparer, Barry T. Rouse, Chunlei Su

Accepted for the council:

Carolyn R. Hodges

Vice Provost and Dean of the Graduate School

To the Graduate Council:

I am submitting herewith a dissertation written by Aarthi Sundararajan entitled "Regulation of B cell response to respiratory viruses". I have examined the final electronic copy of this thesis for form and content and recommend that it be accepted in partial fulfillment of the requirements for the degree of Doctor of Philosophy with a major in Microbiology.

Thandi Onami
Major Professor

We have read this dissertation
and recommend its acceptance:

Mark Y. Sangster

Timothy E. Sparer

Barry T. Rouse

Chunlei Su

Accepted for the Council:

Carolyn R. Hodges
Vice Provost and Dean of the Graduate School

(Original signatures are on file with official student records.)

Regulation of B cell response to respiratory viruses

A dissertation presented for the

Doctor of Philosophy Degree

The University of Tennessee, Knoxville

Aarthi Sundararajan

August 2011

DEDICATION

This dissertation is dedicated to my parents for their constant support and encouragement throughout my graduate studies.

ACKNOWLEDGEMENTS

It is an awesome pleasure to thank those who have made this 'dissertation-completion-dream' possible. I am super, super thankful to my mentor, Dr. Mark Y. Sangster, whose constant support, encouragement and guidance helped me to get to the finish-line of my PhD studies. It has been a great pleasure working and interacting with him. I am grateful for his always-available help plus his patience dealing with my often naive questions associated with my research work and also for helping me to keep my intellectual curiosity broader than my thesis objectives. I am very thankful to him for introducing me to the 'rocking' world of B cells and thanks so much for making research a fun, exciting and rewarding experience.

I am thankful to my committee members, Dr. Thandi Onami, Dr. Timothy E. Sparer, Dr. Barry T. Rouse and Dr. Chunlei Su for providing critical comments and suggestions that have certainly contributed to the shaping of this thesis. I am grateful to Dr. Barry T. Rouse for keeping me motivated during my graduate studies. Wednesdays would have never been the same without his enjoyable journal clubs including intense scientific discussions which have certainly contributed to my broader understanding of this complex field of immunology. I am very grateful to Dr. Thandi Onami, Timothy E. Sparer and Dr. Chunlei Su for providing useful insights into my dissertation work and for their support and encouragement. Special and warm thanks to Dr. Jeffrey Becker for his confidence in me and for his constant support and encouragement throughout my graduate studies. As a visiting graduate student at the University of Rochester, New York (2010-2011), I had a memorable experience interacting with professors at the David Smith Center for Vaccine and Immunobiology. I am very thankful to Dr. David Topham for providing suggestions regarding my dissertation work, for his encouragement and the great Monday lab-meetings. I am also thankful to Dr. Andrea Sant for providing useful insights into the very complex HLA-DR1 studies. I am extremely thankful to all our collaborators who have provided reagents for the current dissertation work. Dr. Samuel H. Speck, Emory Vaccine center and Eric T. Clambey, University of Colorado for providing the 9.5Kb spontaneous deletion mutant virus.

Dr. Andrea Sant, Katie Richards, Francisco Chavez, University of Rochester for providing the HLA-DR1 mice and for the CD4+ T cell-cytokine data, Dr. Richard Webby, St. Jude Children's hospital, for providing the purified NC.

I am extremely grateful to Elizabeth McPherson, for providing me an opportunity to be a graduate teaching assistant and improving my teaching skills. I am thankful to all my students for their fun-filled conversations which made teaching fun. Interacting with them in the lab and doing experiments together was a memorable experience. I am thankful to Nancy Loftis, Rachelle Allen and George Phyllis for making my transition towards a visiting student status go smoothly. My special thanks to Linda Sangster for providing support and encouragement. I am extremely grateful to her for helping me to settle smoothly during my stay at Rochester as a visiting student. This thesis would not be complete without the awesome support of my colleagues at the University of Tennessee (UT), and at David Smith Center for Vaccine and Immunobiology, Rochester. I would like to express warm appreciation to my ex-lab members; Hyemee Joo, Lifang Huan for the early training in the experimental skills. I enjoyed the long and intense scientific interactions with John Harp, Junwei Zeng and Sharvan Sehrawat. Warm and special thanks to Shalini Sharma and Sachin Mulik for their constant support, motivation during my graduate studies. I am also very thankful to Sukanya Iyer and Shalini Sharma for being such rocking and awesome friends outside of the lab environment. My warm thanks to Mitra Azadniv for being an awesome friend and for her help plus encouragement during my last-phase studies at Rochester. As a visiting graduate student at the University of Rochester, I would like to express my gratitude and appreciation to my lab members at Dr. David Topham's lab; Mitra Azadniv, Jane Baer, Kristin Schiebel, Felix Santiago, Hailong Guo, Kris lambert and Andy for making my stay at the lab an enjoyable experience. Thanks to Sarah for giving me company during the late-night experiments.

I express my warmest hugs to my brother and my deepest gratitude and appreciation to my parents. I am thankful to them for providing me the most practical and optimistic advice when I needed it the most and for encouraging me to pursue my dreams.

ABSTRACT

Viruses replicating in the respiratory tract (RT) trigger a wide range of cytokines and chemokines that have antiviral and pro-inflammatory features, instigating an efficient virus- specific B and T cell response that aids in virus- clearance. The majority of antibody secreting cells (ASCs) localizing in the upper RT secrete IgA that can effectively neutralize viruses. In addition, elements of B cell memory are generated that can provide protection from re-infection. Studies examining these aspects, following murine gammaherpesvirus 68 (MHV-68) infection comprise chapter 2 of the dissertation work. Our studies demonstrate that following MHV-68 infection, unlike influenza infection, resulted in a generalized deficiency of virus-specific IgA induction and deficient B cell memory establishment in the respiratory tract. Our studies indicate that features of virus- replication in the RT regulate these aspects of B cell response. These studies lead to the speculation that these features of B cell response may represent an evolutionary adaptation of viruses that establish long-term latency and are transmitted periodically after reactivation and shedding in secretions.

Following cognate interactions with CD4+ T cells, the B cells undergo proliferation, isotype-switching and differentiate towards extrafollicular (low affinity, rapid) or towards germinal center pathway (high affinity). It is not clear what factors regulate these pathways of B cell differentiation, especially in the context of virus infection in the RT. Studies examining these aspects following influenza infection comprise chapter 3 of the dissertation work. Our studies establish a model for the investigation of host and viral factors that modulate the quality and effectiveness of the B cell response to influenza infection. The findings indicate that the quality/nature of the extrafollicular B cell response depends on the nature of the infecting virus. We present evidence that this pathway of rapid antiviral antibody production relates to the production of non-specifically acting factors in the lung and correlates with the cytokine profile of virus-specific CD4+T cells.

In summary, the current dissertation findings point to an influence of virus and host associated factors in regulating features of B cell response in the RT.

TABLE OF CONTENTS

Chapter 3: Regulation of B cell response to influenza virus following infection of the respiratory tract

LIST OF FIGURES AND TABLES

List of Tables:

List of Figures:

Chapter 1

Chapter 2

Chapter 3

ABBREVIATIONS

Abs ..... Antibodies
AID .....Activation-induced deaminase
ASCs .....Antibody-secreting cells
BALT .....Bronchus-associated lymphoid tissue
BCM .....B cell medium
BCR .....B cell receptor
BL .....Burkitt's lymphoma
BM .....Bone marrow
B_{Mem} .....Memory B cell
CLN ..... Cervical lymph node
DCs .....Dendritic cells
dNALT .....Diffuse NALT
EBV .....Epstein-Barr virus
FBS .....Fetal bovine serum
FDCs .....Follicular dendritic cells
GC .....Germinal center
IAV .....Influenza A virus
IFN .....Interferon
IM .....Infectious mononucleosis
i.n. .....Intranasal
KSHV .....Kaposi's sarcoma herpes
LW .....Lung wash
MedLN ..... Mediastinal lymph node
MHV-68 .....Murine gammaherpesvirus-68
MLN .....Mediastinal lymph node
NALT .....Nasal-associated lymphoid tissue
NC .....New-Caledonia virus
NLRs .....NOD-like receptors

NPC .....Nasopharyngeal carcinoma
NW .....Nasal wash
oNALT .....Organized-NALT
PRRs .....Pattern-recognition receptors
RT .....Respiratory tract
SCS .....Sub-capsular sinus
Tfh .....Follicular-helper T cells
TLRs .....Toll-like receptors

Chapter 1

Background and Overview

Overview of the chapter

The respiratory tract (RT) is susceptible to infection by a wide range of pathogens, and the ensuing innate and adaptive immune system mechanisms control the pathogen spread and limit damage to the RT. Understanding immune mechanisms are important for developing effective vaccines. This chapter begins with a review of literature associated with our current understanding of mucosal B cell response in the RT, focusing on aspects relevant to the current dissertation work. Briefly, the current understanding of acquisition of antigen by B cells are discussed, followed by discussion of mechanisms regulating extra follicular and germinal center B cell differentiation pathways. Our current understanding of characteristics and trafficking pattern of memory B cells and plasma cells are discussed. This is followed by a review of T- cell dependent isotype-switching processes in the B cells, with an emphasis on IgA class-switching. The anatomy of RT is discussed, with emphasis on nasal associated lymphoid tissue (NALT). This is followed by an introduction to the models of respiratory viruses used in the current dissertation work; a murine gammaherpesvirus 68 (MHV-68) and influenza A viruses in order to address questions related to the B cell response. The genome features, pathogenesis, immune responses (covering innate, T cell-mediated immunity (CD4+ T cells, CD8+T cells), B cell-mediated immunity) and current vaccine scenario to these respiratory viruses are discussed. The last part of this chapter focuses on conclusions emphasizing some of the questions open in the field, with the directions taken up by the current dissertation work to answer these questions.

Antigen acquisition by B cells

Antigen acquisition by B cells is important for dictating antibody response, cognate interaction with CD4+ T cells and also regulating B cell differentiation.

There are multiple modes for encounter of antigens with follicular B cells [1]. Particulate antigens, such as viral particles and immune complexes gain access to the lymph node through the afferent lymphatics. The lymph fluid initially passes through the sub capsular sinus (SCS) before entering medullary sinus. These antigens gain access to the SCS macrophages present in this area, that are geographically situated over the B cell follicles. These macrophages are in contact with B cells, requiring B-cells derived α1β1 for their development and maintenance [2]. Most importantly, virus particles can be captured by these macrophages and also be displayed to B cells through their follicular tail processes [3-4]. Extensive studies, summarized in [1] have revealed receptors involved in capture of antigen by SCS macrophages. For example, capture of UV-inactivated influenza virus is dependent on the receptor, mannose-binding lectin [5]. Following exposure to antigen, the B cells accumulate in the SCS region, followed by CCR7 up regulation and migration to the T-cell zone [3-4]. Several pathogens directly target and infect SCS macrophages resulting in the production of IFNα/β [6], stimulating antibody production by B cells [7].

Alternatively, antigen bound by non-cognate B cells can transfer antigen to follicular dendritic cells (FDCs), which then provide antigen to cognate B cells. Opsonized antigens are displayed by FDCs, playing an important role in generation of antibody response. FDCs have the ability to display antigen for long periods of time and cognate B cells can capture antigen from FDCs [8]. Lymph node lymphatic endothelial cells can also endocytose viruses and are potentially another candidate for making antigen directly accessible to B cells [4]. In contrast, soluble antigens can also directly gain access to the B cell follicle, through the conduits. Large antigens too large to enter the lymphatic vessels can be presented by DCs to B cells, as evidenced by presence of DCs in SCS and also in the B cell follicles [9]. In the upper RT, antigens can be directly sampled by M cells present in the epithelium overlying NALT [10]. DCs and macrophages are present in the NALT underlying M cells [11], and therefore, have direct access to antigens and possibly provide antigen to B cells.

Regulation of B cell differentiation

Following binding of antigen, B cells receive T cell help in the T-B cell border. This is followed by proliferation of B cells in the follicles, and some of the cells migrate to the extrafollicular areas in the lymph node medullary cords, becoming extrafollicular or short-lived plasma cells, secreting rapid, low-affinity antibodies (Abs). Other B cells in the follicle differentiate into germinal center (GC) B cells, secreting high affinity Abs [12]. Through GC pathway of B cell differentiation, long-lived plasma cells (localizing in the bone marrow; BM) and memory B cells (B_{Mem}). Factors influencing these pathways of B cell differentiation are still unclear. B cells with a strong B cell receptor (BCR) affinity to the antigen take up extrafollicular pathway of differentiation [13]. In contrast, another study demonstrated that BCR affinity is not the decisive factor, and generates both extrafollicular and GC B cells [14-15]. Interestingly, same clones of B cells can be present at both sites [16]. Quality of T-cell help is also an important determinant. T cell independent responses favor stronger extrafollicular B cell response compared to GC. Toll- like receptors (TLR) signals can substitute for T-cell help, stimulating extrafollicular B cell response, but is not sufficient for GC sustenance [17]. Both extrafollicular and GC B cell responses are T cell dependent and in the T-B cell border, the extrafollicular B cell response may be integrin dependent, while GC B cell response may be additionally, SAP dependent [18]. Transcriptional repressors play a major role in the decision making early, with Bcl-6 up regulation associated with GC B cells, while Blimp-1 up regulation is associated with extrafollicular plasma cells [19]. GC B cell responses up regulate interferon regulatory factor 8 (IRF-8) that induces Bcl6, while extrafollicular B cells up regulate IRF-4 that induces Blimp-1 [20]. EBI-2 (G-protein coupled receptor) up regulation favors localization of B cells to extrafollicular sites, while Bcl-6 mediated down regulation of EBI-2 favors localization in the follicles towards GC responses [21-22]. It is largely still unclear what mechanisms control the decision-making, especially in the context of virus infection in the RT.

Follicular-helper T cells (Tfh) are one of the important players in regulating GC responses and interestingly, B cells are also important for Tfh formation. CD40L signaling from Tfh cells may also be important for GC maintenance [12]. IL-21 produced by Tfh cells is also important for GC responses. IL-21 can act in two ways; by inducing formation of Tfh cells [23] and by directly acting on B cells [24-25]. IL-21 is important for IgG1 class switching, proliferation, maintenance and affinity maturation of GC B cells and enhances Bcl-6 expression. Other cytokines, including IL-4 [26]and IL-17 [27] are important for attaining normal GC numbers and maintenance. BCR signaling and FDCs derived integrin and survival signals are also important determinants for formation and maintenance of GCs [12].

B cells trafficking pattern in the respiratory tract

Naive B cells migrate to peripheral lymph nodes in search of antigen and this process is less dependent on CCR7-CCL19/CCL21 axis, but more dependent on CXCR4-CXCL12 and CXCR5-CXCL13 axes. Following exposure to antigen activated B cells increase CCR7 expression, migrating to the T-cell zone, in response to the ligands, CCL19, CCL21 [28-29]. Trafficking to extralymphoid tissues involves down regulation of these receptors and upregulation of other chemokine receptors that aid in migration to inflammatory and mucosal sites. The trafficking of IgA and IgG ASCs are differentially regulated. The IgA antibody secreting cells (ASCs) have trafficking patterns related to the site of induction. For example, IgA ASCs generated in the upper RT preferentially populate the salivary glands and RT, and decreased trafficking to the gut. In contrast, IgG ASCs preferentially traffic to lymphoid tissue and non-mucosal sites of chronic inflammation [30]. The BM is a site for localization of long-lived plasma cells (more IgG and IgM ASCs, and relatively few IgA ASCs) that contribute to the circulating Abs in the serum. IgG and IgA ASCs localize in the BM using the CXCR4-CXCL12 axis [31]. Other axes working in the BM includes CXCR6-CXCL16 and CCR10-CCL28 [30]. Interestingly, CXCL12 is expressed in the epithelium of mucosal tissues [32] and perhaps a parallel system in the RT could contribute to the localization of CXCR4+ASCs to the RT.

IgG ASCs migrate to inflammatory sites (for example, lung, following intranasal infection) under the influence of CXCR3-CXCL9/CXCL10 axis [33]. IgA ASCs expressing CCR10 respond to the ligand CCL28 produced by epithelial cells associated with mucosal tissues of RT and gut [34-35]. In contrast, very few IgG or IgM ASCs are CCR10+ [30]. Following intranasal route of immunization, there is up regulation of CCR10 and $\alpha_4\beta_1$ on IgA ASCs which traffic to the RT in response to their respective ligands, VCAM1 and CCL28 [30]. IgG ASCs expressing low levels of CCR10, $\alpha_4\beta_1$ and CXCR3 may be programmed to enter the RT [30]. B_{Mem} are constantly re-circulating through secondary lymphoid tissues and respond to CCR7, CXCR5, CCR6 and CXCR4 associated axes [30, 36]. CCR10 is not expressed by B_{Mem} [37] and it is not clear what mechanisms govern their migration to the RT. In contrast, CCR9 expression is detectable on B_{Mem} [33], helping them to circulate through mucosal sites associated with the gut.

Regulation of B cells in the RT

GC reactions are considered central to the generation of B_{Mem} and long-lived plasma cells. For example, SAP deficient mice develop short-lived ASCs, but fail to develop GCs, B_{Mem} and long-lived ASCs, emphasizing the importance of signals from T cells in these processes [38-39]. Other signals including over expression of Bcl-2 in B cells lead to increase in B_{Mem} frequencies and ASCs in the BM [40-41]. Reduced IL-21 in the microenvironment contributes to increased B_{Mem} frequencies, but reduced frequencies of ASCs localizing in BM [24-25]. SWAP-70 expression is up regulated in GC B cells, and is down regulated in plasma cells as indicated by studies associated with SWAP-70 deficient mice [42]. Interestingly, ASCs localizing in BM and B_{Mem} are generated, although at reduced frequencies, in the absence of GCs [43-44]. Several mechanisms control maintenance of B_{Mem} [41]. For example, BAFF is important for survival and maintenance of B cells [45] . Spleen is a major repository of IgG B_{Mem} cells [46] and it is unclear what mechanisms govern the maintenance of these cells in this site. Interestingly, in the absence of secondary lymphoid tissues, B_{Mem} are still generated that effectively aid in clearance of influenza virus from RT [47].

Providing survival factors play a major role in maintenance of ASCs in the RT. For example, APRIL over expression in tonsils provide survival niches for IgG and IgA ASCs [41, 48]. It will be interesting to examine if such parallel mechanisms exist in oNALT that are considered equivalents of tonsils.

Regulation of class-switching in B cells

During the antigen-independent phase of B cell development, the B cells diversify the antibody repertoire by a non-homologous end-joining process [49]. Following rearrangement of light chains by V_L-J_L recombination and heavy chains by V_HDJ_H recombination, the mature B cells are IgM^+IgD^+. During the antigen-dependent phase of B cell development, somatic hypermutation, affinity maturation and class-switch recombination occurs, resulting in the generation of high-affinity B cells [49]. The process of class switching in IgM^+IgD^+ B cells (in the IgH - constant region) is important in the generation of different isotypes of antibodies: IgG1, IgG2b, IgG2c/IgG2a, IgG3 and IgA. These class-switched B cells have similar antigen specificity as the precursor cells, but different effector functions [50]. Cytokines from CD4+ T cells involved in cognate interactions with B cells are important in the process of class switching. For example, IgG1 class switching is mediated by IL-4 [51-52], secreted by Th2 cells, while IgG2c class switching is mediated by IFN-γ [53] secreted by Th1 cells. In addition, Th1 cells can inhibit Th2 cells. Although several mechanisms regulate the differentiation of Th1 Vs Th2 cells, it is still unclear how these processes are regulated, especially in the context of a virus infection in the RT.

Regulation of IgA class switching

Class-switching to IgA results in generation of both secreted IgA (sIgA) as well as membrane bound IgA. The sIgA is present as dimeric and oligomeric forms [54]. The J chain is generated by plasma cells and has a dual function [55]. It helps in the interaction of IgA monomers and also interacts with polymeric Ig receptor (pIgR), helping in the process of transcytosis across epithelial cells [56]. The sIgA is secreted in

forms of complexes that also contain a secretory component generated by cleavage of pIgR [57].

The T-cell dependent IgA class switching is dependent on the cytokine TGFβ1 and CD40L mediated mechanisms [58]. The process of IgA class-switching is mediated by switching C_μ to C_α through switch (S) regions which are G-rich regions [59]. Tolecular mechanism for IgA class switching is described in [58]. Briefly, the S region is preceded by intronic exons (I) and a promoter (P), for each constant gene. TGFβ1 mediates the initiation of C_α gene transcription, resulting in the generation of germline I_α - Sα- Cα transcript, from the promoter P_α of I_α exon. This process results in S region to become susceptible to the enzyme, activation induced cytidine deaminase (AID). The AID is important in generation and repair of dsDNA breaks at Sμ and Sα, also resulting in the generation of short half-life, I_α-C_α switch circle transcripts. This is followed by recombinatorial events leading to the generation of m-RNAs for secreted IgA and membrane IgA [58]. AID expression is induced via NF-κB pathway in B cells via CD40L-CD40 interaction [58, 60]. Alternatively, it is also likely that CD40L along with cytokines such as IL-10, IL-2,IL-4,IL-5 and IL-6 may act on B cells and induce autocrine induction of TGFβ1, resulting in IgA class switching [58]. Currently, it is not clear if both these mechanisms operate in an in vivo setting. The source of TGFβ1 in the context of virus infection in the RT is unclear, although certain T cell subsets can secrete this cytokine [58]. Interestingly the IgA class switching effects mediated by TGF-β1 is dependent on concentrations, as low concentrations favor class switching, while higher concentrations inhibit B cell proliferation and differentiation [61]. In addition, T-cell independent mechanisms also regulate IgA class switching, including TLR signaling [62]. In addition, BAFF and APRIL are molecules secreted by DCs that can replace the role of CD40L, mediating class switching to IgA [63].

Characteristics of nasal-associated lymphoid tissue

The nasal-associated lymphoid tissue (NALT) is comprised of organized-nasal-associated lymphoid tissue (oNALT) and diffuse-nasal-associated lymphoid tissue

(dNALT) [64]. The NALT is considered equivalent to waldeyer's ring in humans [64-65].The oNALT is a pair of lymphoid structures present above the palate at the entrance of the nasopharyngeal duct and the epithelium has M cells which sample antigens. In addition, DCs and CD11b+Ia+ macrophages, along with HEVs and B, T cells-rich areas are also present in the oNALT [10]. Interestingly, i.n. administration of reovirus leads to generation of GCs in the oNALT [66]. Characterization of CD4+ T cells in the oNALT revealed that these T cells were capable of differentiating into either Th1 or Th2 cells depending on the kind of antigen exposure [67]. In addition, oNALT is also a site for generating both IgA ASCs and IgA B_{Mem} [46], secreting high affinity IgA Abs [68] that can effectively neutralize viruses in the upper RT. In addition, some studies indicate that IgA-secreting cells in cervical lymph nodes (CLN) originate from oNALT [69]. dNALT is the diffuse lymphoid tissue lining the nasal passages. Both oNALT and dNALT have similar ratios of B and T cells [70]. In contrast, the precursor IgM+B220+ B cells, AID expression and IgA switch transcripts are found in the oNALT but are absent in the dNALT [71]. Unlike oNALT, where the IgA response wanes down towards the end of acute phase of infection, IgA ASCs are found localized in the dNALT over a long period of time following infection [46, 72]. The NALT is also a source for IgA Abs in the nasal wash, which in the context of influenza infection correlates with virus clearance from nose [73].

Models of respiratory virus infection in the current dissertation work

Respiratory virus infection model systems in mice provide insights into the mechanisms important for the resolution of infection. A couple of RT- associated disease models have been described in the current dissertation work; a murine gammaherpesvirus 68 (MHV-68) and influenza A viruses. The acute phase of pathogenesis, including mechanisms of virus control mediated by CD4+ and CD8+ T cells are largely similar between these viruses. The major difference being, that MHV-68 establishes latency and causes systemic disease, while influenza viruses cause a very localized, transient infection restricted mostly to the lungs (See Figure 1.1).

Murine gammaherpesvirus 68

Herpesviruses

The family of herpesviruses is divided into three subfamilies, alpha (α), beta (β) and gamma (γ). The α-subfamily includes herpes simplex (HSV-1, HSV-2) and varicella-zostere virus (VZV), and these viruses have a general tropism for sensory nerve ganglia. HSV-1 is associated with cold sores, HSV-2 with genital lesions, and VSV with shingles. The β-subfamily includes the human cytomegalovirus (HCMV), human herpesvirus (HHV-6, HHV-7) and these viruses have a cellular tropism for monocytes, macrophages, lymphocytes and the salivary gland. HCMV is associated with congenital defects, and is also a causal agent in nosocomial infections in the immuno-compromised individuals.

The γ-subfamily is divided into two genera, *Lymphocryptoviridae* and *Rhadinoviridae*. The *Lymphocryptoviridae* genus includes Epstein Barr virus (EBV), and the *Rhadinoviridae* genus includes Kaposi's sarcoma- associated herpesvirus (KSHV), and also other KSHV-like non-human viruses. The lymphocryptoviruses infect only primates and humans, whereas the rhadinoviruses infect other mammals too, including voles [74-75], mice (Murine gammaherpesvirus 68/ MHV-68 and others), horses (equine herpesvirus 2), cows (bovine herpesvirus 4), pigs and primates [76-83] Molecular phylogenetic analyses have shown that the γ-herpesviruses are closely related to each other, and are very distinct from the α and β herpesviruses [84]. The human γ-herpesviruses have tropism for B cells, epithelial cells and endothelial cells.

MHV-68 as a model system to study gammaherpesvirus immunobiology

The human gammaherpesviruses are species-specific viruses, and as a result, the studies have been restricted to clinical aspects of disease. Infection of mice with a closely related rodent virus, MHV-68 (Murid herpesvirus 4 (MuHV4) / γ-HV68) offers a good small animal model system to study immunological features of human gammaherpesvirus infection [85-88]. Based on the genome properties [89], MHV-68 was classified into gammaherpesvirus family. MHV-68 growth in vitro is efficient, and is

amenable to genetic modifications to study viral gene functions, related to virus replication, latency and reactivation features in the host.

MHV-68 was originally isolated from *Clethrionomys glareolus* (bank vole) in Slovakia [74] and also replicates well in *Apodemus flavicollis* (wood mice) [90]. Two other herpesviruses, MHV-60 and MHV-72 were isolated from bank voles, and viruses MHV-76 and MHV-78 were isolated from wood mice. MHV-Brest was isolated from *Crocidura russula* (Shrew) [91]. In addition, an extensive survey in Slovakia revealed the presence of the virus in rodents, fallow deer, wild boar and sheep. Interestingly, MHV-68 neutralizing antibodies were identified in a set of employees of the institute of virology, Slovak academy of sciences [92].

Human diseases associated with γ-herpesviruses

The γ-herpesviruses are known to induce lymphoproliferative diseases and cancer. EBV and KSHV are associated with both benign and malignant lymphomas, along with those associated with smooth muscle cell and endothelial cell origin. The mechanisms behind the tumor induction is unclear, but there are indications that tumorigenesis is triggered when viruses infect across-species [80] or most commonly in cases of immuno-compromised individuals. The magnitude and outcome of infection is also influenced by the age of the individual when they acquire the infection. In addition, the stage of the life cycle of the virus also plays a critical role in determining the outcome of infection.

For example, EBV infection in young children is asymptomatic, while infection acquired during adulthood is associated with infectious mononucleosis (IM) [93]. Reactivation of EBV in HIV patients results in oral hairy leukoplakia (OHL) and immunoblastic lymphomas and tumors of muscle origin. In young adults with X-linked immunodeficiencies, EBV infection results in a severe case of IM, resulting in death. During latency stages of EBV infection, the disease may progress to Burkitt's lymphoma (BL) [94-95] and epithelial tumor associated nasopharyngeal carcinoma (NPC). In addition, EBV infection is widespread in the human population [96]. EBV infection is

also associated with other diseases such as T-cell lymphomas, gastric carcinomas and Hodgkin's disease. The association of EBV with breast carcinoma and hepatocellular carcinoma is not clear. EBV is also associated with several autoimmune disorders such as multiple scelorosis, rheumatoid arthritis, and diabetes.

KSHV is associated with Kaposi's sarcoma (KS) [97], primary effusion lymphoma (PEL) or body cavity based lymphoma [98],and multicentric Castleman's disease (MCD)[99] MCD is characterized by lymphadenopathy, fever and splenic infiltration [100]. It is also associated with hyper IL-6 production and inflammation. Interestingly, PEL and MCD are of B cell origin and KS is of endothelial cell origin. In children, primary infection with KSHV is associated with a febrile maculopapular skin rash [101]. In case of a primary infection in adults that are immunosuppressed, have bone marrow failure, splenomegaly and fever [102]. KSHV may also be transmitted to new hosts by organ transplants [103]. KSHV is also associated with sarcoidosis [104], multiple myeloma [105] and severe primary pulmonary hypertension [106].

Genome features of MHV-68

The complete genome of MHV-68 has been sequenced [89]. The viral genome is a linear ds DNA, with 118,823bp of unique sequence, G+C content of 46% and consists of multiple copies of 1.2Kb terminal repeat flanking the unique sequence [75]. In addition, the genome has a couple of internal repeats called *Bam* repeats (these repeats have a *BamH*I restriction site) present as 40bp repeats and 100bp repeats. The virus encodes 80 gene products, with 21 genes that are herpesvirus family common genes. These genes comprise 25% of viral genome. More than 40 genes are gammaherpesvirus subfamily common genes, and there are16 unique MHV-68 specific genes, designated as M1-M9, M10 a, b, c, M11-M14. Some of the major MHV-68 specific gene functions are compiled and listed in Table 1.1. In addition, several of the MHV-68 genes are homologous to cellular genes and also to the human gammaherpesviruses [107]. The herpesvirus gene expression following infection is classified into immediate early (IE), early (E), early-late (E-L) and late (L) genes.

MHV-68 associated genes falling into these categories have been described, based on DNA microarray anaysis, RT PCR analysis, following infection in murine epithelial cells [108]. Kinetics of MHV-68 genes following intranasal infection in Balb/c mice has revealed that there are differential patterns of viral gene expression in the lungs, mediastinal lymph node (MLN) and in the spleen [109].

MHV-68 pathogenesis

The natural route of infection of MHV-68 is not known. For other animal gammaherpesviruses, the route of infection seems to be through the respiratory tract. In addition, viral DNA has been detected in the lungs of captured wood mice, suggesting intranasal route of infection and transmission through aerosols as a likely normal route of infection and spread [90]. The intranasal (i.n.) route of infection is the most commonly used method of inoculation of MHV-68. Oral exposure of MHV-68 to mice resulted in replication in the intestinal epithelium, and the virus survived in the acidic gastric environment. In addition, MHV-68 spread systemically, and established latency with similar kinetics to that of the i.n. route of infection [110]. On the other hand, a recent study demonstrated that MHV-68 given orally is poorly infectious [111], suggesting i.n. as a possible route of natural infection. The other route of inoculation has been intra-peritoneal (i.p.) inoculation and this result in seeding virus directly to the spleen. In addition, the roles of M2 and M11 are evident only through i.n. infection, and their functions are by-passed in the i.p. method of infection [112-113].

Following i.n. method of infection, the virus replicates efficiently in the respiratory tract of mice. Replication patterns of the virus has been studied in great detail using a bioluminescence imaging system in whole mouse, using a recombinant MHV-68 expressing firefly luciferase [114] and also by monitoring the luciferase expression by a charge-coupled-device camera scanning [111]. MHV-68 replicates efficiently in both the upper and the lower respiratory tract. Following intranasal infection with 10^4 PFU (note: this is the dose that we are using in the majority of our studies), the virus is initially detected in the nose and in the lungs, and is cleared from these sites by day 10.

This has been demonstrated by several other studies too [115-116]. Following from day's 7- 10-post infection, the virus can be detected in the draining lymph nodes; mediastinal lymph node (MLN) and the cervical lymph nodes (CLN), with a higher proportion in the superficial cervical lymph nodes than in the deep cervical lymph nodes. By day 10, the virus could also be detected in the spleen [111]. In addition, by day 8, the virus was detected in the salivary glands, and by two weeks, in the peritoneum. Interestingly, some virus was also detectable 1-2 months post infection in the nose, and in the salivary glands, indicating possible virus reactivation sites [114].

Recently, some of the studies have implicated the role of MHV-68 associated factors that affect the virus replication in the respiratory tract. One of the extensively studied factors is the thymidine kinase (TK). Intranasal inoculation of TK deficient mutants, resulted in failure to replicate in the nose, but could still replicate efficiently in the lungs, as measured by luciferase imaging [117]. Interestingly, the TK deficient mutants were undetectable in both the nose and lungs by plaque assay [118], highlighting the level of sensitivity of detection by the two methods. In addition, ORF27 gene product is involved in cell-to-cell spread, and is important during the acute phase of infection [119]. Following disruption of ORF61, which encodes for the large subunit of ribonucleotide reductase demonstrated defective upper and lower respiratory tract infection [120].

Following infection in the lungs, MHV-68 replicates productively in the alveolar epithelial cells, mononuclear cells [116]. It is not clear what cells are targeted in the upper respiratory tract, but recent studies using TK mutants highlighted the possibilities [117-118]. Specifically, the TK mutant still replicated in B cells, driving their proliferation, and therefore raising the speculation that MHV-68 probably does not infect B cells in the upper respiratory tract. Interestingly, TK mutants failed to replicate in the macrophages. MHV-68 infection in mice results in lung inflammation and bronchiolitis. Interestingly, a closely related strain, MHV-76 infection resulted in a more rapid clearance from the lungs, and also increased inflammatory response in the lung [121]. MHV-76 is a natural

isolate that has an identical genome to that of MHV-68, except a 9.5Kb region on the left end of the unique region is deleted. The 9.5 Kb region has 12 genes; M1, M2, M3, M4, and eight vtRNAs. By day 3 post-infection, macrophages infiltrate the lungs, followed by CD8 T cells, peaking at day 7. In addition, there is also a massive increase in the number of circulating Vβ4+ CD8 T cells, which is similar to the infectious mononucleosis disease [122]. The inflammation is cleared by 14 days post infection, but the mononuclear cells are still visible in the lungs up to 30 days post infection [116]. MHV-68 replication can also be detected at distant sites, such as the adrenal glands. In the lungs, although the virus establishes latency in the B cells, macrophages and dendritic cells, but during the long-term, latent virus is found only in the B cells [123]. The lung epithelial cells have also shown to be a site of persistence [124]. The virus enters the MLN following infection in the lungs, and infects B cells, macrophages and dendritic cells. Following infection, the B cells undergo expansion, and there is an increase in the number of latently infected B cells [56] (see Figure 1.2).

The latently infected B cells migrate from the MLN to the spleen by 14 days post-infection. The latently infected B cells also expand in the spleen, resulting in splenomegaly. In the spleen, the latency is established in B cells [59], dendritic cells and macrophages [49, 123]. Interestingly, among the B cells, there is a preference for latency establishment in activated B cells that are associated with germinal center reaction [57] and memory B cells [125] . This feature also syncs with the observations associated with EBV [126-127]. In addition, blood also carries latently infected virus through isotype-switched B cells [123]. The latently infected B cells also migrate to non-lymphoid sites such as the vascular endothelial cells [128]. Interestingly, the ability to establish latency is independent of the lytic infection [129-130]. This feature is also evident in TK deficient mutants that demonstrate attenuated lytic replication, but still can establish latency efficiently [118]. Latently infected B cells migrate to the mucosal sites and reactivate.

Reactivation of virus is important for virus transmission to a new host and also for expanding the pool of latently infected cells [131-132]. Several agents, such as phorbol esters, sodium butyrate, calcium ionophore, etc, can stimulate the reactivation of latent gammaherpesviruses . In vitro studies with MHV-68 infected B cell lymphoma cell line, S11, revealed the importance of RTA (lytic transactivator) in the process of reactivation of MHV-68 [133]. Interestingly, administration of LPS and cPG intra-peritoneal to the mice that have been infected with MHV-68 intranasally resulted in reactivation of the virus in lungs, with increased CD8 T cell responses. In addition, the resulting reactivation resulted in increased frequencies of latently infected cells [134]. MyD88 $^{-/-}$ mice infected with MHV-68 have a defect in reactivation [135]. Several studies also indicate a direct role for NF-κB in MHV-68 reactivation. Specifically, NF-κB activation results in establishment of latency [136], whereas down-regulation of NF-κB activation results in reactivation of virus [137]. The exact mechanism of reactivation through this pathway is unknown. MHV-68 associated genes are also involved in the process of reactivation. One of the most important genes is a transcriptional activator (RTA)/ORF50. Mutations in RTA result in failure to reactivate and constitutively active RTA results in failure to establish latency [138]. Plasma cell differentiation can also result in reactivation of virus, and this seems to be modulated by MHV-68 associated M2 gene; absence of M2 results in failure to reactivate [139].

Vaccination strategies

Peptide and subunit vaccination strategies targeting lytic and latent proteins reduce lytic replication and latency, but do not affect long-term latency establishment [140-142]. gp150-expressing vaccinia virus immunized mice were protected from infectious mononucleosis, but did not affect latency establishment following challenge with live virus [132]. Heat- inactivated vaccine reduced lytic replication, but did not prevent establishment of long-term latency following challenge with live virus [132]. Interestingly, live-attenuated viruses that are deficient in latency establishment are very effective in controlling latency load following challenge with live virus. These live

attenuated viruses were created by over expressing RTA, using different strategies [138, 143-144] or by deletion of ORF73 [145].

MHV-68 Immune response

Innate response

MHV-68 infection in type I IFNR-/- mice results in an increased mortality and a rapid spread to the lymph nodes. In addition, these patterns of pathogenesis were also evident in IRF-1 deficient mice [146]. In contrast, following infection of MHV-68 in type II IFNR-/- mice, there is severe fibrosis, with an increased pro-inflammatory cytokines. Interestingly, the pathology associated with the infection of MHV-68 in type II IFNR-/- mice is dependent on CD4+ and CD8+ T cells [114]. MHV-68 infection results in an increased production of IFN-γ by T cells [147]. IFN-γ does not play an important role in virus control during both acute and latent phases of infection [114, 117]. In addition, although there are strain differences, with BALB/c mice infected with MHV-68 demonstrating increased IFN-γ production in the lungs, as compared to C57/BL6 mice, the viral gene expression is similar in both the strains [148]. MHV-68 infection in IFN-γ -/- mice did not result in IL-4 and IL-5 production [117]. IL-6 is one of the predominating cytokines produced following MHV-68 infection [147]. MHV-68 infection in IL-6-/- mice does not influence virus replication or latency or the immune response [149]. MHV-68 infection also induces IL-10 [147], mediated by M2 gene product [150]. MHV-68 infection in IL-10-/- mice results in increased production of IL-12 ,with increased splenomegaly [116]. Along these lines, MHV-68 infection in IL-12-/- mice demonstrated increased lytic and latent virus load, with decreased IFN-γ production [116].

Following MHV-68 infection, there is an increase in expression of chemokines, such as RANTES, eotaxin, MIP-1α. MIP-1β, IP-10, MCP-1 in the lungs. There is also an increased expression of MCP-1, RANTES, MIP-1α, eotaxin and MCP-1 in the BAL [151]. In addition, there is also upregulation of chemokine receptors, such as CCR1, CCR2, CCR3, CCR5 and CXCR3 [151-152]. CXCR3-/- mice infected with MHV-68 display delayed virus clearance, with delayed T cell recruitment [153]. The pattern of

chemokine expression observed is similar to the pattern observed following other respiratory viruses infection. Interestingly, the chemokines are expressed in the lungs in two distinct patterns. The first sets of chemokines are expressed rapidly, while the second patterns of chemokines have delayed kinetics, and were expressed up to a month post-infection [152]. MHV-68 carries two gene products, M3 and ORF74, which modulate the chemokine response. ORF74 encodes a CXCR2 chemokine receptor homologue [154], and M3 protein binds CC and CXC chemokines [155]. Although M3 is secreted in large amounts in the lung, it has no effect in vivo in modulating the host chemokine response [152]. Interestingly, there are also genetic differences in the pattern of cytokine and chemokine induction. Overall, the BALB/c mice displayed increased cytokine and chemokine induction as compared to the C57BL/6 mice. But, this increase did not translate into differences in virus clearance in the lungs and also in terms of latency establishment [148].

T-cell response

In CD8+ T cell depleted BALB/c mice; following high dose MHV-68 infection, there is an increased mortality, with increased virus load [156], which is not observed in CD8+T cell deficient C57BL/6 mice . Such host genetic differences are also reflected in MHV-68 infected β_2-microglobulin deficient mice (lack CD8+ T cells). MHV-68 infected β_2-microglobulin on a BALB/c background displayed lymphoproliferative disease [157], in contrast to the C57BL/6 background that displayed no disease. In contrast to the situation following LCMV infection [158], the MHV-68-specific CD8+ T cell response is independent of the CD4+ T cell help [159]. Interestingly, in CD4+ T cell depleted C57BL/6 mice; a chronic wasting disease is observed [115], and in this scenario, the CD8+ T cells are not defective [159]. Not surprisingly, mice depleted with both CD4+ and CD8+ T cells resulted in mortality [160]. Therefore, CD8+ T cells play an important role in controlling lytic phase of replication but are not effective in controlling long-term infection. One possible reason could be the role of MHV-68 encoded CD8+ T cell immune evasion gene products, such as K3, expressed during both lytic and latent phase of infection, that degrade TAP [161] and also degrades MHC class I heavy

chains [162]. A more recent role for K3 in down-regulating MHC-Class I in migratory and lymph node dendritic cells has been identified, an immune evasion strategy that could aid in establishment of virus persistence [163]. In addition, M3, a chemokine binding protein, can also inhibit CD8+T cell function [164].

The MHV-68 peptides that are associated with the majority of the CD8+ T cell response during the acute and persistent phase of infection have been well-characterized [165]. The peptide-specific CD8+ T cell response are measured through intracellular IFN-γ staining. The kinetics of the CD8+ T cell response is typical of other respiratory viruses, such as influenza viruses. Following intranasal infection of MHV-68, there is a steady increase in the CD8+ T cell response from day 10 in the MLN and spleen, until the end of lytic infection. The MHV-68 specific CD8+ T cells recovered from BAL and MLN, spleen display distinct groups of peptide specificity [165-166]. In addition, the frequencies of MHV-68 specific memory CD8+ T cell precursors were similar to influenza [166].

An interesting feature of CD8+ T cell response to MHV-68 is the expansion of activated Vβ4+ CD8+ T cell population in the peripheral blood and lymphoid tissue during the end of acute phase and is detectable up to a month after infection [122, 167]. This feature is similar to the infectious mononucleosis syndrome induced by EBV in humans. The expansion of this population of CD8+ T cells is independent of MHC-class I [165], and is dependent on the presence of B cells and CD40L interaction through CD4+ T cells [168]. Interestingly, during the mononucleosis state, there is a decrease in the activity and the number of CD4+CD25+FoxP3+ cells, indicating a feature of immune dysregulation [169].

Following depletion of CD4+ T cells in B-cell deficient mice, there is increased virus titers in lungs during the acute phase of infection, demonstrating direct control of virus by CD4+ T cells [170]. The CD4+ T cells control virus in both acute and latent phases of infection primarily through IFN-γ production [171]. They also provide help to the B cells [172]. In contrast, following influenza infection, CD4+ T cells do not control

virus directly, but instead function by providing B cell help [173]. CD4+ T cells also play a critical role in the development of splenomegaly [174] and also for the expansion of Vβ4+ CD8+ T cells [168]. The CD4+ T cells play an important role in controlling latency [129, 143, 175] via IFN-γ production [176]. The frequencies of MHV-68 specific CD4+ T cell response determined by IFN-γ ELISPOT assay during acute phase of infection revealed a steady increase in MLN and spleen. Interestingly, a CD62L lo and CD44hi feature is maintained over long-term [177], which is contrasting to other respiratory viruses [178].

B-cell response

B cells through antibody production control persistent MHV-68 infection [179]. Passive transfer of both neutralizing and non-neutralizing antibodies control acute virus replication primarily through host IgG Fc receptors [180]. The glycoprotein, Gp150 aids in epithelial cell infection [181] and interestingly, antibodies against Gp150 do not neutralize the virus [182]. Following infection of B cells *in vitro* with MHV-68, there is an increased IL-6 and IgM production, with higher CD69 expression [172]. MHV-68-specific B cell response has been well-characterized in the draining lymph nodes, spleen and bone-marrow. The analysis revealed an earlier B cell response in the MLN compared to other sites. Overall, the response is delayed compared to other respiratory viruses. In addition, the B cell response is skewed towards IgG2b and IgG2c response, characteristic of a Th1 response. There is also an absence of virus-specific IgA in the draining lymph nodes, a feature inconsistent with other respiratory viruses. In addition, there is also a substantial component of nonspecific antibody production following MHV-68 infection, a feature dependent on CD4+ T cells in vivo [183]. The respiratory mucosa is a critical site for MHV-68 entry, replication, latency establishment, reactivation and transmission, but little is known about the B cell mediated mucosal immunity to the virus. These aspects are addressed in the current dissertation work.

Influenza A virus

Genome and virus replication features

Influenza viruses are enveloped, negative strand, single-stranded RNA viruses and belong to the *orthomyxoviridae* family. Influenza viruses are classified as types A, B and C. Influenza A viruses (IAVs) are the most pathogenic type, infecting humans [184-185].

IAVs genome has eight RNA segments, coding for up to 11 proteins. The RNA segments include nucleoprotein (NP), viral polymerase complex comprised of PB1, PB2 and PA proteins. In contrast, proteins matrix protein (M1), hemagglutinin (HA), neuraminidase (NA), ion channel protein (M2), non-structural proteins (NS1 and NS2, with NS1 being found in virus infected cells) are associated with the surface of virus (See Figure 1.3) [184-185].

IAVs are subtyped according to the surface antigens HA and NA. So far 16 subtypes of HA and 9 types of NA have been described in birds. The lung epithelial cells of the upper and lower RT are targeted in the mammals [186]. Along with epithelial cells, other cells including monocytes, macrophages are infected [187]. Genetic variations are common in IAVs and allow efficient escape from the immune system. Antigenic drift is characterized by increased point mutations in the virus results in generation of a new virus that enables the new virus to evade adaptive immune system and antiviral treatments. In contrast, antigenic shift is characterized by genetic re-assortment in double infected cells resulting in generation of viruses that have altered surface structures, compared to the parent strains [186].

IAVs binds sialic-acid containing receptors through the HA receptors. The virus is endocytosed through clathrin-dependent mechanism. Low pH of 5-6 in the endosomes favors fusion of viral and endosome membranes, resulting in the release of nucleocapsids into the cytoplasm. These nucleocapsids are then transported into the nucleus where viral mRNA is synthesized using the viral polymerase complex (primary

transcription). The viral mRNAs are transported back to the cytoplasm where translation occurs and the new set of proteins synthesized is transported back to the nucleus which mediates secondary transcription that includes synthesis of complementary RNA (cRNAs) and secondary vRNAs. The secondary vRNAs are transcribed into mRNAs that are transported into the cytoplasm where translation occurs and synthesis of structural proteins occurs. The structural proteins are transported into the nucleus where assembly of nucleocapsids occurs. These nucleocapsids are transported into the cytoplasm and plasma membrane where budding and release of virus particles occurs. (See Figure 1.4) [184-185]

Influenza virus immune response

Innate response

Following i.n. infection of IAVs, the epithelial cells, alveolar macrophages, dendritic cells in the RT are exposed to virus particles which recognize the virus through pattern-recognition receptors (PRRs). This interaction leads to the induction of cytokines and chemokines [188]. The TLR (Toll-like receptors) family is a classic example of PRRs [189]. TLR3 and TLR7/8 has been shown to be important for the recognition of viral RNA [190-191]. TLR3 activation is associated with the induction of IFNβ and other pro-inflammatory cytokines and chemokines. The role of TLR signaling in anti-viral effects and in adaptive immune response is evident in studies associated with TLR-deficient mice [186]. Following IAV infection, plasmacytoid DCs (pDCs) are the major candidates involved in production of type I IFNs, recognizing viral RNA via TLR7 and PKR. In contrast, myeloid DCs recognize viral RNAs by RIG-1 [186, 188]. NOD-like receptors (NLRs) are another class of PRRs. Inflammasomes is an important component of this class of receptors, and NLRP3 deficient mice have deficient innate response to IAV infection [192]. Along these lines, IL-1β deficient mice have reduced inflammatory response, with increased mortality and morbidity and deficient CD4+ T cell activation and decreased IgM response [193-194]. Retinoic acid-induced gene I (RIG-I)-like receptors (RLRs) is another class of PRRs that includes RIG-I and melanoma differentiation-associated protein (Mda) 5. RIG-I is activated by cytoplasmic single

strand 5'-triphoshate RNA and Mda-5 is activated by double-stranded RNAs. The signaling via these receptors initiates expression of type I IFN and other pro-inflammatory cytokines [186]. IAVs inhibit the expression of type I IFNs via NS1 in several ways [195].

IAVs infected alveolar macrophages produce pro-inflammatory cytokines including IL-6, TNF-α, IL-1β and IL-18 [185, 187, 196-197]. Infected lung epithelial cells secrete monocyte chemoattractant protein 1 (MCP-1) that attracts monocytes to the lung, differentiating into DCs and macrophages. Numerous studies have added information regarding the quality of cytokines and chemokines induced following influenza infection [185, 187]. The innate cytokine and chemokine response is important for recruitment of dendritic cells to the draining lymph nodes. Following influenza virus infection, the lung-resident dendritic cells up regulate the expression of MHC class II, costimulatory molecules, such as CD80, CD86 and CD40. These dendritic cells migrate to the draining lymph node, under the influence of the chemokine receptor, CCR7 and initate the adaptive immune response in the lymphoid tissue [198-199].

T cell response

Following influenza virus infection, CD8+ T cell response is regulated by several factors including FasL expression on DCs, TCR avidity, costimulation and inflammatory features in the lung [188, 200]. Within 6-7 days post infection, virus-specific T cells traffic to the lung, in response to several chemokines and chemokine receptor expression in the lung [201]. Virus-specific CD4+ and CD8+ T cells in the lung secrete IFN-γ and TNF-α and induce apoptosis of infected epithelial cells through FAS-FASL interactions or by secretion of perforin and granzymes. In contrast, CD4+ T cells also secrete IL-2 and IL-10 [188, 202-203]. CD8+ T cells play a critical role in virus clearance, as demonstrated by studies associated with mice lacking CD8+ T cells [204].

B cell response

The typical pattern of mucosal B cell response in the RT following influenza infection is depicted in Figure 1.5. Briefly, following influenza virus infection, virus-specific IgM ASCs are generated in the draining lymph nodes, CLN and MLN. The early IgM response is dwarfed within a day or two by a peak of ASCs producing predominantly IgG isotypes. The response in the CLN, which is recognized as an IgA-inductive site, typically includes a substantial proportion of IgA ASCs. IgA production is a less consistent feature of the MLN response, although a prominent early peak of IgA ASCs is seen in the MLN following infection with some influenza subtypes. An Ab response develops in the oNALT with the same kinetics as those in the CLN and MLN, but interestingly consists almost exclusively of IgA ASCs. Ab is produced locally by IgA and IgG antibody secreting cells (ASCs) that home to the RT. The majority of ASCs that localize in the upper RT secrete IgA [72], which is transcytosed across epithelial cells to establish a virus-neutralizing barrier at the mucosal surface. In addition to locally produced Ab, circulating IgG can enter respiratory tissues (particularly in the lower RT) by transudation, and this would be increased by virus-induced inflammation. Circulating IgG levels steadily increase from approximately day 7 after infection, initially reflecting Ab production in responding lymphoid tissues and later in the bone marrow (BM). The numbers of antiviral ASCs in all responding lymphoid tissues rapidly diminish after the elimination of infectious virus. However, antiviral Abs at the respiratory mucosa (particularly IgA) and in the blood are maintained long-term by the durable ASC populations that are established in the RT and the BM, respectively [46].

Virus-specific Abs plays an important role in the clearance of influenza virus [205]. In addition, virus-specific IgM early on in the B cell response is critical for virus clearance, reducing mortality and also protection from influenza-induced lung pathologies [206]. There is also an important role in virus clearance for other isotype-switched Abs [207]. The cognate interaction between CD4+ T cells and B cells are important for B cell proliferation and isotype-switching [208]. Virus-specific IgA is CD4+ T cell dependent during the early stages of infection [209]. In addition, virus-specific IgG Abs can be generated in the absence of CD4+T cells and are also protective in nature

[210]. B cell memory is characterized by long-lived plasma cells and B_{Mem}. The generation of long-lived IgG ASCs is dependent on CD40 signaling as indicated [211] and these ASCs localize in the BM. Over long-term post infection, virus-specific IgG and IgA ASCs localize in the lung. In contrast, IgA ASCs localize in the dNALT. Virus-specific B_{Mem} circulate continuously and disperse to secondary lymphoid tissues, with spleen as a major repository of IgG B_{Mem}. In addition, both IgA and IgG B_{Mem} frequencies were maintained in the lung long-term after infection [46].

APPENDIX

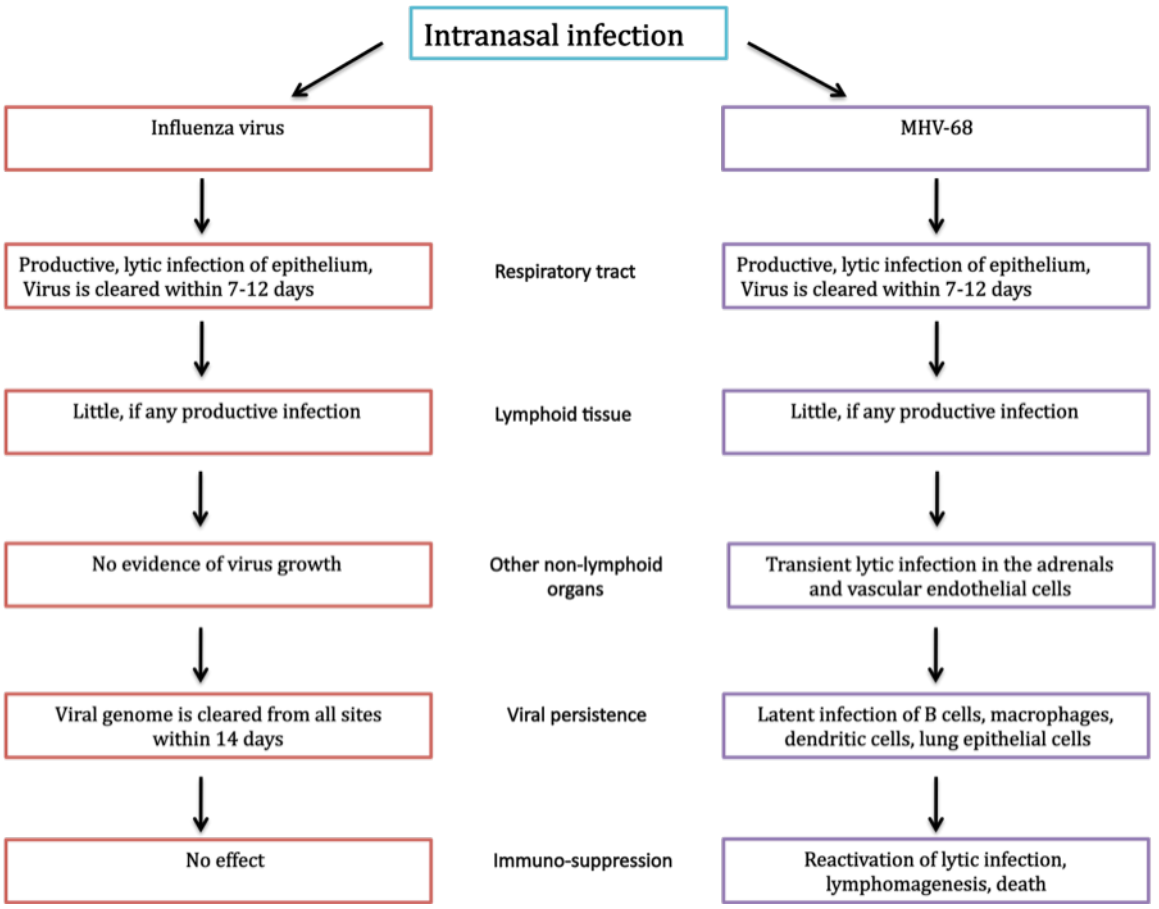

Figure 1.1 Comparable acute phase pathogenesis following influenza virus or MHV-68 infection of the respiratory tract, adapted from [212]

TABLE 1.1 MHV-68 specific gene functions, adapted from [213]

Gene	Biochemical function	Pathogenesis deficit
M1	Secreted super-antigen like, induces expansion and activation, and increased IFN-γ from Vβ4+ CD8 T cells [214]	Increased reactivation [130]
M2	Modulation of BCR signal transduction [215], induces host IL-10, promotes plasma cell differentiation [139]	Failure to reactivate [139], increased long term latency [216]
M3	Secreted chemokine binding protein [217]	Decreased latency amplification [218]
M4	Not determined	Latency establishment deficit [219]
ORF8	gB, receptor binding	Essential in vitro
ORF11	Tegument protein	Lytic replication deficit
K3	Degrades MHC class I and TAP	Latency amplification deficit
ORF21	Thymidine kinase	Severe lytic replication deficit
ORF22	Virion fusion protein	Essential in vitro
ORF27	Cell-cell spread	Lytic replication deficit
ORF50/RTA	Lytic cycle transcriptional activator	Over-expression removes latency
ORF51	gP 150	Release deficit in vitro, normal replication in vivo
M11	Bcl-2 homolog, anti-apoptotic	Reduced latency amplification and pathogenecity
ORF73	Episome maintenance	Severe latency deficit

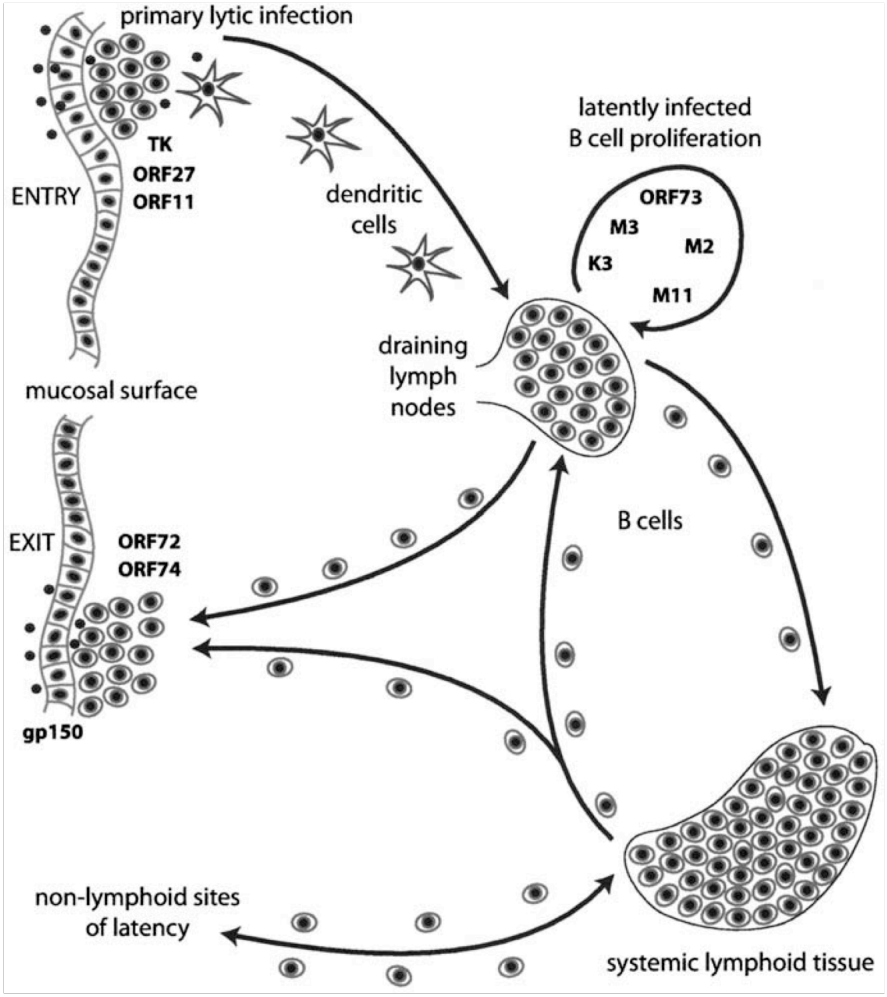

Figure 1.2. MHV-68 pathogenesis [213], highlighting the important proteins involved in various stages of the virus pathogenesis. Mucosal surfaces are the key sites of entry, replication, reactivation and transmission to a new host.

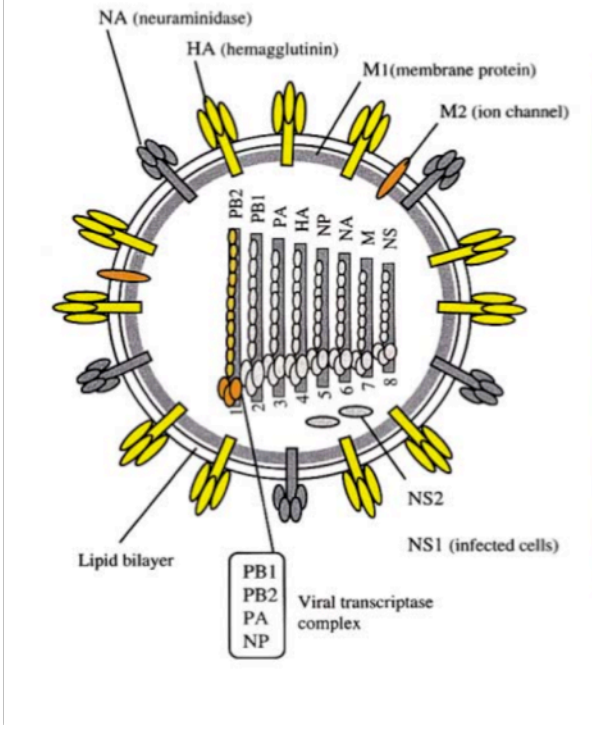

Figure 1.3. Influenza A virus genome and structural features, adapted from [185]

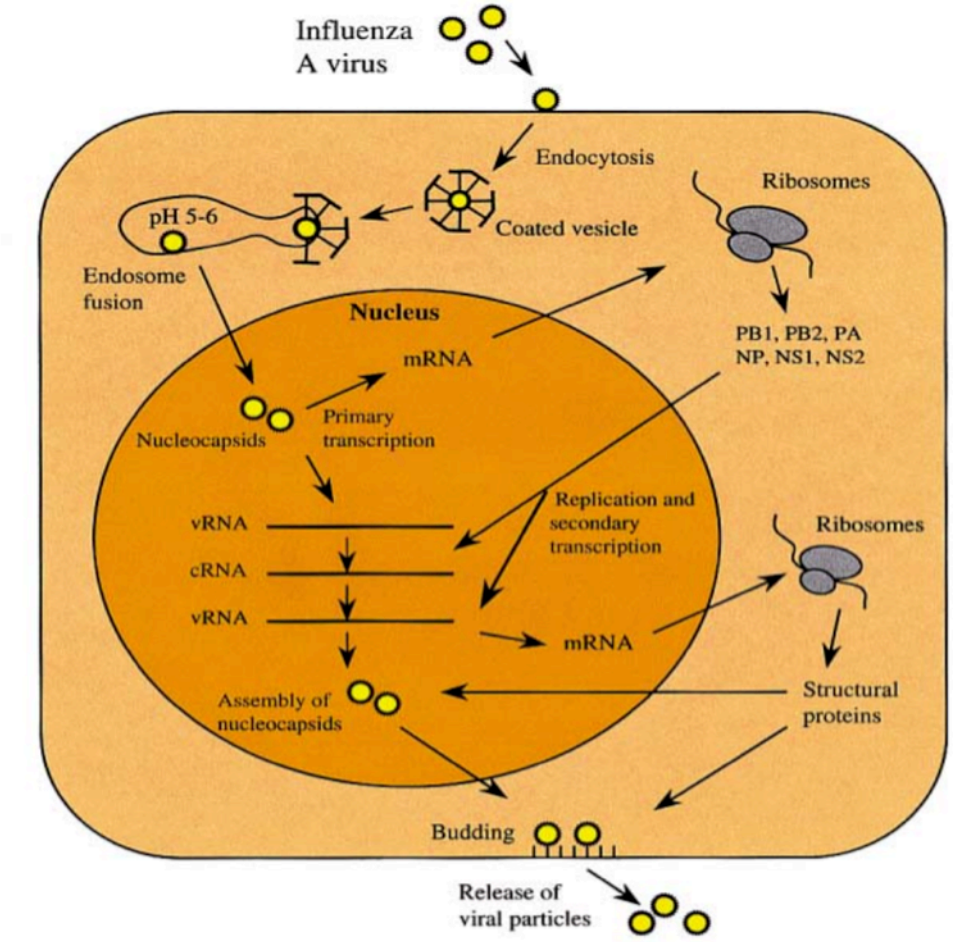

Figure 1.4. Influenza A virus replication depicting virus life-cycle inside cells [185]

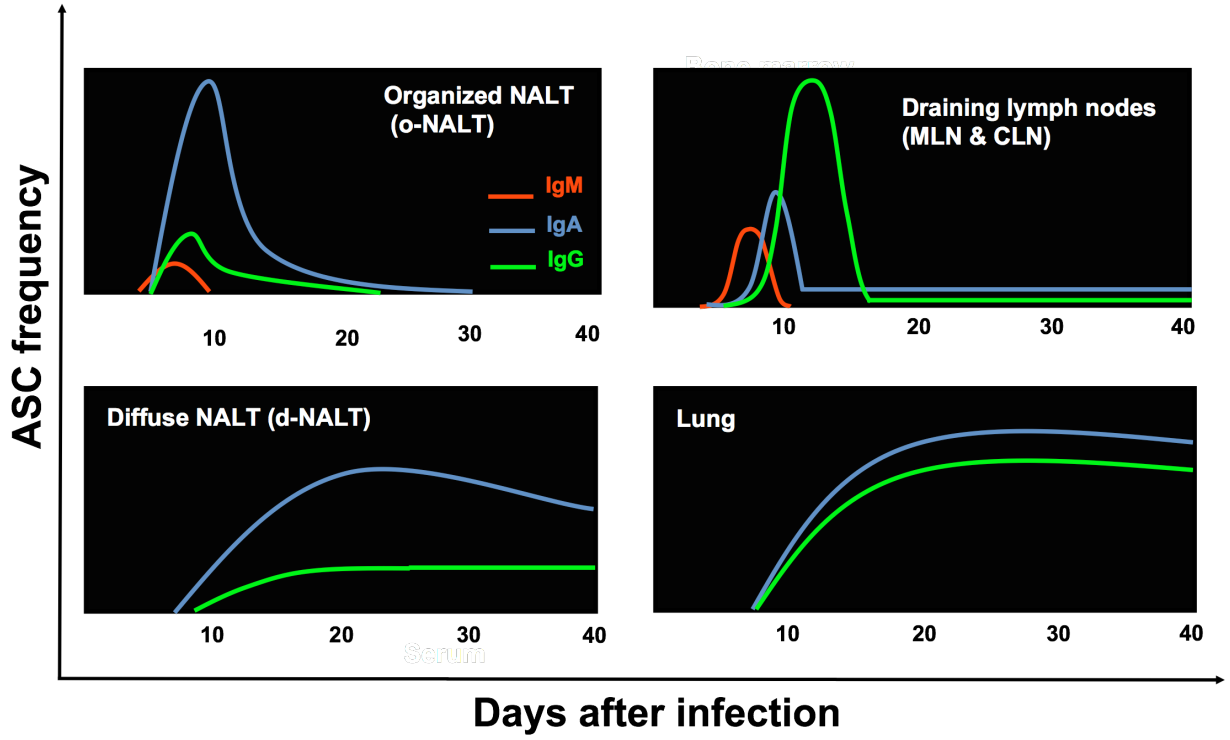

Figure 1.5. Typical pattern associated with mucosal B cell response to a virus replicating in the respiratory tract.

Chapter 2

Regulation of B cell response to a murine gammaherpesvirus-68 (MHV-68) following infection of the respiratory tract

Introduction

A broad range of viruses representing multiple families enter the body via the respiratory tract (RT) and undergo a phase of replication in the respiratory mucosa. Although innate mechanisms provide early-acting antiviral activity, optimal control of primary viral infection of the RT is typically dependent on the development of Ag-specific B and T cell responses. Highly effective B cell- and T cell-mediated antiviral mechanisms operate at sites of viral replication and the kinetics of development of these responses suggest that all play a role in viral clearance and recovery from infection [188].

Studies over many years have generated a comprehensive picture of the development of B cell responses against viruses that target the RT and the role of Abs in viral clearance and long-term protection against re-infection. Much of this work was done using mouse models of acute infection with negative strand RNA viruses such as influenza A virus and murine parainfluenza type 1 (Sendai) virus [220-221]. Infection with these viruses is highly localized and transient; productive replication is restricted to epithelial cells from the nasal mucosa to the lower airways and recovery is associated with the complete elimination of virus from the body. B cell responses are first evident in secondary lymphoid tissues that drain the respiratory mucosa; most notably in the organized nasal-associated lymphoid tissue (oNALT), considered the murine equivalent of human tonsils [222], and in the cervical (CLN) and mediastinal (MLN) lymph nodes, which drain the upper and lower RT, respectively. The rapidity of the B cell response relates to Ag load, but virus-specific Ab production typically begins with the appearance of IgM Ab-secreting cells (ASCs) in the CLN and MLN 5-6 days after infection. The early

IgM response is dwarfed within a day or two by a peak of ASCs producing predominantly IgG isotypes. The response in the CLN, which is recognized as an IgA-inductive site, typically includes a substantial proportion of IgA ASCs. IgA production is a less consistent feature of the MLN response, although a prominent early peak of IgA ASCs is seen in the MLN following infection with some influenza subtypes. An Ab response develops in the oNALT with the same kinetics as those in the CLN and MLN, but interestingly consists almost exclusively of IgA ASCs. Ab production in the spleen matches the pattern in the CLN and MLN but is delayed by 2-3 days, presumably reflecting the time required for Ag transit from the lung [46]. From as early as 7 days after RT infection, Abs resulting from de novo B cell activation in secondary lymphoid tissues access sites of viral replication in the RT and contribute to viral clearance.

Ab is produced locally by IgA and IgG antibody secreting cells (ASCs) that home to the RT. The majority of ASCs that localize in the upper RT secrete IgA [72], which is transcytosed across epithelial cells to establish a virus-neutralizing barrier at the mucosal surface. In addition to locally produced Ab, circulating IgG can enter respiratory tissues (particularly in the lower RT) by transudation, and this would be increased by virus-induced inflammation. Circulating IgG levels steadily increase from approximately day 7 after infection, initially reflecting Ab production in responding lymphoid tissues and later in the bone marrow (BM). Infectious virus is typically cleared from the RT between 7 and 10 days after infection, correlating with the appearance of antiviral Ab in this location. The numbers of antiviral ASCs in all responding lymphoid tissues rapidly diminish after the elimination of infectious virus. However, antiviral Abs at the respiratory mucosa (particularly IgA) and in the blood are maintained long-term by the durable ASC populations that are established in the RT and the BM, respectively [46].

Murine gammaherpesvirus 68 (MHV68), belonging to the gammaherpesvirus sub-family, also targets the RT when administered intranasally (i.n.) to laboratory mice. Productive viral replication occurs in epithelial cells and mononuclear cells in the upper and lower RT [116]. Concurrently; a lifelong latent infection of B lymphocytes [59], macrophages [49], dendritic cells [123], and pulmonary epithelial cells [124] is established. Within a few days of infection, the virus spreads via the blood to a variety of

distal sites, notably glandular tissues such as the salivary and mammary glands, where transient, low level replication may occur. Control of the acute phase of MHV68 infection, with clearance of infectious virus from the RT by 10-12 days [156, 174], is mediated primarily by cytotoxic $CD8^+$ T cells [156], and also effector $CD4^+$ T cells that function via secretion of IFN-g [170]. These cells, together with antiviral Abs, continue to regulate the long-term persistent phase and the occasional re-emergence of infectious virus in the lungs and elsewhere [160, 179]. Features of the host response to MHV68 infection include a massive splenomegaly peaking after approximately 2 wk [174] and reflecting expansion of the B cell (primarily) and T cell populations, and an infectious mononucleosis-like condition characterized by an increased frequency of activated $CD8^+$ T cells in the peripheral blood [122, 168]. MHV68 infection in the mouse has many parallels with human Epstein Barr virus (EBV) infection and is considered a convenient experimental system that may provide valuable insights into g-herpesvirus infections in general [87, 89].

Analyses of the B cell response to MHV68 infection that have been performed indicate a pattern that in many ways matches that described above for other viruses that replicate in the RT. Vigorous MHV68-specific B cell responses developed first in the CLN and MLN and somewhat later in the spleen. These responses, characterized by early IgM production followed by increased numbers of ASCs producing IgG isotypes, gradually waned after peaking between 2 and 3 wk after infection. A long-lasting ASC population was established in the BM and maintained high levels of circulating virus-specific IgG. However, in marked contrast with the situation for other respiratory viruses, MHV68-specific IgA ASCs were absent from the responding lymph nodes, most notably the CLN [183]. In response to this observation, the current study was undertaken to comprehensively evaluate the B cell response to MHV68 infection, with an emphasis on the induction of virus-specific IgA and the establishment of Ab-mediated antiviral protection in the RT. Our analysis identifies a generalized deficiency in the MHV68-specific IgA response that is a consequence of a strong bias towards Th1 cytokine production. In addition, our studies also demonstrate deficient mucosal B cell memory following MHV-68 infection. We speculate that this may represent an evolutionary

adaptation of viruses that establish long-term latency and are transmitted periodically after reactivation and shedding in secretions. Our findings also have implications for the control of g-herpesvirus infections by vaccination.

Materials and Methods:

Viruses

MHV-68 (clone G2.4) was grown in owl monkey kidney cells and the stock titer was determined by plaque assay on NIH3T3 cells. Purified MHV-68 used for the immunoassays was prepared by sucrose density gradient centrifugation (collected at the interface of 30% and 60% sucrose gradients). The spontaneous deletion mutant, γHV68Δ9473 and the relevant WT γHV68 was obtained from Dr. Samuel Speck, Emory Vaccine center, Atlanta. Inactivated MHV-68 was prepared by UV-irradiating purified MHV-68, with a dose of 5000 rad. The UV-irradiation was carried out in Stratalinker, UV- crosslinker (model 2400). An H1N1 Influenza A virus, A/New Caledonia/99 virus (NC), used for comparative studies was grown in the allantoic cavity of embryonated hen's eggs. Purified NC (obtained from Dr.Richard Webby, St.Jude Children's hospital, Memphis) was used for immunoassays. Inactivated NC was prepared by treating purified virus with β-propiolactone. The protein estimation in the purified virus was estimated by the Bradford assay [223].

Mice

C57BL/6J (B6) mice and mice deficient in IFN-γ signaling, B6.129S7-Ifngr1^{tm1Agt}/J (IFNγ R-/-) mice were purchased from the Jackson Laboratory (Bar Harbor, ME). Mice were housed under pathogen-free conditions and after virus infection, were housed in BSL2-level containment. Females were used in all experiments and were infected at the age of 8-12 wk of age. The Animal Care and Use Committee of the University of Tennessee approved animal procedures.

Infection and sampling

Mice were anesthetized i.p. with Avertin (2,2,2-tribromoethanol), followed by i.n. infection with viruses in 30μl of Dulbecco's PBS. MHV-68 was administered as a dose of 10,000 PFU [183], unless indicated. NC was administered at a comparable dose of 40,000 EID_{50}. The anaesthetized mice were exsanguinated via the retroorbital plexus before tissue sampling. The superficial cervical lymph nodes (CLN) and the right posterior mediastinal lymph node (MLN) were collected and gently disrupted between frosted ends of microscope slides to generate single-cell-suspensions. The cells were re-suspended in IMDM (Invitrogen) containing L-glutamine (2 mM), sodium pyruvate (1 mM), penicillin (100 IU/ml), streptomycin (100 μg/ml), gentamycin (10 μg/ml), $5x10^{-5}$ M β-mercaptoethanol and 10% FCS (Complete medium). Bone marrow (BM) cell suspensions were obtained by flushing femurs and tibiae. This was followed by RBC removal by using RBC lysis buffer (Sigma). Cell populations from o-NALT and d-NALT were collected as described previously [70]. Briefly, using the microscope, o-NALT was collected attached to the palate and cells were prepared by teasing. Cells in the d-NALT were recovered by digesting tissue lining the nasal passages with collagenase type I, followed by isolation by Percoll gradient centrifugation, as described for lungs. o-NALT and d-NALT were pooled from a set of three to four mice in order to obtain enough cells for the assay. Lungs were perfused with cold Dulbecco's PBS, followed by fine mincing and incubation for 1hr at 37°C in complete medium that contained 4 mg/ml collagenase type II (Invitrogen). The cells from the lung were resuspended in 40% isotonic Percoll and gently layered over 75% isotonic Percoll (GE healthcare). The cells layered over the gradient was centrifuged at 2000 rpm for 20 min at 25°C and the cells at the interface of 40% and 75% isotonic Percoll was collected and washed with complete medium. Sera were collected from clotted blood. Nasal washes (NW) and lung washes (LW) were collected as described previously [224]. Briefly, NW was carried out by flushing 0.5ml of wash solution (0.1% BSA, antibiotics-PBS) into the trachea towards the nose, collected as it drained from the nares. LW was collected by injecting 1 ml of wash solution through a 1 ml syringe into the trachea, and collected back. The process

was repeated 4-5 times before final recovery. NW and LW were clarified by brief centrifugation and stored at -80°C, until further analysis. Lungs and nasal mucosa (NM) to be titrated for plaque assay were homogenized in 1 ml HBSS (Invitrogen) containing antibiotics and 0.1% BSA. The homogenates were clarified by centrifugation and the supernatants were stored at -80°C, until further analysis.

ELISPOT assay

The virus- specific ASCs were determined by ELISPOT assay as described previously [183]. Briefly, purified virus was detergent disrupted, and plated at 1 μg/100μl/well in a 96- well multiscreen HA filter plates (Millipore). Following overnight incubation at 4°C, the plates were washed with PBS and blocked with complete medium for 1hr, 37°C, 5% CO_2. 5X serial dilutions of cell suspensions were prepared in complete medium, and 100μl of the cells were added to the washed plates, beginning with 10^5 cells/well, unless indicated. The plates were incubated for 4 hrs, 37°C, 5% CO_2. This was followed by washes with Dulbecco's PBS and 0.1% Tween-PBS. Alkaline phosphatase (ALP) conjugated isotype-specific goat anti-mouse Abs (Southern biotech) were diluted 1/500 in 5% BSA-PBS and added as 100μl/well, followed by overnight incubation at 4°C. After washing both sides of the plate, spots were developed at room temperature with 1 mg/ml of 5-bromo-4-chloro-3-indolyl phosphate (Sigma) in diethanolamine buffer. Thereafter, the plates were washed and dried. Each spot represents an antibody-secreting cell, and were enumerated visually by using an Olympus SZX9 microscope.

ELISA assay

The virus-specific Abs was determined by ELISA assay as described previously [183]. Briefly, purified virus was detergent disrupted, and plated at 0.25 μg/ 50 μl/well in a 96-well Nunc ImmunoMaxiSorp plates (Fisher-scientific). Following overnight incubation at 4°C, the plates were washed with 0.05% Tween-PBS and blocked with 3% BSA-PBS for 90 min at room temperature. Serial dilutions of serum or nasal wash (NW)

or lung wash (LW) samples were prepared in 0.1% BSA-0.05%Tween-PBS, and 50 μl of the dilutions were added to the washed plates. The plates were incubated for 4hrs at room temperature and followed by washes. Alkaline phosphatase (ALP) conjugated isotype-specific goat anti-mouse Abs (Southern biotech) were diluted 1/600 to 1/1000 in 1% BSA-PBS and added as 100μl/well, followed by overnight incubation at 4°C. After washing the wells, the plates were developed with *p*-nitrophenyl phosphate (Sigma) in diethanolamine buffer. After 20 min, absorbance at 405nm was read using a *Vmax* kinetic microplate reader (Molecular devices). The virus- specific Ab titer is expressed as the reciprocal of the highest dilution that gave an absorbance value more than twice that for the samples from naive mice. For some experiments, concentrations of Abs were calculated from standard curves based on purified mouse Ig standards (Southern biotech).

Memory B cell assay

Virus- specific memory B cells (B_{Mem}) were determined by memory B cell assay as previously described [46]. Briefly, in a 96-well round bottom plate, two-fold dilutions of cell-suspensions, beginning with 10^5 cells/well and were incubated for 3 days with 10^6 X-ray irradiated (3000 rad) syngeneic naive splenocyte feeders and 0.1μg of inactivated virus. For MHV-68-specific memory B cell assays, UV-inactivated virus was used and for NC-specific memory B cell assays, β-propiolactone-inactivated virus was utilized. Following incubation, the cells were washed and transferred to detergent-disrupted virus coated plates, and ELISPOT assay (as described above) was carried out. Pre-existing virus-specific ASCs were also enumerated at the time of sampling by a direct *ex vivo* ELISPOT assay. Following ELISPOT analysis, the wells were scored positive for virus-specific B_{Mem} if progeny ASC numbers were greater than twice the mean pre-existing ASC. The virus-specific B_{Mem} frequencies were calculated from the number of negative wells per cell dilution by extrapolation to the dilution that gave 37% negative wells [225]. B_{Mem} frequencies of less than one per 10^5 input cells could not be accurately determined. Virus-specific IgG and IgA B_{Mem} were defined as cells that generated IgG and IgA ASCs respectively, after in vitro stimulation.

Plaque assay

The virus titration on the homogenates derived from lung and NM were determined by plaque assay as described previously [133]. Briefly, 10-fold serial dilutions of the homogenates were prepared in DMEM (Biowhittaker) media supplemented with antibiotics and 10% FBS. 0.5 ml of the serial dilutions was added to 6-well plates that had been previously seeded with a 70% confluent monolayer of NIH3T3 fibroblast cells. Dr. Tim Sparer, University of Tennessee provided the NIH3T3 cells. The infected cells were incubated for 1hr at 37°C, 5% CO_2. Following incubation, the virus dilutions were removed from cells. The infected cells were overlayed with a freshly prepared 3ml/well of 1.5% carboxy methyl cellulose (CMC) (Sigma) and 2X MEM media (Invitrogen) in a 1:1 v/v composition. The 2X MEM media was supplemented with 2x the amount of everything that was added to DMEM media, resulting in a 1X concentration in the overlay. This was followed by incubating the plates for 5-6 days at 37°C, 5% CO_2. After 5-6 days, the overlay was removed and 1 ml of 1/50 of glutaraldehyde (Acros) was added to each well for 10 min at room temperature to fix cells to plate. The glutaraldehyde was removed and 1ml/well of Coomassie blue stain was added. The staining was carried out for 45 min at room temperature, followed by washing and air-drying. The plaques were counted under microscope and PFU/ml was determined. Each plaque represents one plaque-forming unit.

Statistics

The statistical comparisons of mean values were performed using non-parametric Mann-Whitney test (*p <0.05, **p <0.01).

Results

Deficient MHV-68-specific IgA and IgG1 induction in the RT

Initial experiments evaluated the virus-specific B cell response in B6 mice infected i.n. with a sublethal dose of MHV68. The B cell ELISPOT assay was applied to

enumerate virus-specific ASCs, including those generated during the acute response in secondary lymphoid tissues that drained the RT and also those that localized in the RT and BM that maintained long-term Ab production. NW and BAL were analyzed by ELISA to identify antiviral Abs available at the mucosal surfaces of the upper and lower RT. For comparison with the MHV68-specific response, a limited analysis of the virus-specific response to i.n. infection with influenza A virus, NC was determined. The B cell response to NC represented the typical mucosal B cell response following RT infection. As described previously for the CLN and MLN, MHV68 infection generated a vigorous virus-specific ASC response, with early IgM production followed by a consistent predominance of IgG2b and IgG2c ASCs; IgA ASCs were essentially absent from both lymph nodes (Figure 2.1 A, D). Notably, few if any IgA ASCs were generated at any time in the oNALT (Figure 2.1 G), a site where IgA production typically predominates in the response to viruses that replicate in the RT [72]. Intranasal administration of a higher dose of MHV-68 did not change the profile of the B cell response (Figure 2.1 C, F). As expected, IgA was prominent in the NC-specific ASC response in the oNALT, in particular (Figure 2.1 H) and in the CLN (Figure 2.1 B). In addition, NC infection resulted in generation of high frequencies of IgG1 ASCs in the CLN and MLN (Figure 2.1 B, E). In contrast, IgG1 generation was largely absent from the MHV68-specific response (Figure 2.1 A, D), suggesting a stronger bias towards the induction of Th1 cytokines following MHV-68 infection. Similar trends were observed in the proportion of isotype-switched virus-specific ASCs generated following MHV-68 or NC infection of the RT (Figure 2.2)

Virus-specific ASC populations were established in the BM after both MHV68 (Figure 2.3 A) and NC (Figure 2.3 B) infection. Small numbers of MHV68-specific IgA ASCs were present in the BM on day 56, perhaps reflecting IgA ASC generation in the spleen later in the course of infection [183]. Virus-specific serum Ab levels closely reflected the differences in the ASC responses to MHV68 and NC infection. The IgG2b and IgG2c isotypes clearly predominated in serum after MHV68 infection (Figure 2.3 C), whereas IgG1, IgG2b, and IgG2c were at similar levels after NC infection (Figure 2.3 D). IgA was consistently detected in the acute phase of infection after NC but not following

MHV68 infection. MHV-68-specific IgA was detected in the serum on day 56, reflecting IgA ASCs localization in the BM at this time-point.

In contrast to the situation following NC infection, where IgA ASC localization in the RT correlated with IgA in the nasal washes, abbreviated as NW (Figure 2.4 F) and lung washes, abbreviated as LW (FIG. 4. J), virus-specific IgA was not detected in the NW (Figure 2.4 E) or LW (Figure 2.4 I) following MHV68 infection. MHV68-specific IgG was present in the LW from day 7 after infection (Figure 2.4 G) and also following NC infection (Figure 2.4 H). This probably reflects transudation of circulating Ab.

Deficient MHV-68-specific B cell localization in the RT

During the acute phase of infection, the localization of ASCs in the d-NALT (NM) and lung was dramatically decreased after MHV68 (Figure 2.4 A, C) compared with NC infection (Figure 2.4 B, D). Interestingly, this applied not only to IgA ASCs, but also to IgG ASCs, suggesting a generalized difference in the regulation of ASC localization in the RT following MHV68 and NC infection. The analysis was extended to the memory phase of infection 56-84 days post infection. The deficiencies in MHV-68-specific ASC localization in the NM (Figure 2.5 A) and lung (Figure 2.5 B), compared to NC infection were also reflected during the memory phase of infection. MHV-68-specific IgA was not detectable in the NW (Figure 2.5 C), compared to NC infection (Figure 2.5 D). The MHV-68-specific IgG titers in the LW (Figure 2.5 E) were similar to the situation following NC infection (Figure 2.5 F). Compared to acute phase of infection, MHV-68-specific IgA titers during the memory phase were detectable in the LW (Figure 2.5 G), although lower titers as compared to NC (Figure 2.5 H), probably reflecting the transudation of IgA from serum (Figure 2.5 C).

Following influenza virus infection, virus–specific memory B cell (B_{Mem}) pool is established, which provide resistance to re-infection. The virus-specific B_{Mem} disperse to various secondary lymphoid organs such as the spleen and the MLN and are found in high frequencies in the lung, providing localized protection [46]. Following MHV-68 or

NC infection, the virus-specific IgG B_{Mem} response was analyzed using an ELISPOT based limiting dilution analysis [46, 226]. The frequencies of MHV-68-specific IgG B_{Mem} and NC-specific IgG B_{Mem} were comparable in the MLN and in the spleen. Surprisingly, both MHV-68 and NC- specific IgG B_{Mem} were found in low frequencies in the lung (Figure 2.6), perhaps reflecting virus modulated differences in the regulation of localization of immunologic memory in the RT. The generation of secondary MHV-68-specific B cell response was determined by intranasal infection of mice that received splenocytes derived from either MHV-68 immune mice or naive mice. A strong secondary MHV-68-specific IgG response was evident in the group of mice that received immune cells, compared to the group of mice that received naive cells. In addition, similar to the primary response, MHV-68-specific IgA was completely absent in the secondary response (Figure 2.7). Measurement of MHV68 titers demonstrated a transient phase of productive infection in both the upper and lower RT, with clearance of infectious virus by day 9 (Figure 2.8).

Differential modulation of influenza-specific IgG and IgA response in the RT following MHV-68 and influenza virus co-infection

As NC infection of the RT induced a strong IgA and IgG1 production, a group of mice were co-infected with MHV-68 and NC and were compared with groups of mice that had been infected with either MHV-68 or NC. The purpose of co-infection studies was to determine if the MHV-68 induced environment in the RT influence NC-specific mucosal B cell response. The mice were first infected with MHV-68, and four hours later, infected with NC. The MHV-68- specific B cell response in the co-infected mice was identical to the mice that received MHV-68 alone. In contrast, the NC-specific B cell response in the co-infected mice was modulated by MHV-68 infection. In the co-infected mice, the NC-specific B cell response in the MLN exhibited down-regulated IgG1 response, compared to NC single infected mice (Figure 2.9 & 2.10). In contrast, the NC-specific IgA response in the oNALT (Figure 2.9 & 2.10) and in the draining lymph nodes

was identical to the NC-specific response in the mice that received NC alone. Lack of effect of MHV-68 on the generation of X-31-specific IgA response was also observed following MHV-68 and X-31 co-infection (Figure 2.12, 2.13 & [46]). In contrast to the IgA response, but similar to the pattern observed with MHV-68 and NC co-infection, the down-regulation of IgG1, with an up-regulation towards IgG2c response was apparent in the draining lymph nodes of MHV-68 and X-31 co-infected mice, compared to X-31 alone-infected mice (Figure 2.12 & 2.13). MHV-68-specific B cell response in the X-31 co-infected mice remained unaltered, a feature consistent with NC co-infection studies.

Increased influx of MHV-68-specific IgG influx into the lung following MHV-68 and influenza virus co-infection

Following MHV-68 infection of the RT, there is a weak influx of virus-specific ASCs into the RT. As NC infection of the RT induced a strong influx of ASCs into the upper and lower RT, co-infection of MHV-68 and NC was carried out in order to test the influence of MHV-68 induced environment on NC -specific ASC influx into the RT. The localization of NC or MHV-68-specific ASCs into the BM, NM or lung was not affected by co-infection (Figure 2.11). Although not statistically significant, there was a trend towards increased MHV-68-specific ASCs in the lungs of co-infected mice. In contrast, following MHV-68 and X-31 co-infection studies, the influx of MHV-68-specific ASCs into the lung were significantly increased (Figure 2.14 A), compared to single infection, not affecting X-31-specific ASC localization into the lung (Figure 2.14 A). The influx of X-31 (Figure 2.14 B) [46] or MHV-68-specific (Figure 2.14 C) ASCs into the NM were not affected as a result of co-infection.

MHV68-specific IgA induction requires viral replication

To determine whether MHV68 replication was a requirement for deficient virus-specific IgA induction, a concentrated preparation of MHV68 was inactivated by UV treatment prior to i.n. administration. It was necessary to administer a dose of inactivated particles equivalent to 30 µg of viral protein in order to generate consistently measurable B cell responses in the draining lymph nodes. Responses to inactivated MHV68 were relatively weak compared with responses to live virus infection, and they also differed substantially in Ab isotype profile. Inactivated MHV68 elicited predominantly IgA production in the CLN (Figure 2.15 A, B). The response in the MLN included a small IgA component, as well as IgG1 ASCs that were absent in the response to live virus (Figure 2.15 C, D).

Secondary B cell response to inactivated MHV-68 in the RT

Similar to the live virus infection, a single dose of the inactivated MHV-68 did not induce localization of ASCs in the NM and lung. However, the group of mice that had been primed with inactivated MHV-68 and thereafter challenged with the inactivated MHV-68 three weeks later, demonstrated a massive influx of virus-specific IgG and IgA ASCs into the NM (Figure 2.16 F) and into the lung (Figure 2.16 E). In addition, the challenge also resulted in a strong secondary response to inactivated virus in the CLN (Figure 2.16 C) and in the MLN (Figure 2.16 D), which included both IgA and IgG1 components. Priming mice with inactivated MHV-68 i.n. followed by live virus infection also resulted in a secondary B cell response in the CLN (Figure 2.16 A) and in the MLN (Figure 2.16 B) that included both IgA and IgG1 components. This reflects the ability of the live virus to activate a secondary B cell response induced by inactivated virus irrespective of the Ab isotype. The secondary B cell response to inactivated MHV-68 following challenge with live virus was weaker compared to the secondary B cell response following challenge with inactivated MHV-68.

MHV-68 acute phase replication associated gene products are not involved in down-regulating IgA response, but enhances influx of IgG ASCs into the lung

The virus-specific IgA induction following inactivated MHV-68 administration indicates an influence of live virus replication on modulating the IgA response. These findings suggest the possibility that MHV-68 associated gene products expressed during acute virus replication down-regulate the IgA response. To address this possibility, B cell response following intranasal infection of a spontaneous deletion mutant, γHV68Δ9473 was determined. The mutant virus lacks approximately 9.5 Kb of the unique coding sequence of MHV-68 genome [227]. This locus has at least twelve MHV-68 specific genes including *M1, M2, M3, M4* and eight viral t-RNA-like genes [89] that are expressed both during acute virus replication and during persistence [108, 112, 228-231]. Although the importance of this locus following an intranasal infection of γHV68Δ9473 was not completely characterized, an analysis following intranasal infection of MHV-76, another gammaherpesvirus isolate that has the locus deletion identical to γHV68Δ9473, revealed this locus to be important for acute virus replication in the lung and also for decreasing the host inflammatory response in the lung [121]. These findings suggest the possibility that MHV-68 may utilize this locus to down-regulate host IgA response. In addition, *M3* encodes for a chemokine binding protein, which is expressed in copious amounts in the lung [109, 155]. M3 can bind to several chemokines with high affinity [217], and therefore could potentially down-regulate the influx of virus-specific ASCs into the NM and lung.

The B cell response in the draining lymph nodes to the γHV68Δ9473 (Figure 2.17 A, C) did not induce either IgG1 or IgA, and in these aspects were identical to the response to the corresponding WT γHV-68 (Figure 2.17 B, D). Interestingly, the IgG2c response was enhanced in the mice infected with γHV68Δ9473 compared to the mice infected with WT γHV-68. In addition, no virus-specific IgA was induced in the oNALT (Figure 2.17 E). There was an increased influx of IgG ASCs into the lung (Figure 2.17 F)

following γHV68Δ9473 infection, compared to the WT γHV-68 infection, with no changes in the influx of ASCs into the NM (Figure 2.17 G).

MHV-68 specific IgA is induced following infection in the IFN-γR-/- mice

As the MHV-68-specific gene products were not involved in the direct regulation of IgA and IgG1 induction, other features of MHV-68 replication in the RT, including a biased Th1 cytokine response [147] can potentially regulate the mucosal B cell response. Th1 responses can directly down regulate Th2 responses [232]. In addition, MHV-68 infection in the IFN-γR-/- mice results in induction of fibrosis, characterized by increased levels of TGFβ1 [233], a critical IgA class-switch factor [58, 61, 234-236]. Therefore, the change in the cytokine profile in these mice following MHV-68 infection could influence the B cell response. MHV-68 infection in the IFN-γR-/- mice generated IgA response in the CLN (Figure 2.18 A) and in the MLN (Figure 2.18 B) compared to the response in the WT mice. In contrast, IgA response was not generated in the oNALT of the IFN-γR-/- mice (Figure 2.18 F). IgG1 was also induced in the IFN-γR-/- mice following MHV-68 infection, indicating a role for IFN-γ in down-regulating Th2 cytokine mediated class-switching mechanisms. Interestingly, the IgG2b proportions were increased, with a decrease in IgG2c proportions in the IFN-γR-/- mice following MHV-68 infection (Figure 2.19).

Virus- specific ASC localization in the RT is impaired following infection in the IFN-γR-/- mice

IFNγ induction in the RT following virus infection is an important signal for initiating chemokine cascade in the lung that can attract the immune cells to the RT. The MHV-68-specific localization of ASCs into the lung (Figure 2.18 C) and NM (Figure 2.18 D) of IFN-γR-/- mice were comparable to the localization following infection of the

WT mice. Although the MHV-68-specific IgA ASCs were generated in the draining lymph nodes of IFN-γR-/- mice, these ASCs failed to localize the RT. Interestingly, NC-specific IgA and IgG ASCs also failed to localize in the lungs of IFN-γR-/- mice, compared to WT mice (Figure 2.18 E). This indicates that the lack of localization of MHV-68-specific IgA and IgG ASCs in the lung following MHV-68 infection of the IFN-γR-/- mice might be reflective of an inherent defect for ASCs to migrate to the lung in the absence of IFNγ signaling.

Discussion

The B cell response to acute respiratory viruses that replicate in the RT, such as influenza virus and parainfluenza type 1 virus includes a substantial component of IgA [220-221]. MHV-68, a persistent gammaherpesvirus, following RT infection in mice offers as a good animal model for studying EBV immunobiology in vivo. Analysis of B cell response to MHV-68 revealed a marked contrast with the situation for other respiratory viruses. MHV68-specific IgA ASCs were absent from the responding lymph nodes [183]. Our analysis extends these studies, providing a comprehensive picture of the state of mucosal B cell response to MHV-68 infection of the RT. The analysis is compared with a typical mucosal B cell response generated following i.n. infection with a comparable dose of influenza A virus, NC. In addition, the current analysis also provides mechanistic insights into the regulation of B cell response to MHV-68 in the RT.

One of the peculiar features, as demonstrated before, was an absence of IgA induction in the CLN following MHV-68 infection. This is surprising as CLN is a biased site for IgA induction following infection of RT [237-238]. Studies with other respiratory viruses have demonstrated that unlike oNALT in the upper RT, the draining lymph nodes have a larger proportion of IgG responses compared to IgA proportions. Increasing the load of MHV-68 in the RT increased the IgG proportions, but failed to induce an IgA response. This excludes the possibility of availability of low levels of

antigen in the environment down-regulating MHV-68-specific IgA response. oNALT in the upper RT predominantly generates IgA ASCs following NC or other influenza viruses induction [46, 72]. In contrast, MHV-68 infection failed to generate IgA response in the oNALT. The lack of IgA generation was not associated with poor replication of MHV-68 in the RT, as MHV-68 replicated efficiently both in the nasal mucosa Figure 2.8, [111, 114] and in the lung Figure 2.8, [115-116]. In fact, MHV-68 titers in the lung were comparable to the NC titers in the lung (data not shown). Failure to detect MHV-68-specific secretory IgA in the NW and LW raises the scenario that along with the absence of IgA ASC generation, the secretion of IgA is also impaired, reflecting different levels of down-regulation of IgA by MHV-68 in the RT. Compared to the acute phase B cell response, some IgA ASCs were detectable in the BM during the memory phase of infection. Along these lines, IgA Abs were detected in the serum and in the LW, perhaps reflecting IgA ASCs generated in the spleen [183] as a result of ongoing virus persistence and basal reactivation of virus.

In contrast, the quantity of IgG responses was comparable between MHV-68 and NC infection, indicating an isotype-specific, selective down-regulation of virus-specific IgA following MHV-68 infection. The absence of IgA at mucosal surfaces in the upper RT extended into the memory phase of infection and this demonstrates a generalized deficiency of IgA induction following MHV-68 infection. All isotypes of the virus-specific Ab can be protective in nature, but lack of IgA offers defective Ab mediated protection, particularly at mucosal surfaces. The presence of influenza-specific IgA in the nasal passages has particularly anti-viral effects [134]. The absence of IgA at mucosal surfaces confers a selective advantage to MHV-68, as features of pathogenesis of virus, such as replication, latency establishment, reactivation and transmission are associated with mucosal surfaces of the RT [213]. EBV is detected in the secretions at tonsillar surfaces [134], which are equivalent to oNALT in mice [222]. Our studies demonstrating lack of IgA generation in the oNALT and also lack of secretory IgA Abs in the nasal wash following MHV-68 infection, perhaps reinforces the situation with EBV infection, facilitating virus replication and latency establishment in the RT, also favoring transmission to a new host. Although currently, there are no gammaherpesvirus

transmission models available, it would be potentially of interest to pursue the development of such models that demonstrate the role of IgA mediated mucosal protection to gammaherpesvirus infection.

Our studies indicate that IgA and IgG induction mechanisms are differentially regulated in the RT. Following MHV-68 infection; the B cell response includes a bias towards IgG2b/IgG2c and no IgG1 induction. In contrast, NC infection of the RT has both IgGb/IgG2c and IgG1 components. This is perhaps reflective of the cytokine profile studies that demonstrate lack of typical Th2-associated cytokines such as IL-4, IL-5 following MHV-68 infection [147], compared to other respiratory viruses, for example following sendai virus infection [239]. The effects of down regulation of Th2 associated cytokines by MHV-68 is also evident in the co-infection studies with MHV-68 and NC, which resulted in the down-regulation of NC-specific IgG1, favoring a strong bias towards IgG2c switching in the co-infected mice. In contrast, MHV-68-specific IgG isotype profile in the co-infected mice was identical to MHV-68 single infected mice. These results indicate a role for MHV-68 replication induced non-specific factors that perhaps favor the establishment of a biased Th1 environment in the RT involving a strong component of IFN-γ. The features associated with this environment may be critical determinants regulating IgG isotype class switching mechanisms. Although we did not evaluate the cytokine profile of CD4+ T cells associated with co-infected and single-infected mice, the change in NC-specific IgG isotype pattern in the co-infected mice compared to NC single infected mice is indicative of a role for a biased component of IFN-γ derived form CD4+ T cells in modulating the IgG isotype class switching. IFN-γ production from CD4+ T cells during the process of cognate interaction with B cells is critical for the generation of virus-specific IgG2c [53]. In contrast, IL-4 production from Th2 cells is important for IgG1 isotype class switching [51-52]. It is also likely that the polarized Th1 environment following MHV-68 infection may play a direct role in down-regulating Th2 differentiation [232]. This line of thinking is also observed in our studies with inactivated MHV-68 administration i.n. which resulted in the induction of IgG1 response in the MLN. Indeed, inactivated MHV-68 is a relatively poor IFN-γ inducer, compared to live virus [135]. MHV-68 infection in the IFN-γR-/- mice causes pulmonary

fibrosis associated with enhanced induction of Th2 cytokines including IL-4 [233]. In lieu of the altered cytokine pattern, we observed generation of IgG1 ASCs in the MLN of IFN-γR-/- mice infected with MHV-68. These findings favor the argument that a polarized Th1 environment can significantly down regulate Th2- mediated IgG1 class switching mechanisms. Interestingly, following a 9.5 Kb spontaneous deletion mutant (γHV68Δ9473) infection [227], the IgG2c response in the MLN was enhanced, reflecting a role for this region in regulating B cell response to MHV-68 in ways that is not yet clear. Additional step-wise characterization through individual loss-of-function mutants will be important to delineate the exact role of this region in regulating the B cell response to MHV-68.

Although IgA class switching can occur via T cell-dependent and T-cell independent mechanisms [58], studies with influenza virus have demonstrated that the early generation of virus-specific IgA is entirely dependent on CD4+ T cell help [209]. CD40-CD40L interactions and TGF-β1 are known to regulate the classical T cell-dependent IgA class switching mechanisms [50, 58, 240]. CD40-CD40L interaction initiates NF-κB activation in B cells, leading to induction of activation induced cytidine deaminase (AID) [60]. AID is critical for class switch recombination process and IgA class switching [241]. Low concentrations of TGF-β1 is important for initiating C_α transcription, resulting in the generation of germline C_α transcripts that makes the transcripts amenable to the actions of AID, inducing IgA CSR [61]. Although the source of TGF-β1 in the context of T cell-dependent scenario is not clear, certain subsets of CD4+ T cells can directly secrete TGF-β1 [242] and perhaps induce IgA class switching. Alternatively, Th2-derived cytokines, such as IL-4, IL-5 and IL-10 may also stimulate B cells to secrete endogenous TGF-β1 that can induce IgA class switching in an autocrine fashion [243]. The other possibility is that TGF-β1 secreted by CD4+ T cells or in an endogenous manner by B cells may be important for the generation of IgA plasmablasts which following exposure to Th2-derived cytokines may differentiate and proliferate into IgA plasma cells [10]. In contrast, our studies demonstrate no roles for Th2 mediated IgA induction as the NC- specific IgA induction in the upper and lower RT was not

affected in the co-infected mice, although NC- specific IgG1 induction was impaired in these mice. Unlike IgG isotypes, the IgA class-switching mechanism is not inhibited by the polarized IFN-γ environment, contrary to a study that demonstrated direct inhibition of TGFβ1-mediated IgA class switching by IFN-γ signaling on B cells [244]. Although we did not compare the proportions of TGF-β1 secreting CD4+ T cells following NC or MHV-68 infection, unlike NC, MHV-68 establishes latency in all the antigen presenting cells [49, 57, 59] and therefore can potentially down regulate the differentiation of subsets of TGF-β1 secreting CD4+ T cells that aid in IgA class switching.

Our studies indicate that the deficient IgA induction following MHV-68 infection is a feature associated with virus replication, as inactivated MHV-68 induced a predominating IgA response in the CLN, with some IgA response being generated in the MLN as well. The induction of predominantly IgA ASCs in the CLN, compared to MLN following inactivated virus administration is also evident in studies with influenza [226]. This may be indicative of features associated with inactivated virus, which are perhaps sampled by M cells in the epithelial cells of NALT to the DCs resulting in the selective generation of IgA committed plasmablasts [10]. These cells may then migrate to the CLN through the efferent lymphatics and therefore, following inactivated virus administration, there is mainly appearance of IgA ASCs in the CLN. In contrast, live virus replication may be associated with induction of other mechanisms that favor generation of ASCs in the CLN, rather than migration of ASCs from NALT, resulting in the localized generation of IgG ASCs and IgA ASCs in the CLN. Induction of IgA to inactivated MHV-68 implicated features of live virus replication in down regulating IgA response. But, MHV-68 associated gene products expressed during the acute phase of infection did not influence IgA induction as demonstrated by our studies with the 9.5Kb spontaneous deletion mutant, γHV68Δ9473. It would be interesting perhaps to examine TGFβ1 induction following administration of inactivated MHV-68.

Availability of increased TGF-β1 in the environment can contribute to IgA induction to live virus, as observed with our studies following MHV-68 infection in the IFN-γR-/- mice. MHV-68 infection in these mice is characterized by pulmonary fibrosis

with increased TGFβ1 induction [233]. Interestingly, MHV-68 infection in the IFN-γR-/- mice failed to induce IgA response in the oNALT, pointing towards a differential regulation of IgA induction in the upper and lower RT. Alternatively; it is also likely that the pattern of fibrosis may be associated in the lower RT and not with the upper RT, contributing to differential induction of TGF-β1 in the upper and lower RT following infection of MHV-68 in the IFN-γR-/- mice. The B cell response in the draining lymph nodes of these mice also included increased IgG2b proportions. This may reflect the ability of TGFβ1 to induce both IgA and IgG2b class switching. Interestingly, IL-21 causes an effective down-regulation of TGFβ1-mediated class switch to IgG2b, without influencing TGFβ1 mediated effects on class-switch to IgA. Therefore, the strikingly strong IgG2b component in these mice may also reflect decreased IL-21 in the TGF-beta rich microenvironment [245]. Further characterization of cytokine profiles in the upper and lower RT of these mice will be required to address these issues.

The B cell response to respiratory viruses replicating in the RT includes generation of cellular elements of B cell memory, consisting of virus-specific ASCs producing IgG and IgA, as well as concentrations of B_{Mem} that localize in the RT [46]. In contrast to NC and other influenza virus infection, MHV-68 infection resulted in a weak influx of IgG ASCs into the RT at all times post-infection. This is surprising, as both NC and MHV-68 generated comparable IgG responses in the draining lymph nodes. Mechanisms regulating trafficking of ASCs into the lung and NM are not clear. IgG ASCs expressing CXCR4 traffic to BM in response to the corresponding ligand, CXCL12 [31]. This feature does not seem to be compromised following MHV-68 infection, as there is comparable IgG ASCs localization in the BM following NC or MHV-68 infection. In addition, IgG ASCs expressing CXCR3 traffic to inflammatory sites [246]. Following MHV-68 or influenza infection, there is an apparent inflammation in the lung, with both viruses inducing BALT structures [247-248]. But, the inflammation induced in the lung following MHV-68 infection may be compromised as indicated by studies following MHV-76 infection of the RT. MHV-76 is a gammaherpesvirus isolate that has genes missing similar to the spontaneous deletion mutant, γHV68Δ9473. Studies with this isolate revealed the importance of this region in down-regulating the

inflammatory response in the lung [121], raising questions that perhaps, the lung inflammation induced by MHV-68 is sub-optimum. In support of this line of thinking, our analysis of B cell response to γHV68Δ9473 revealed increases in the frequencies of ASCs in the lung. Significant increases were not observed in the NM, compared to the frequencies following WT virus infection. The ASCs localizing in the NM are mostly IgA ASCs, and as γHV68Δ9473 infection similar to the WT virus failed to generate IgA ASCs, the influx of ASCs into the NM remained comparable. The increased influx of ASCs into the lung may also reflect the lack of effects of the chemokine binding protein, M3 in the mutant virus. M3 is secreted in large amounts in the lung during the acute phase of infection [217], and may contribute to the modulation of inflammation in the lung. Although, a previous study demonstrated no changes in the chemokine pattern in the lung following infection with a virus lacking M3 coding sequence [152], there could be localized effects of M3 that can modulate the immune response. It is not known if M3 is secreted in the NM. Therefore, the weak influx of IgG ASCs into the lung, perhaps are modulated by the threshold of inflammation in the RT, dictated by the nature of infecting virus. These lines of thoughts were also apparent following infection with different strains of influenza, as NC (a non-mouse adapted virus) infection of the RT resulted in lower frequencies of IgG and IgA ASCs localizing in the lung and NM, compared to the X-31 or PR8 infection (mouse adapted viruses) [46]. Inflammation in the lung as a possible stimulus for attracting IgG ASCs into the lung was also evident following inactivated MHV-68 or inactivated influenza administration, which attracted little IgG ASCs to the lung [226]. Co-infection with X-31 encouraged significant influx of MHV-68-specific ASCs into the lung, and this kind of a trend was also observed following NC and MHV-68 co-infection, although not statistically significant. This could reflect the increased inflammation or other factors in the lung by X-31, compared to NC infection. Alternatively, the nature of infecting virus may modulate the induction of ASCs that are inherently programmed to enter the RT.

The IgA ASCs generated in the lymph nodes draining the RT are pre-programmed to migrate to the lung [249]. Therefore, it is surprising that although IgA ASCs were generated in the draining lymph nodes of IFN-γR-/- mice, they failed to

migrate to the lung. The failure of IgA and IgG ASCs to migrate to the lung seems to be an inherent defect in these mice as NC infection of IFN-γR-/- mice also resulted in reduced appearance of IgA and IgG ASCs in the lung. These studies also emphasize a role for IFNγ in modulating the influx of ASCs into the RT. Following inactivated X-31 administration i.n., there is a preferential localization of IgA ASCs in the lung and NM [226]. In contrast, in the lung, although the magnitude of MHV-68-specific IgA ASCs was comparable to the X-31-specific IgA ASCs, the administration of inactivated MHV-68 resulted in localization of both IgG and IgA ASCs in the lung. These differences may be due to the generation of higher frequencies of IgG ASCs in the MLN following inactivated MHV-68 administration, compared to those induced following inactivated X-31 administration [226].

IgG B_{Mem} frequencies in the MLN and spleen following MHV-68 and NC infection were similar, but both the viruses-specific IgG B_{Mem}'s failed to localize in the lung. In contrast, following X-31 infection, greater frequencies of IgG B_{Mem} localized in the lung [46]. It is not clear what mechanisms govern the trafficking properties of B_{Mem} into the lung. This may reflect properties of IgG B_{Mem}, similar to ASCs , being modulated by the nature of infecting virus and threshold of inflammation in the lung. Induction of BALT does not seem to be a requisite for attracting or maintaining ASCs or B_{Mem} in the lung, as BALT is induced following influenza or MHV-68 infection. Perhaps, the properties of BALT induced following MHV-68 infection may be different from that following influenza infection, as BALT seems to be a latent reservoir for MHV-68 [248]. In contrast to the situation following influenza infection, IgA B_{Mem} is not generated following MHV-68 infection, as indicated by the adoptive transfer studies.

Priming mice with inactivated MHV-68 i.n. generated elements of both IgG and IgA B_{Mem}, as indicated by the strong secondary B cell response in the draining lymph nodes following challenge with inactivated MHV-68 or live MHV-68. The B cell response induced by the challenge possessed typical secondary B cell response features, characterized by a reduction in IgM response and an increase in the isotype-switched B cell responses compared to the primary response. These studies indicate that the down-regulation of induction of both IgA ASCs and IgA B_{Mem} are modulated by features

of virus replication. The generation of a secondary B cell response with IgG1 and IgA components indicates that the live MHV-68 has the ability to differentiate B_{Mem} to ASCs irrespective of the Ab isotype. Interestingly, priming mice with inactivated MHV-68 generated both IgG, IgA B_{Mem} that following differentiation with inactivated MHV-68 localized in the lung and NM. Our studies indicate that inactivated MHV-68, in contrast to live virus can induce IgA, and also enhance localization of both IgG and IgA ASCs in the upper and lower RT.

In summary, the current studies provide a comprehensive picture of B cell response to MHV-68 in the upper and lower RT and also address possible mechanisms contributing to MHV-68 mediated down regulation of virus- specific IgA and IgG1. In addition, these studies provide a platform for testing inactivated MHV-68 as a potential vaccine strategy in providing mucosal protection to gammaherpesvirus infection. The findings lead to the speculation that deficient B cell-mediated mucosal protection modulated by virus replication may represent an evolutionary adaptation of viruses that establish long-term latency and are transmitted periodically after reactivation and shedding in secretions.

APPENDIX

Figure 2.1. Virus-specific B cell response in the upper and lower respiratory tract. B6 mice were infected i.n. with 10,000PFU of MHV-68 or 40,000 EID_{50} of NC. The kinetics of MHV-68- specific ASC response in the CLN (A), MLN (D) and o-NALT (G) is shown. For comparison, limited analysis of NC-specific ASC response was determined in the CLN (B), MLN (F) and o-NALT (H). Virus-specific ASC response in the CLN (C) and MLN (F) was determined on day 10 post-infection with a higher dose of MHV-68 ($2x10^5$ PFU). The ELISPOT assay was performed on cell suspensions of CLN and MLN derived from individual mice, and for o-NALT, the cell suspensions were pooled from three to four mice. The ASCs producing virus-specific IgM, IgG1, IgG2b, IgG2c, IgG3 and IgA were determined. Results are expressed as a frequency of ASCs per 10^5 nucleated cells. The mean + SE for the draining lymph nodes is shown for five to twelve individual mice and the mean + SE for o-NALT is shown for three to six sets of pooled samples.

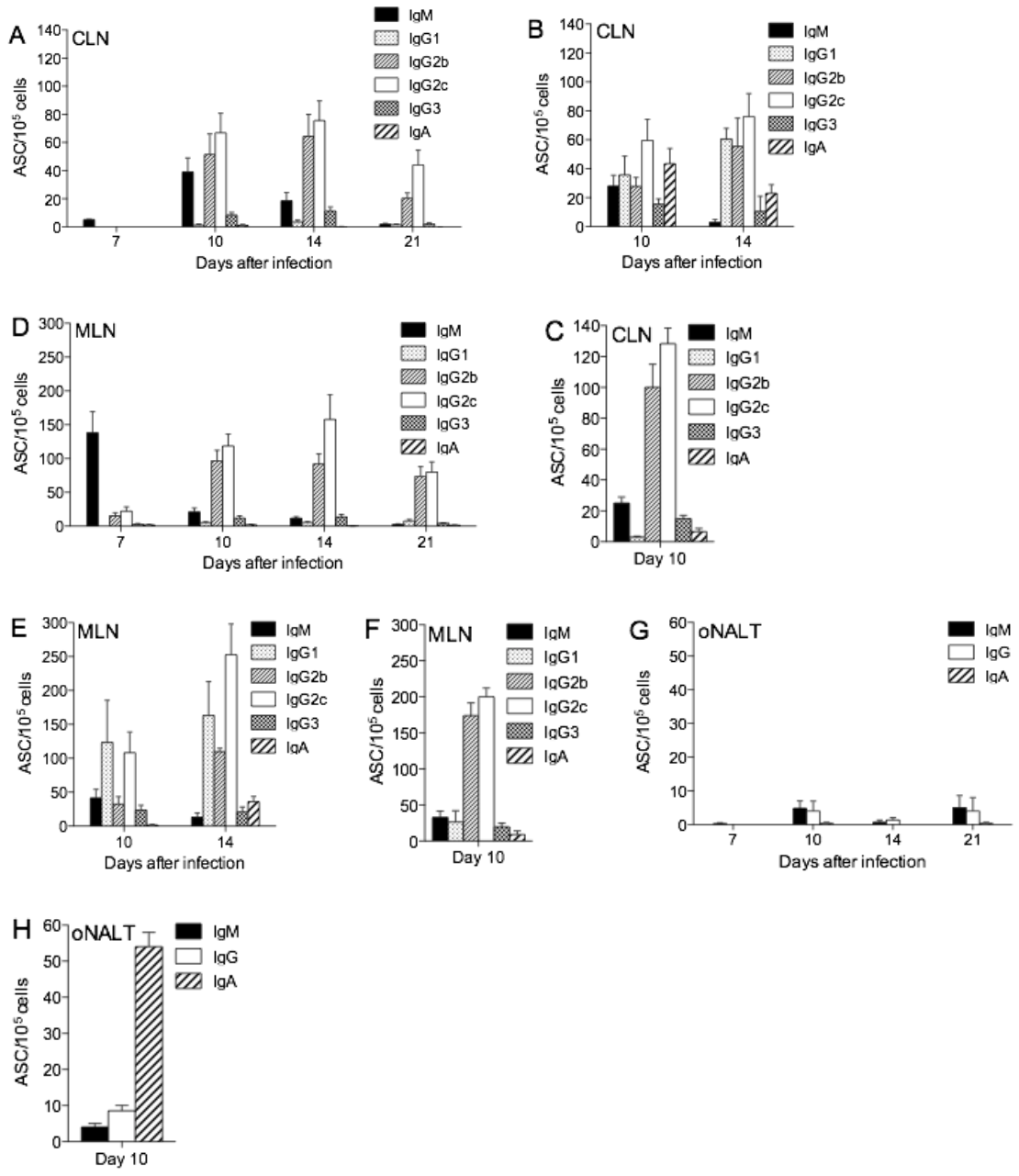
A
CLN
ASC/10^5 cells
Days after infection
IgM
IgG1
IgG2b
IgG2c
IgG3
IgA
B
CLN
C
CLN
Day 10
D
MLN
E
MLN
F
MLN
G
oNALT
IgG
H
oNALT

Figure 2.2. Proportion of isotype switched virus- specific ASCs in the upper and lower respiratory tract. Following 10 days post infection, the proportions were determined in the CLN and MLN following MHV-68 infection (A & C respectively) and following NC infection (B & D respectively). Proportions of MHV-68 and NC-specific IgA ASCs among the total (IgM, IgG, IgA) virus-specific ASCs in the o-NALT (E) is shown.

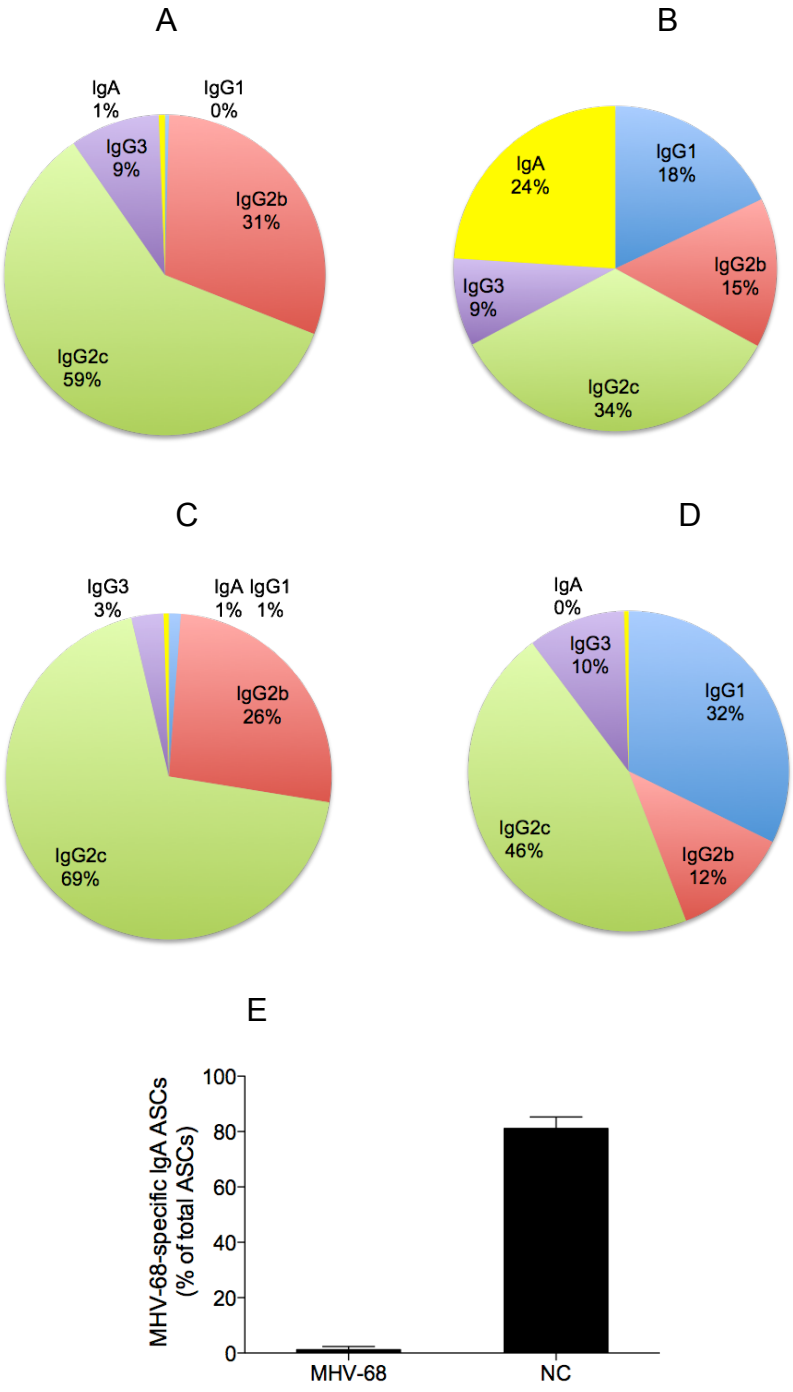
A
IgA 1%
IgG1 0%
IgG3 9%
IgG2b 31%
IgG2c 59%
B
IgA 24%
IgG1 18%
IgG2b 15%
IgG3 9%
IgG2c 34%
C
IgG3 3%
IgA 1%
IgG1 1%
IgG2b 26%
IgG2c 69%
D
IgA 0%
IgG3 10%
IgG1 32%
IgG2c 46%
IgG2b 12%
E
MHV-68-specific IgA ASCs (% of total ASCs)
100
80
60
40
20
0
MHV-68
NC

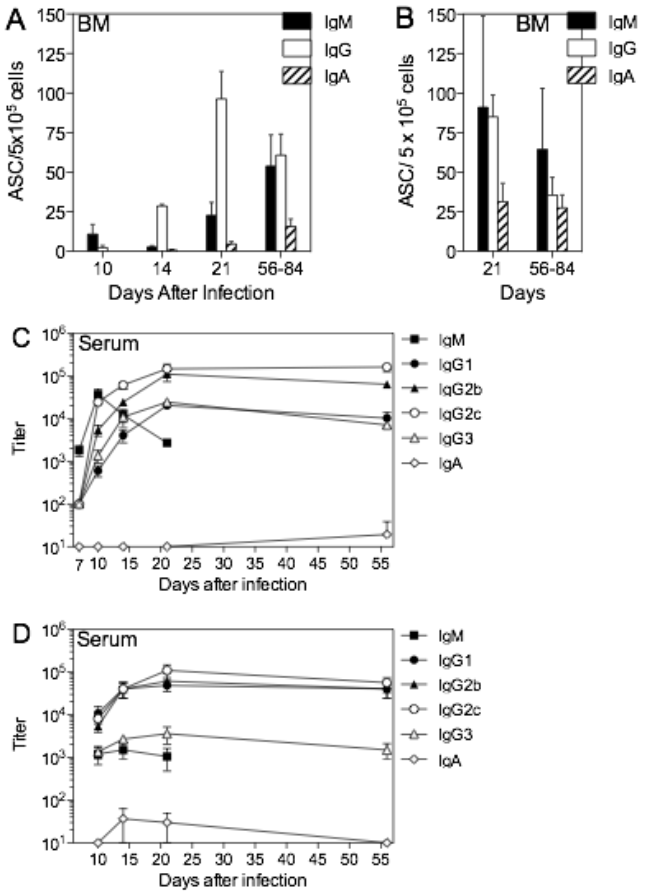

Figure 2.3. Circulating virus-specific B cell response. The kinetics of MHV-68-specific ASC response in BM (A) was determined following MHV-68 infection and compared with a limited NC-specific ASC analysis in BM (B). ELISPOT assay was performed on cell suspensions derived from individual mice and numbers of cells producing virus-specific IgM, IgG, and IgA were determined. Results are expressed as a frequency of ASCs per $5x10^5$ nucleated cells. The mean + SE is shown for five to thirteen individual mice. The kinetic analysis of virus-specific IgM, IgG1, IgG2b, IgG2c, IgG3 and IgA serum Ab levels were determined following intranasal infection with MHV-68 (C) and NC (D). ELISA assay was performed to determine virus- specific titers by end-point titration. The mean + SE is shown for four individual mice.

Figure 2.4. Virus-specific B cells localization in the RT during the acute phase of infection. The kinetics of MHV-68 -specific ASCs in the NM (A) and lung (C) was determined by ELISPOT assay. The analysis was compared with the NC-specific ASCs in the NM (B) and lung (D) on day 21 post infection. The mean + SE for lung is shown for three to ten individual mice. The mean + SE for NM is shown for three to five sets of pooled samples from individual infected mice. The samples were analyzed as described in legend to figure 1. Following infection with MHV-68 or NC infection, ELISA assay was performed to determine the levels of MHV-68-specific Ab levels in the NW (E) and LW (G,I) and NC-specific Ab levels in the NW (F) and LW (H,J). The mean + SE is shown for five to thirteen individual mice. The samples were analyzed as described in legend to figure 2.

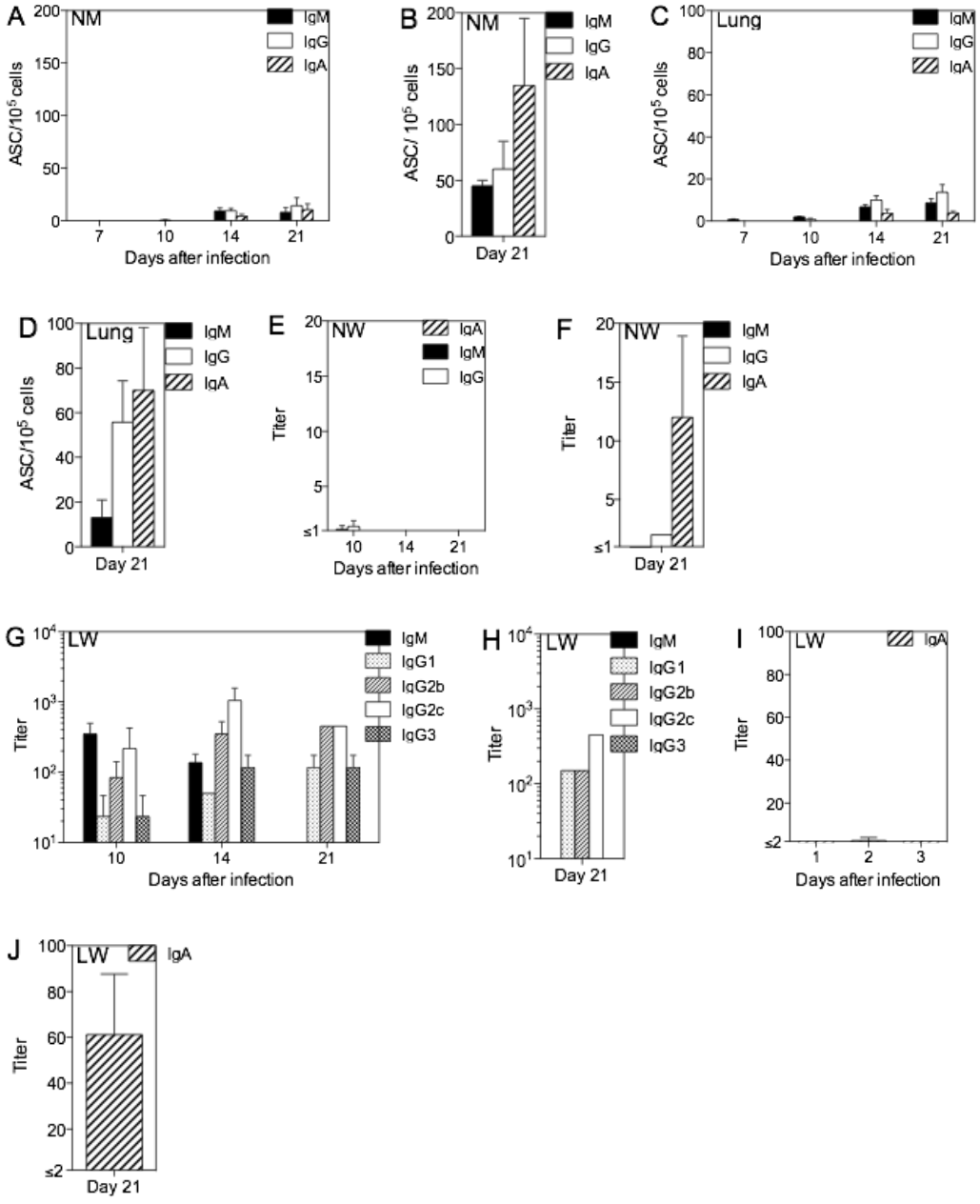
A
NM
IgM
IgG
IgA
ASC/10^5 cells
Days after infection
B
NM
Day 21
C
Lung
D
Lung
E
NW
Titer
F
NW
G
LW
IgG1
IgG2b
IgG2c
IgG3
H
LW
I
LW
J
LW

Figure 2.5. Virus-specific B cells localization in the respiratory tract during the memory phase. 56-84 days after infection, the virus -specific ASCs in the NM (A) and lung (B) was determined by ELISPOT assay following intranasal infection with MHV-68 or NC. Results are expressed as a frequency of ASCs determined per animal. ELISA assay was performed to determine the levels of MHV-68-specific Ablevels in the NW (C) and LW (E, G) and NC-specific Ab levels in the NW (D) and LW (F, H) following infection with MHV-68 or NC respectively. The mean + SE is shown for three to six individual mice. The samples were analyzed as described in legend to figure 2.

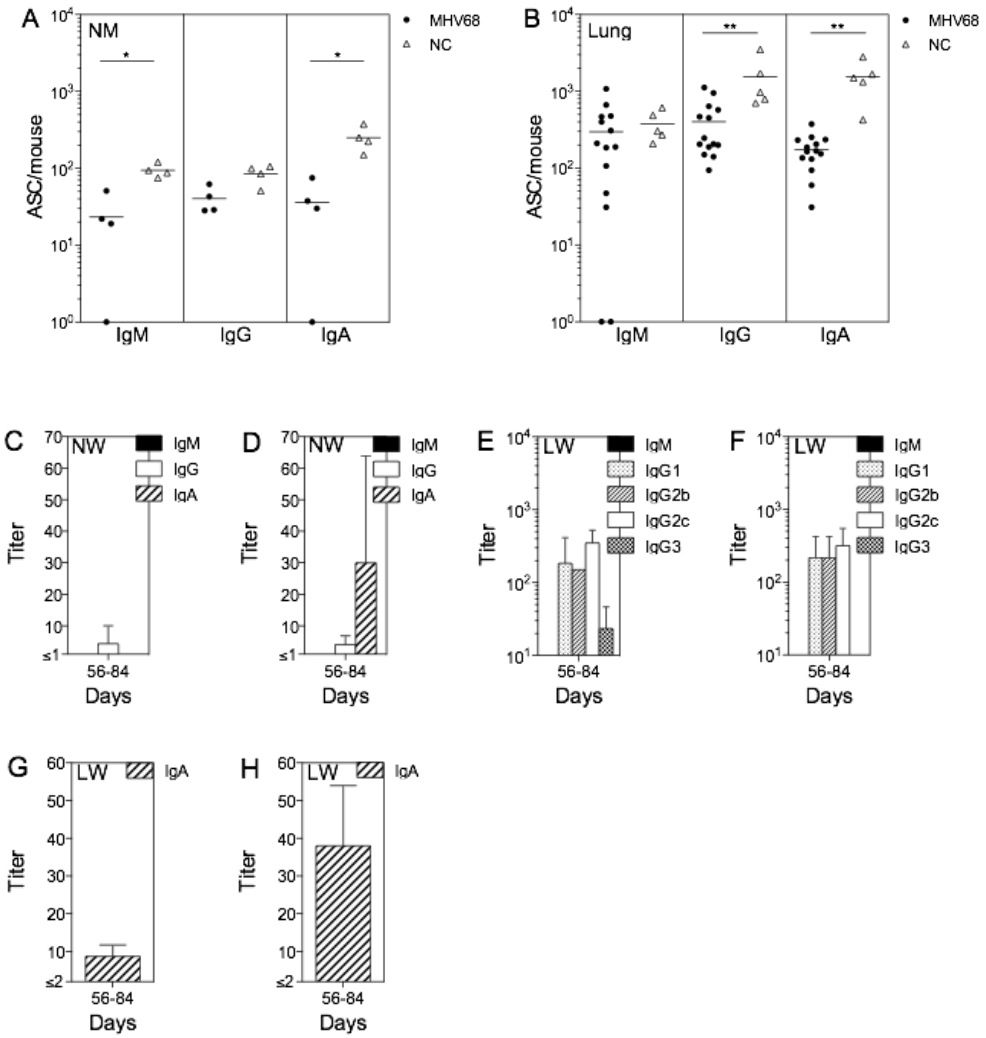
A
NM
MHV68
NC
ASC/mouse
IgM
IgG
IgA
B
Lung
C
NW
Titer
Days
56-84
D
E
LW
IgG1
IgG2b
IgG2c
IgG3
F
G
H

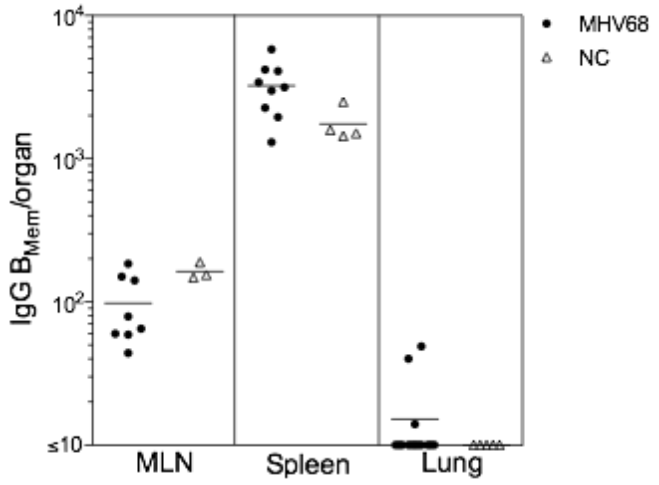

Figure 2.6. Quantitative analysis of virus-specific IgG B_{mem} in the MLN, spleen and lung. B6 mice were sampled 8-12 wk after i.n. infection with MHV-68 or NC. IgG B_{Mem} frequencies are expressed as proportions per organ, determined by LDA based on *in vitro* stimulation of B_{Mem} by inactivated virus to differentiate into ASCs. The stimulation was carried out by incubating B_{Mem} with 0.1µg of inactivated virus. The scatter of the data with the mean is shown.

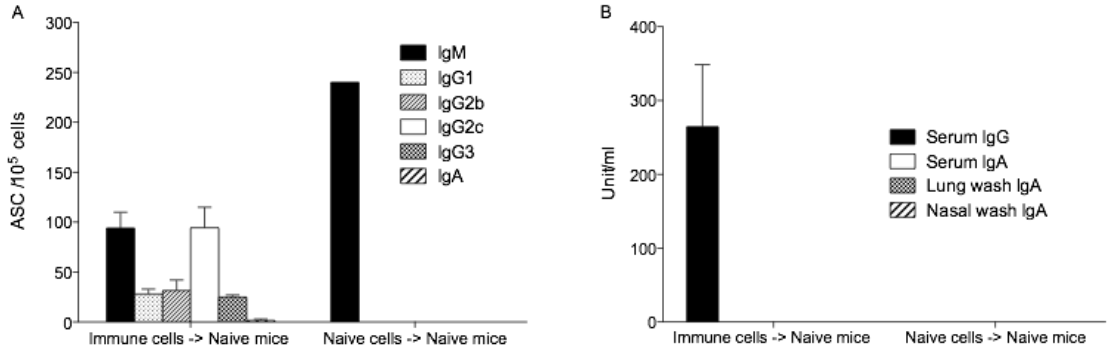

Figure 2.7. MHV-68-specific secondary B cell response. Splenocytes from MHV-68 immune B6 mice or naïve B6 mice were adoptively transferred into irradiated (400 rad) naïve B6 mice. Each mouse, $3x10^7$ cells were transferred via i.p and i.v routes. Following the transfer, the recipient mice were i.n. infected with 10,000 PFU of MHV-68. 7 days after infection, the recipient mice were sampled and the frequency of MHV-68-specific ASCs was determined by ELISPOT assay in the MLN (A). Results are expressed as a frequency of ASCs per 10^5 nucleated cells. The level of MHV-68-specific Abs in the serum, nasal wash and lung wash on day 7 post-infection was determined by ELISA assay (B). The concentrations of Abs were determined by standard curves generated by using purified mouse immunoglobulin standards. The mean + SE is shown for three individual mice.

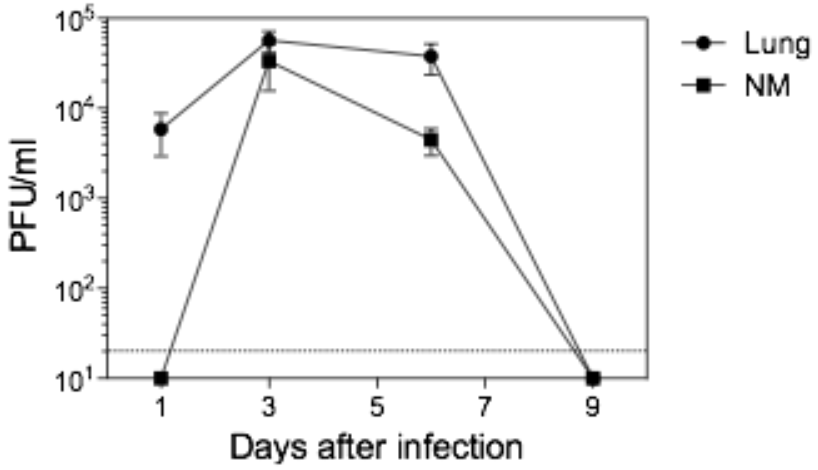

Figure 2.8. MHV-68 replication in the upper and lower respiratory tract. B6 mice were infected with 10,000 PFU of MHV-68 i.n. and at indicated times after infection, lungs and NM were harvested and virus titers determined in the homogenates by plaque assay on NIH3T3 cells. The horizontal dotted line indicates the sensitivity of the assay, determined as 20 PFU/ml. The mean + SE is shown for three to six individual mice.

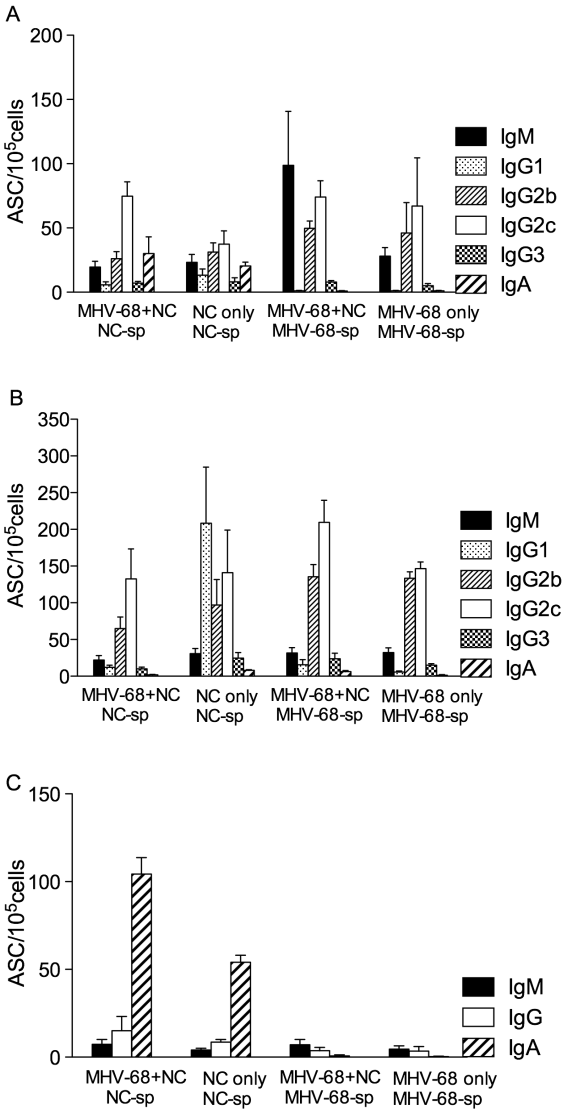

Figure 2.9. Virus-specific B cell response following co-infection of MHV-68 and NC. B6 mice were infected i.n. with 10,000 PFU OF MHV-68 and after four hours, infected with 40,000 EID_{50} of NC. The ASC response in the CLN (A), MLN (B), o-NALT (C) is shown. The ELISPOT assay for CLN and MLN was performed on cell suspensions derived from individual mice and for o-NALT on pooled samples from three mice. Results are expressed as a frequency of ASCs per 10^5 nucleated cells. The mean + SE for the CLN and MLN is shown for three to four individual mice.

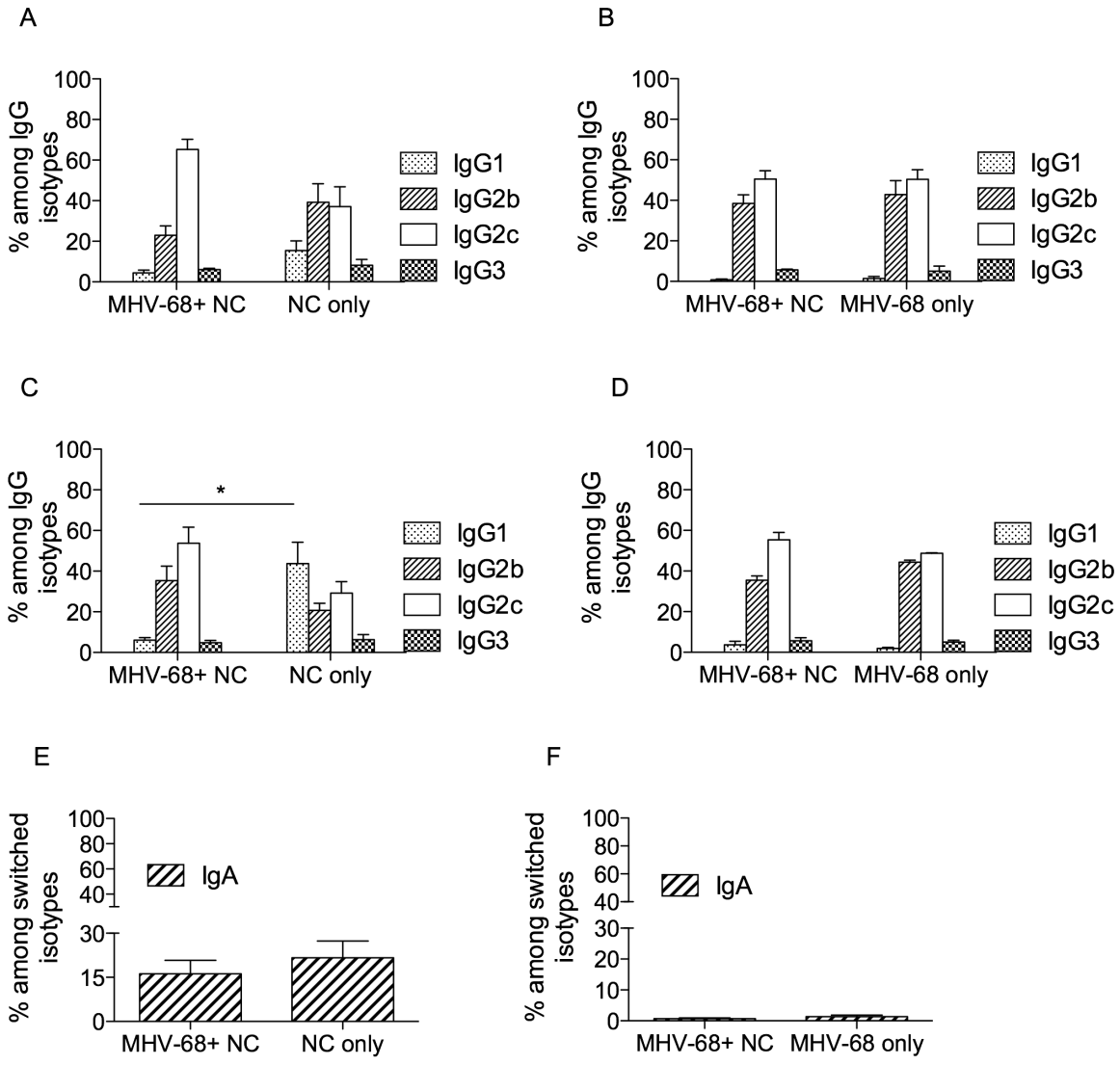

Figure 2.10. Proportions of isotype-switched virus-specific B cells following MHV-68 and NC co-infection. NC-specific ASC response in the CLN (A), MLN (C) and in the oNALT (E) is shown. MHV-68-specific ASC response in the CLN (B), MLN (D) and in the oNALT (F) is shown.

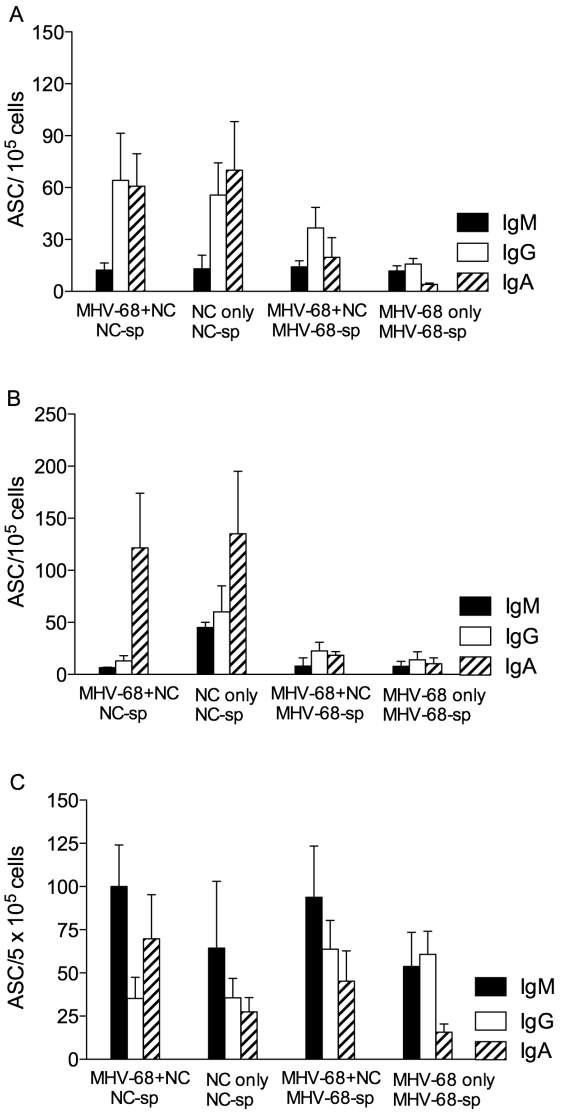

Figure 2.11. Virus-specific B cell response following co-infection of NC and MHV-68. B6 mice were infected i.n. with 40,000 EID_{50} of NC and after four hours, were infected with 10,000PFU of MHV-68. The ASC response in the lung (A), d-NALT (B), BM (C) on 34-35 days post infection is shown. The ELISPOT assay for lung and BM was performed on cell suspensions derived from individual mice and for d-NALT on sets of pooled samples from three mice. Results are expressed as a frequency of ASCs per 10^5 nucleated cells for lung and d-NALT and as ASCs per $5x10^5$ nucleated cells for BM. The mean + SE for lung, d-NALT and BM is shown for three to seven individual mice.

Figure 2.12. Virus-specific B cell response following co-infection of MHV-68 and X-31. B6 mice were infected i.n. with MHV-68 and after two days, infected with X-31. X-31-specific ASC response in the co-infected mice are indicated as follows; CLN (A), MLN (B), oNALT (C), dNALT (I). X-31-specific ASC response in X-31 alone-infected mice are indicated as follows; CLN (G), MLN (H). MHV-68-specific ASC response in the co-infected mice are indicated as follows; CLN (D), MLN (E), oNALT (F). The ELISPOT assay for CLN and MLN was performed on cell suspensions derived from individual mice and for o-NALT on pooled samples from three mice. The mean + SE for the CLN and MLN is shown for three to eight individual mice.

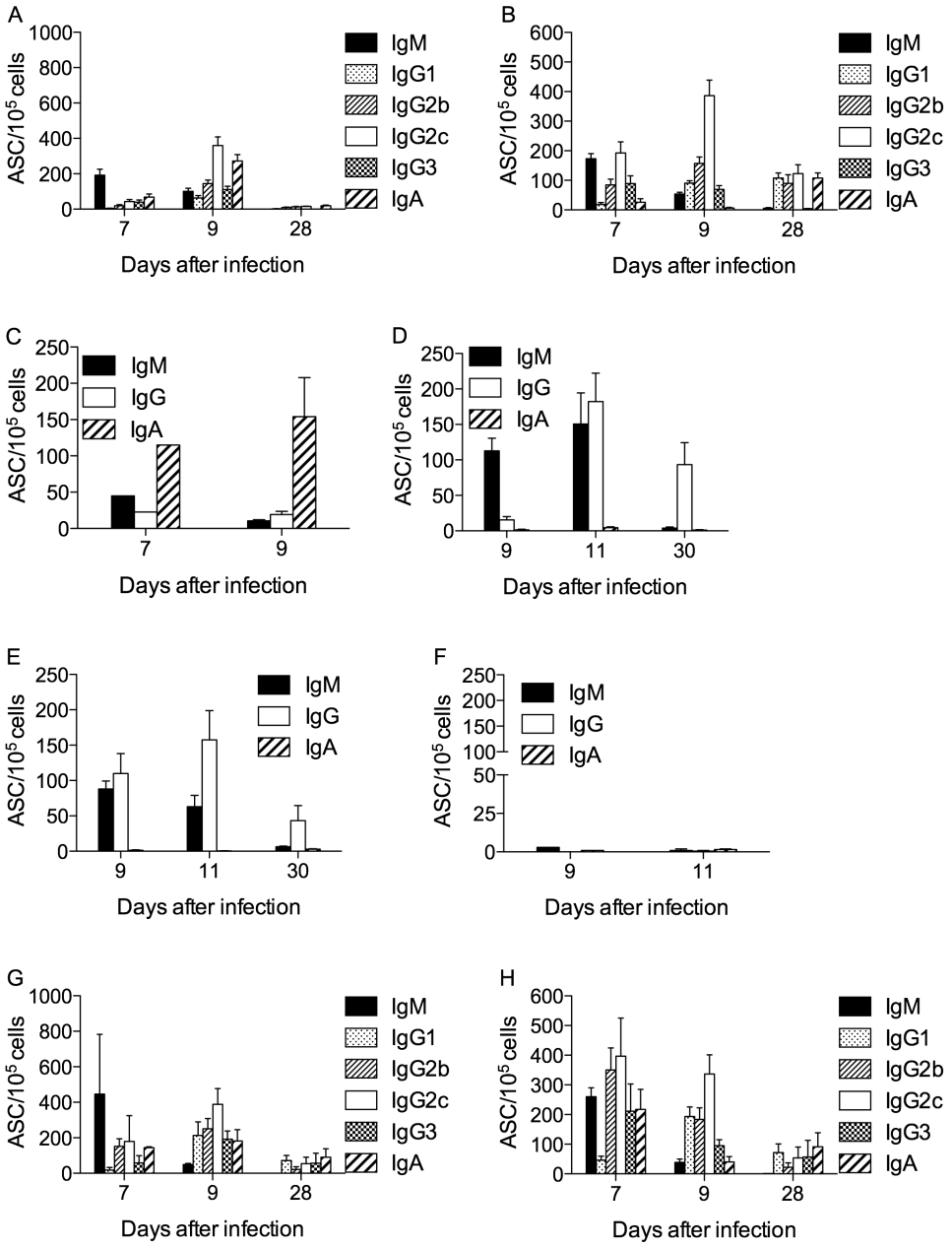
A
ASC/10^5 cells
1000
800
600
400
200
0
7
9
28
Days after infection
IgM
IgG1
IgG2b
IgG2c
IgG3
IgA
B
ASC/10^5 cells
600
500
400
300
200
100
0
7
9
28
Days after infection
IgM
IgG1
IgG2b
IgG2c
IgG3
IgA
C
ASC/10^5 cells
250
200
150
100
50
0
7
9
Days after infection
IgM
IgG
IgA
D
ASC/10^5 cells
250
200
150
100
50
0
9
11
30
Days after infection
IgM
IgG
IgA
E
ASC/10^5 cells
250
200
150
100
50
0
9
11
30
Days after infection
IgM
IgG
IgA
F
ASC/10^5 cells
250
200
150
100
50
25
0
9
11
Days after infection
IgM
IgG
IgA
G
ASC/10^5 cells
1000
800
600
400
200
0
7
9
28
Days after infection
IgM
IgG1
IgG2b
IgG2c
IgG3
IgA
H
ASC/10^5 cells
600
500
400
300
200
100
0
7
9
28
Days after infection
IgM
IgG1
IgG2b
IgG2c
IgG3
IgA

Figure 2.13. Proportions of isotype-switched virus-specific B cells following MHV-68 and X-31 co-infection. X-31-specific IgG1 response is down regulated, while IgG2c response is enhanced following MHV-68 and X-31 co-infection. The X-31-specific ASC response in the CLN (A), MLN (B) and in the oNALT (C) is shown. Results are shown for three to eight individual mice. The co-infected mice were sampled on day 11-post MHV-68/ day 9-post X-31 infection and the X-31 only infected mice sampled on day 9 post X-31 infection.

A

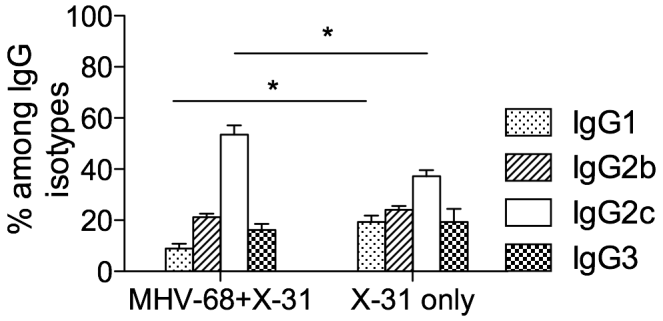
100
80
60
40
20
0
% among IgG isotypes
*
*
IgG1
IgG2b
IgG2c
IgG3
MHV-68+X-31
X-31 only

B

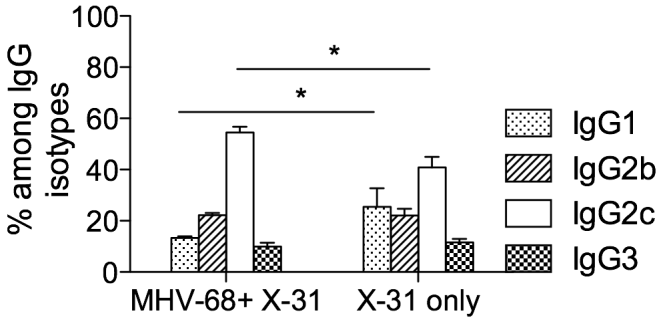
100
80
60
40
20
0
% among IgG isotypes
*
*
IgG1
IgG2b
IgG2c
IgG3
MHV-68+ X-31
X-31 only

C

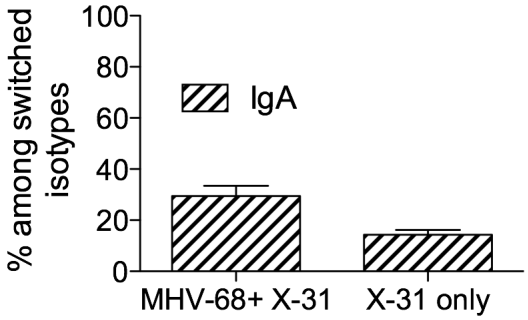
100
80
60
40
20
0
% among switched isotypes
IgA
MHV-68+ X-31
X-31 only

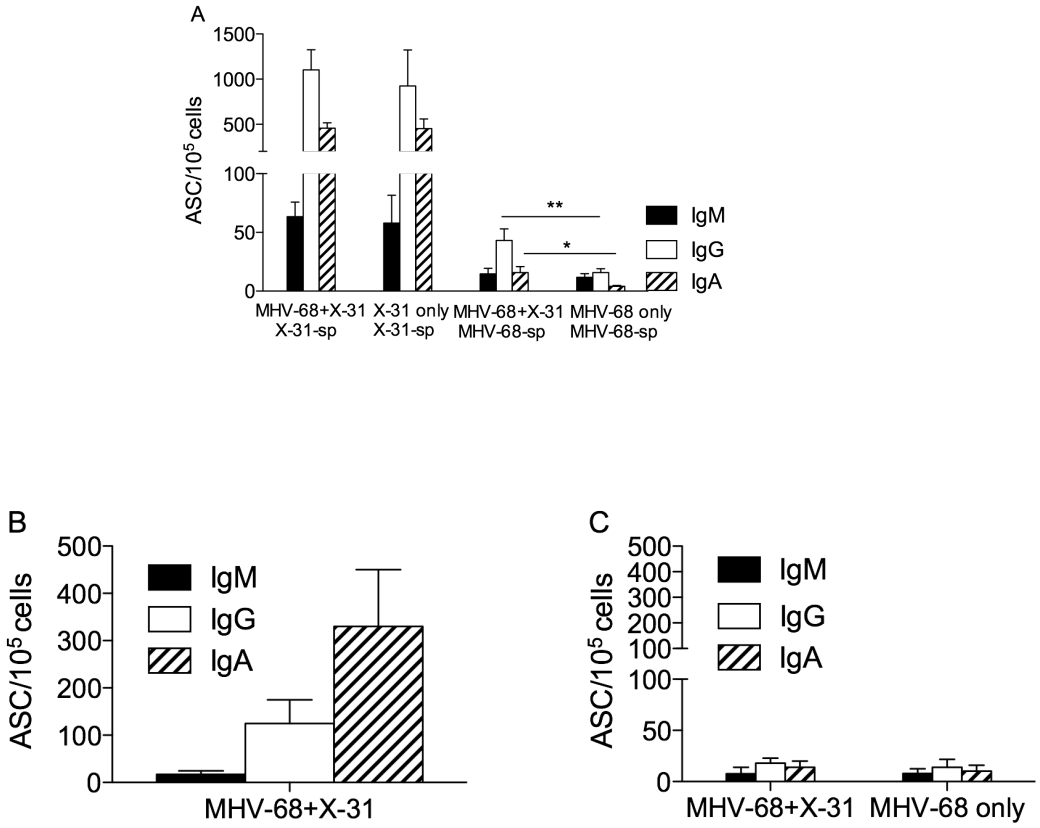

Figure 2.14. Virus-specific B cell response following co-infection of MHV-68 and X-31. Virus-specific ASC response in the lung (A) on day 30 post MHV-68 infection/day 28 post X-31 infection, comparing co-infected and respective single infected mice is shown. X-31-specific ASC response in the dNALT (B) of co-infected mice on day 28 post infection is shown. MHV-68-specific ASC response in the dNALT (C), comparing co-infected and MHV-68 alone on day 30 post-infection is shown. The ELISPOT assay for lung was performed on cell suspensions derived from individual mice and for dNALT on sets of pooled samples from three mice. The mean + SE for lung dNALT is shown for three to twelve individual mice. Results are expressed as a frequency of ASCs per 10^5 nucleated cells.

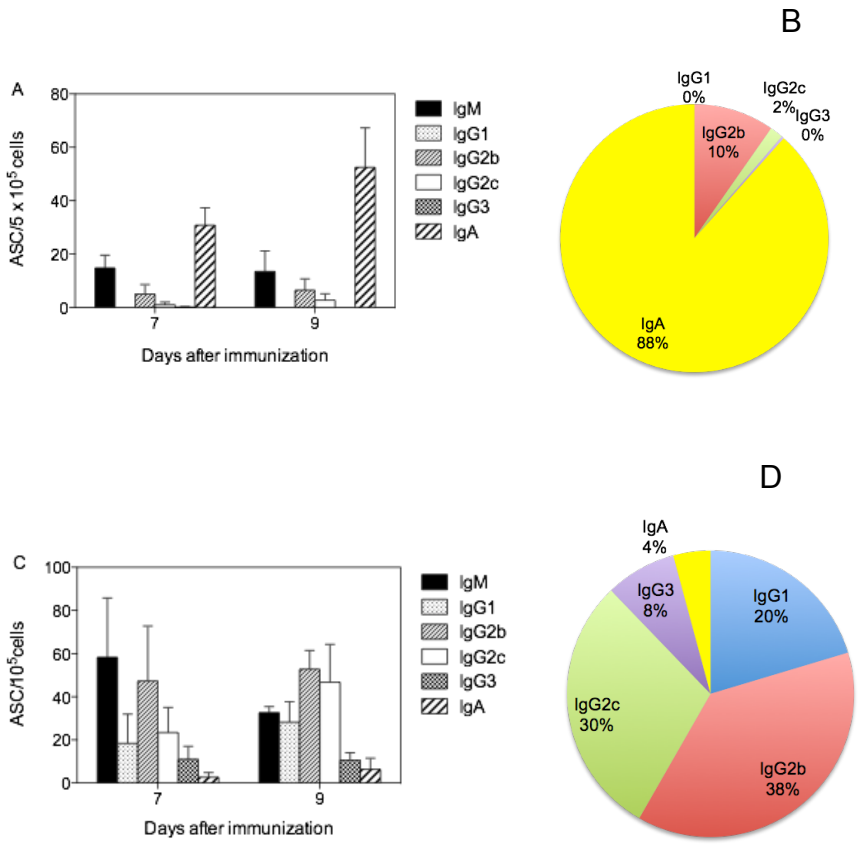

Figure 2.15. MHV-68-specific B cell response to inactivated virus. C57BL/6 mice were i.n. administered with 30µg of UV-inactivated MHV-68. The MHV-68 -specific B cell response was determined by ELISPOT assay in the CLN (A) and in the MLN (C). Results in the CLN are expressed as a frequency of $5x10^5$ of nucleated cells and in the MLN as a frequency of 10^5 nucleated cells. The proportions of isotype switched virus-specific ASCs in the CLN (B) and MLN (D) are shown. The mean + SE is shown for three to six individual mice.

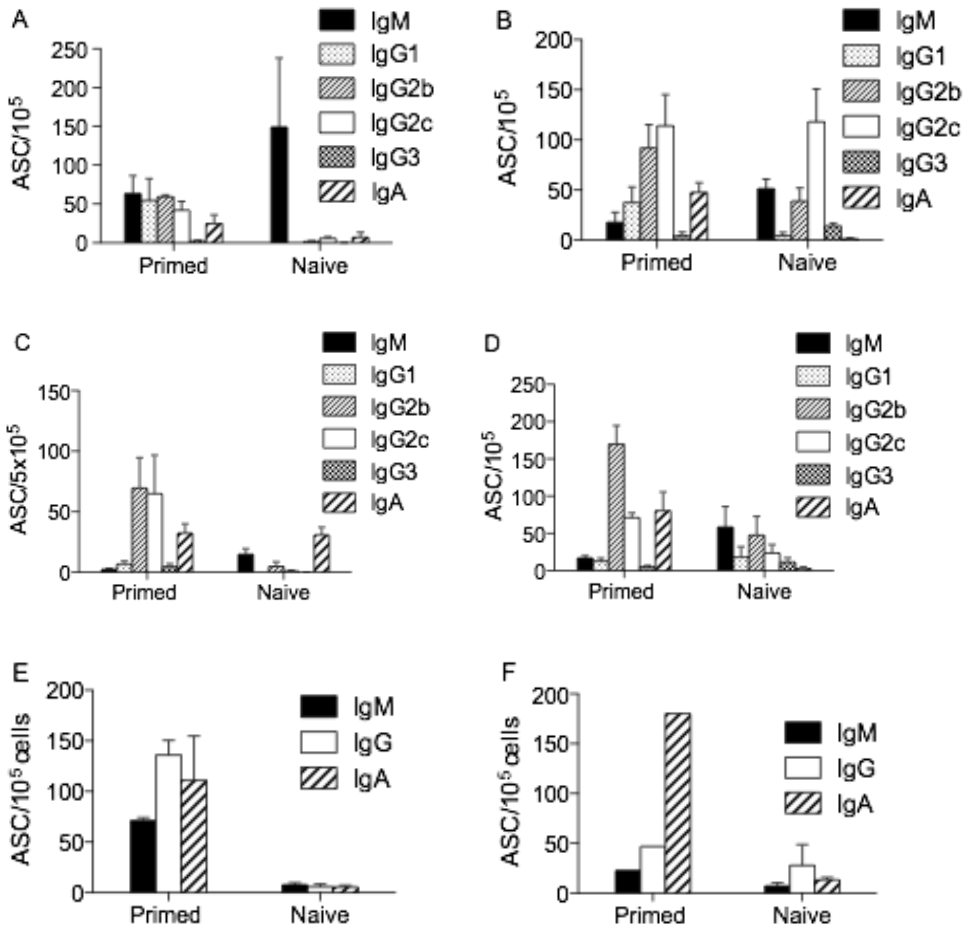

Figure 2.16. MHV-68-specific secondary B cell response following priming with inactivated MHV-68. 3 wks post i.n. immunization of B6 mice with 30µg of inactivated MHV-68, the mice were either challenged with $2x10^5$ PFU of MHV-68 or boosted with 30µg of inactivated MHV-68. MHV-68-specific B cell response in CLN (A), MLN (B) following challenge with the live virus is shown. Results are expressed as a frequency of 10^5 cells. The mean + SE is shown for four individual mice. The MHV-68 -specific response in the CLN (C), MLN (D), lung (E) and d-NALT (F) following challenge with the inactivated virus was determined. As a result of a weaker B cell response, results in CLN are expressed as a frequency of $5x10^5$ cells, and results in other sites are expressed as a frequency of 10^5 cells. The mean + SE for CLN, MLN and lung is shown for three to seven individual mice.

Figure 2.17. Virus-specific B cell response to γHV68Δ9473. B6 mice were i.n. administered with $4x10^5$ PFU of γHV68Δ9473 or WT γHV68. The frequencies of MHV-68- specific ASCs following γHV68Δ9473 infection in the CLN (A) and MLN (C) is shown. For comparison, MHV-68-specific B cell response to WT γHV68 in the CLN (B) and in the MLN (D) was determined. In addition, comparison of frequencies of MHV-68-specific ASCs following γHV68Δ9473 or WT γHV68 infection was determined in the o-NALT on day 10 post-infection (E), lung (F) and in the d-NALT (G) on day 21 post infection. Results are expressed as ASCs per 10^5 nucleated cells, determined by ELISPOT assay. The mean + SE for MLN, CLN and lung samples are shown for four to eight individual mice. The mean + SE for o-NALT and d-NALT is shown for three sets of pooled samples.

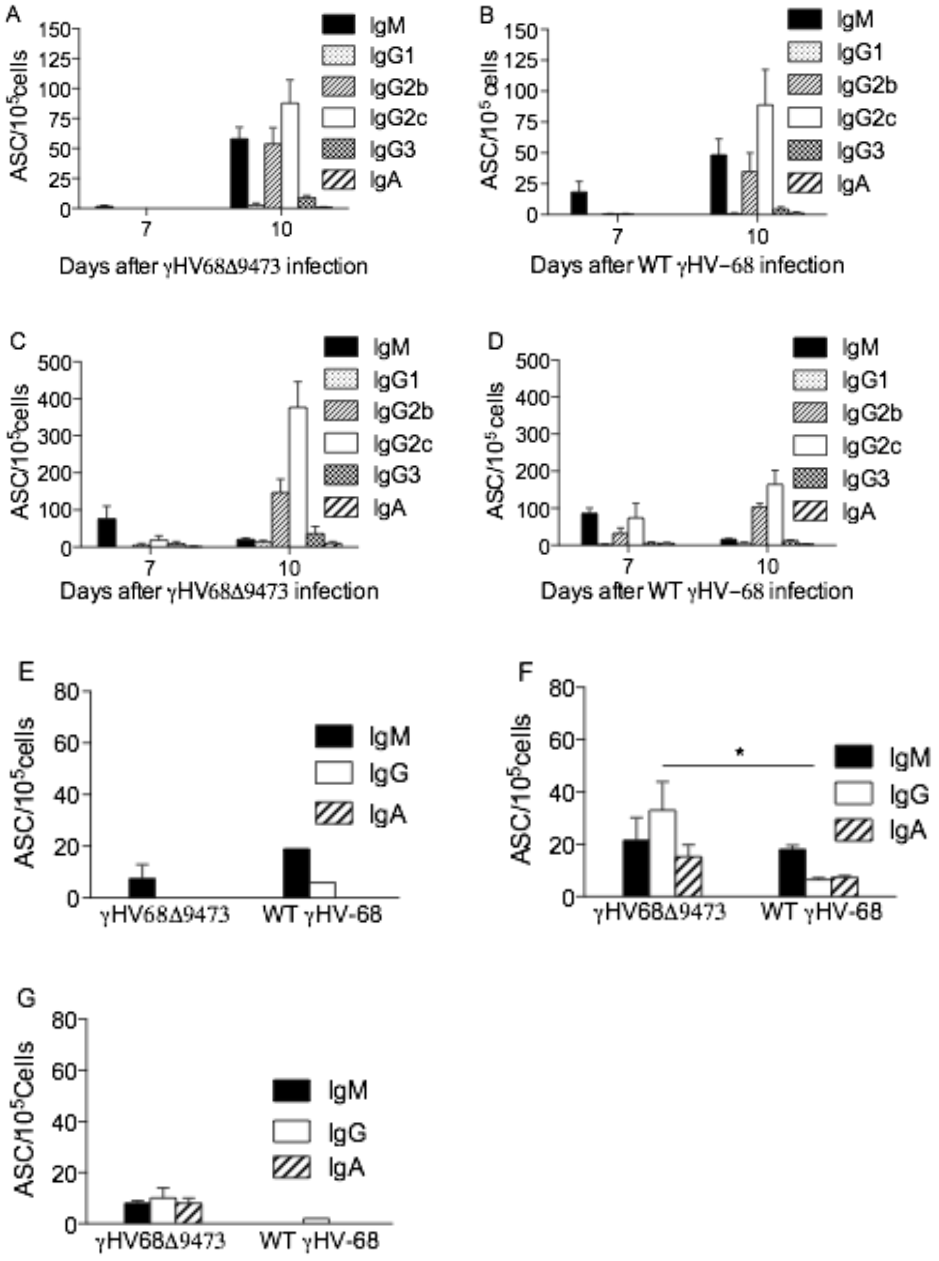
A
ASC/10^5cells
150
125
100
75
50
25
0
7
10
Days after γHV68Δ9473 infection
IgM
IgG1
IgG2b
IgG2c
IgG3
IgA
B
ASC/10^5 cells
Days after WT γHV−68 infection
C
ASC/10^5cells
500
400
300
200
100
Days after γHV68Δ9473 infection
D
Days after WT γHV−68 infection
E
ASC/10^5cells
80
60
40
20
IgM
IgG
IgA
γHV68Δ9473
WT γHV-68
F
*
G
ASC/10^5Cells

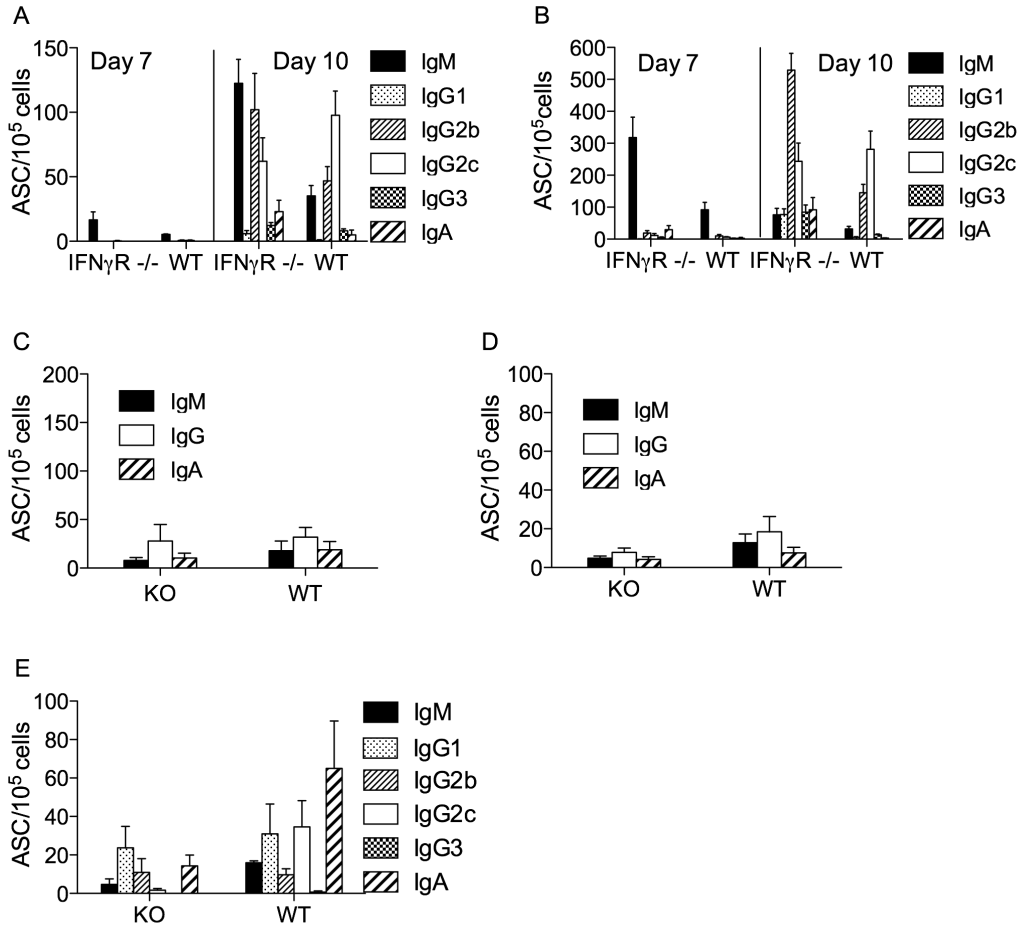

Figure 2.18. MHV-68-specific B cell response in the IFN-γR-/- mice. B6.129S7-Ifngr1^{tm1Agt}/J (designated as IFNγR-/-) and the background strain, B6 mice (designated as WT) were i.n. administered with 10^4 PFU of MHV-68. The frequencies of MHV-68-specific ASCs were determined by ELISPOT assay on the cell-suspensions derived from CLN (A), MLN (B), dNALT(C) and lung (D). The frequencies of NC-specific ASCs in the lung (E) are shown. The lung and d-NALT analysis were carried out on day 21-26-post infection. Results are expressed as ASCs per 10^5 nucleated cells. The mean + SE for MLN, CLN and lung samples are shown for three to six individual mice. The mean + SE for d-NALT is shown for three sets of pooled samples.

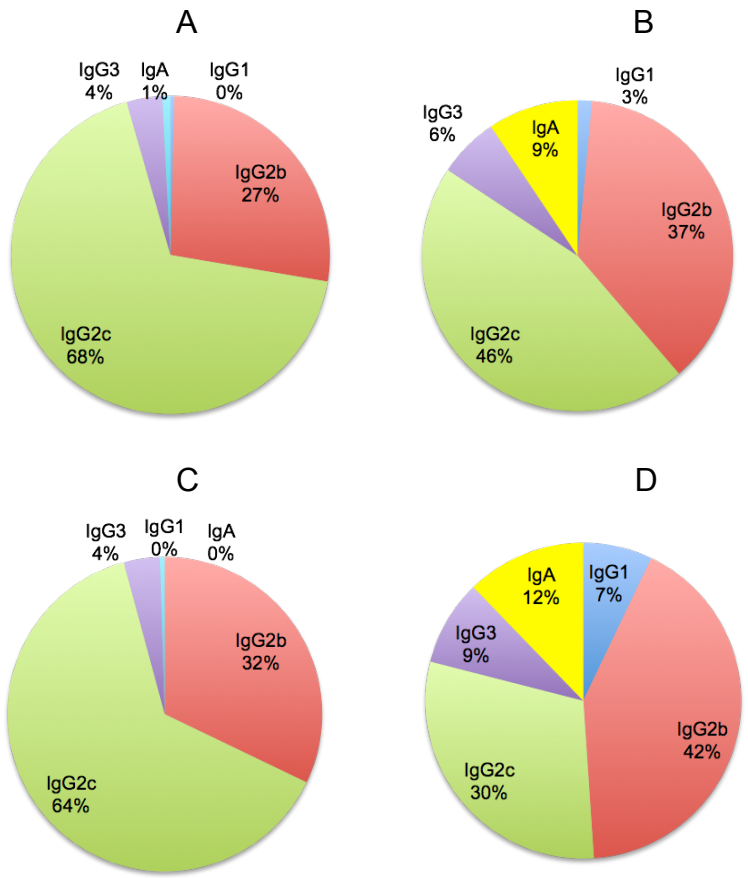

Figure 2.19. Proportion of class-switched MHV-68-specific ASCs in the IFN-γR-/- mice. Responses in the CLN and MLN following infection in the WT mice (A & C respectively) and IFN-γR-/- mice (B & D respectively) are shown.

Chapter 3

Regulation of B cell response to influenza virus following infection of the respiratory tract

Introduction

Studies of mouse models of influenza A virus infection have produced a comprehensive picture of disease pathogenesis and the innate and adaptive antiviral mechanisms that contribute to viral clearance and recovery [220-221]. The initial phase of influenza virus replication in epithelial cells of the upper and lower respiratory tract, as well as viral targeting of local macrophages and dendritic cells, triggers the rapid release of a range of cytokines and chemokines with antiviral and pro-inflammatory activity [188]. In addition to limiting viral replication in the respiratory tract, these processes are critical for the optimal activation of Ag-specific B and T cells and the development of adaptive immunity. The ultimate elimination of infectious virus from the respiratory tract is dependent on B and T cell-mediated mechanisms, such as the destruction of virus-infected cells by infiltrating cytotoxic CD8 T cells, and the antiviral activity of progressively increasing antibody levels [250-251].

Optimal virus-specific antibody production following influenza infection in the mouse is dependent on CD4 T cell help for B cells [252]. Although some antiviral antibodies can be generated in the absence of CD4 T cells, antibody production is substantially more vigorous and effective following collaborative interactions between CD4 T cells and B cells [210]. CD4 T cells provide cognate signals and secreted factors that drive B cell activation and differentiation and induce antibody isotype switching. After cognate interactions of peptide:MHC class II (MHC II)-bearing B cells with CD4 T cells, activated B cells may differentiate via the extrafollicular pathway to rapidly generate a population of short-lived virus-specific antibody-secreting cells (ASCs) [19],

or they may enter B cell follicles and initiate germinal center reactions where long-lasting populations of ASCs and memory B cells expressing high affinity antiviral antibody are formed [253] . The progression of B cells through the germinal center reaction is dependent on a second phase of a cognate T cell help delivered by follicular helper T cells [254]. Regulation of the differentiation options available to B cells responding to influenza infection is not well understood. In addition, little is known about the relationship between the repertoire and quality of the influenza-specific CD4 T cell response and the provision of cognate help for an optimally effective B cell response.

Recently, the influenza-specific CD4 T cell response was comprehensively characterized in HLA-DR1 transgenic (DR1) mice, which express as a transgene a hybrid MHC II molecule consisting of the peptide-binding domain of human HLA-DR1 and a membrane-proximal region of mouse origin [255]. Infection of DR1 mice with A/New Caledonia/20/99 (NC) (H1N1) resulted in a virus-specific CD4 T cell response that was predominantly restricted to the transgenic MHC II molecule. The response repertoire was exceptionally broad and included multiple strong epitopes in the four viral proteins analyzed: HA, NA, NP, and nonstructural protein 1 (NS1) [256]. Although initially used as a tool for the identification of MHC II-restricted epitopes that may be relevant to responses in humans, DR1 mice now provide a model that is well-characterized at the level of CD4 T cell responses to a recently circulating influenza virus.

In the current study, the virus-specific B cell response in DR1 mice following NC infection was analyzed as a step towards relating characteristics of the influenza-specific CD4 T cell response to B cell response parameters and the effective production of antiviral antibodies. C57BL/10 (B10) mice, which share the non-MHC genetic background of DR1 mice and provide a contrasting CD4 T cell response pattern, were included for comparison. Whereas the NC-specific CD4 T cell repertoire in DR1 Tg mice, as described above, was particularly broad, B10 mice displayed a much narrower repertoire with fewer epitopes largely confined to the NA and NP. We demonstrate striking differences between DR1 and B10 mice in the virus-specific B cell response to NC infection. These differences were substantially diminished when different influenza

strains were used for infection and by non-specific effects during concurrent infection with NC and an unrelated virus. Overall, our findings indicate that the nature/quality of the extrafollicular B cell response depends on the nature of the infecting virus. We present evidence that this pathway of rapid antiviral antibody production relates to the production of non-specifically acting factors in the lung and correlates with the cytokine profile of virus-specific CD4 T cells.

Materials and Methods

Viruses

Influenza A viruses, A/New Caledonia/99 virus (NC) and A/Puerto Rico/8/1934 virus (PR8) were grown in the allantoic cavity of embryonated hen's eggs. Purified NC (obtained from Dr.Richard Webby, St.Jude Children's hospital, Memphis) and purified PR8 was used for immunoassays. MHV-68, a gammaherpesvirus (clone G2.4) was grown in owl monkey kidney cells and the stock titer was determined by plaque assay on NIH3T3 cells. Purified MHV-68 used for the immunoassays was prepared by sucrose density gradient centrifugation (collected at the interface of 30% and 60% sucrose gradients).The protein estimation in the purified virus was estimated by the Bradford assay [223]. Purified HA (Protein Sciences Corp. Meriden, CT) and purified NP (provided by Dr. Andrea Sant, University of Rochester, Rochester) were used in some of the immunoassays.

Mice

The HLA-DR1 transgenic mice (B10.M/J-TgN-DR1) [255] were obtained from D. Zaller (Merck) through Taconic laboratories and were maintained in the pathogen-free facility at the University of Tennessee according to institutional guidelines. These mice express a chimeric HLA-DR1 class II molecule, whose peptide binding domain is derived from human HLA-DR1, while the membrane proximal domains are derived from

murine I-E. This design facilitates interaction with murine CD4 T cells. For comparison, B10 mice (C57BL/10) were purchased from the Jackson Laboratory (Bar Harbor, ME). Mice were housed under pathogen-free conditions and after virus infection, were housed in BSL2-level containment. Females were used in all experiments and were infected at the age of 8-12 wk of age. The Animal Care and Use Committee of the University of Tennessee approved animal procedures.

Infection and sampling

Mice were anesthetized i.p. with Avertin (2,2,2-tribromoethanol), followed by i.n. infection with viruses in 30μl of Dulbecco's PBS. NC was administered at 40,000 $EID_{50,}$ PR8 at $25EID_{50,}$ MHV-68 at 10,000 PFU [183], unless indicated. The anaesthetized mice were exsanguinated via the retroorbital plexus before tissue sampling. The right posterior mediastinal lymph node (MLN), spleen were collected and gently disrupted between frosted ends of microscope slides to generate single-cell-suspensions. The cells were re-suspended in IMDM (Invitrogen) containing L-glutamine (2 mM), sodium pyruvate (1 mM), penicillin (100 IU/ml), streptomycin (100 μg/ml), gentamycin (10 μg/ml), $5x10^{-5}$ M β-mercaptoethanol and 10% FCS (Complete medium). Bone marrow (BM) cell suspensions were obtained by flushing femurs and tibiae. This was followed by RBC removal by using RBC lysis buffer (Sigma). Lungs were perfused with cold Dulbecco's PBS, followed by fine mincing and incubation for 1hr at 37°C in complete medium that contained 4 mg/ml collagenase type II (Invitrogen). The cells from the lung were resuspended in 40% isotonic Percoll and gently layered over 75% isotonic Percoll (GE healthcare). The cells layered over the gradient was centrifuged at 2000 rpm for 20 min at 25°C and the cells at the interface of 40% and 75% isotonic Percoll was collected and washed with complete medium. Sera were collected from clotted blood.

ELISPOT assay for B cells

The virus- specific ASCs were determined by ELISPOT assay as described previously [183]. Briefly, purified virus was detergent disrupted, and plated at 1 μg/100μl/well in a 96- well multiscreen HA filter plates (Millipore). Following overnight incubation at 4°C, the plates were washed with PBS and blocked with complete medium for 1hr, 37°C, 5% CO_2. 5X serial dilutions of cell suspensions were prepared in complete medium, and 100μl of the cells were added to the washed plates, beginning with 10^5 cells/well, unless indicated. The plates were incubated for 4 hrs, 37°C, 5% CO_2. This was followed by washes with Dulbecco's PBS and 0.1% Tween-PBS. Alkaline phosphatase (ALP) conjugated isotype-specific goat anti-mouse Abs (Southern biotech) were diluted 1/500 in 5% BSA-PBS and added as 100μl/well, followed by overnight incubation at 4°C. After washing both sides of the plate, spots were developed at room temperature with 1 mg/ml of 5-bromo-4-chloro-3-indolyl phosphate (Sigma) in diethanolamine buffer. Thereafter, the plates were washed and dried. Each spot represents an antibody-secreting cell, and were enumerated visually by using an Olympus SZX9 microscope.

ELISA assay

The virus-specific Abs was determined by ELISA assay as described previously [183]. Briefly, purified virus was detergent disrupted, and plated at 0.25 μg/ 50 μl/well in a 96-well Nunc ImmunoMaxiSorp plates (Fisher-scientific). For HA and NP- specific Ab detection, the required concentrations of these proteins were dissolved in PBS and directly added to the plates. Following overnight incubation at 4°C, the plates were washed with 0.05% Tween-PBS and blocked with 3% BSA-PBS for 90 min at room temperature. Serial dilutions of serum or nasal wash (NW) or lung wash (LW) samples were prepared in 0.1% BSA-0.05%Tween-PBS, and 50 μl of the dilutions were added to the washed plates. The plates were incubated for 4hrs at room temperature and followed by washes. Alkaline phosphatase (ALP) conjugated isotype-specific goat anti-mouse Abs (Southern biotech) were diluted 1/600 to 1/1000 in 1% BSA-PBS and added

as 100μl/well, followed by overnight incubation at 4°C. After washing the wells, the plates were developed with *p*-nitrophenyl phosphate (Sigma) in diethanolamine buffer. After 20 min, absorbance at 405nm was read using a *Vmax* kinetic microplate reader (Molecular devices). The virus- specific Ab titer is expressed as the reciprocal of the highest dilution that gave an absorbance value more than twice that for the samples from naive mice. For some experiments, concentrations of Abs were calculated from standard curves based on purified mouse Ig standards (Southern biotech).

HA- specific Antibody affinity ELISA

This is a modified ELISA assay, based on Sodium thiocyanate (NaSCN) displacement of low-affinity Abs. Through titration of sera in the presence of various concentrations of NaSCN (Sigma), a discriminating concentration of 0.75M NaSCN was identified (data not shown). Briefly, the dilutions of sera were incubated in the HA-coated wells. This was followed by addition of 0.75M NaSCN or PBS (as a control) to the wells, and 15 min incubation at RT was carried out. This was followed by washes, and incubation for 2 hrs at RT in the presence of ALP-conjugated IgG goat anti-mouse Ab (Southern biotech). Thereafter the plates were developed as described above, and read using a *Vmax* kinetic microplate reader (Molecular devices). A standard curve based on purified mouse Ig standards (Southern biotech) was used for the calculation of concentrations of Abs in the sera. This was followed by calculation of Avidity index (AI). AI = Concentration of Abs with NaSCN/Concentration of Abs without NaSCN x 100.

Flow cytometry

The cells derived from MLN were stained with the appropriate combination of FITC-labeled PNA (Vector laboratories), Alexa-647-labeled anti-FAS (BD biosciences), PE (Cy7)-labeled anti-CD4 (RM4-5, BD biosciences), anti-CD8 (53-6.7, ebioscience), PE (Cy5.5)-labeled anti-CD19 (eBio 1 D3, ebioscience), PerCP-labeled anti-B220 (RA3-6B2, BD biosciences), APC labeled anti-CD138 (281-2, BD biosciences) after blocking of the Fc receptor with naive serum at 4°C. Data were acquired by using LSR II (BD biosciences) and analyzed by using FloJo (Tree Star). For characterization of cells, a

gate was drawn to include lymphocyte populations from FSC Vs SSC. This was followed by removal of doublets and was gated on live cell populations using live/dead fixable aqua dead cell stain kit (Invitrogen). For identifying germinal center B cells, the cells were gated on B220+ populations, followed by gating on PNA+FAS+ cells. For identifying plasma cells, the cells were gated on B220lo/int CD138+ cells.

Cytokine production by influenza-specific CD4+ T cells analysis

Briefly, enriched CD4+ T cells from MLN were cultured in vitro with APCs and a range of class-II restricted peptide epitopes. Cytokine production was determined by ELISPOT assay after 24 hrs [256].

Statistics

The statistical comparisons of mean values were performed using non-parametric Mann-Whitney test (*p <0.05, **p <0.01).

Results

Altered NC-specific extrafollicular ASC response in DR1 mice

Initial experiments compared the virus-specific B cell response in DR1 and B10 mice following intranasal infection with the H1N1 influenza virus NC. Infection in both mouse strains was sublethal and virus was completely cleared from the lung after transient replication. Virus titers in the lung on days 1, 3, 5, and 8 after infection were similar in DR1 and B10 mice, indicating comparable Ag loads [268] A strong virus-specific IgM and IgG ASC response was evident in the draining mediastinal lymph node (MedLN) of DR1 and B10 mice on day 8, whereas IgG ASCs were essentially absent from the MedLN of DR1 mice at this time [268]. The response in the MedLN of B10

mice was typical of previously reported influenza-specific B cell responses in a range of mouse models and included a strong IgG2b and IgG2c component. In contrast, when a NC-specific IgG response developed in DR1 mice (see MedLN on day 14), it was strongly biased to IgG1 production [268] (Figure 3.1 A, B). NC-specific ASC localization in the bone marrow of DR1 and B10 mice reflected the kinetics and isotype profile of responses in lymphoid tissues [268]. Infection with a high (sublethal) dose of NC did not substantially modify the differences between DR1 and B10 mice in the characteristics of the NC-specific ASC response in the MedLN [268].

The B cell response in the MedLN after NC infection was also characterized by flow cytometry. On day 8, the percentage of $B220^+$ B cells (mean ± SD) was similar in the MedLN of DR1 and B10 mice (50.52 ± 3.398 and 50.44 ± 5.072, respectively). Contrary to the pattern for NC-specific ASCs measured by ELISPOT assay, the proportion of $B220^{int}$ $CD138^+$ phenotype of ASCs generated by the extrafollicular pathway was similar between DR1 and B10 mice (Figure 3.2 B, D). In contrast, the proportion of germinal center cells (PNA^+ Fas^+) in the $B220^+$ cell population was approximately 3-fold higher in DR1 mice, suggesting stronger germinal center activity. The proportion of germinal center B cells increased from day 8 to day 10 in B10 mice, but remained significantly lower than in DR1 mice (Figure 3.6 B, D). Depletion of CD4 T cells essentially eliminated NC-specific ASCs in the MedLN of B10 mice on day 8, establishing that the early ASC response in B10 reflected T-dependent B cell differentiation and not T-independent antibody production (Figure 3.2 E). Overall, our findings indicate more rapid generation of NC-specific isotype-switched B cell response in B10 mice that was largely absent from DR1 mice.

Discordance between ELISA measurements of NC-specific serum antibodies and virus neutralization titers

Measurement of NC-specific serum antibody levels by ELISA demonstrated a significantly more rapid IgG response in B10 compared with DR1 mice; primarily reflecting increased IgG2b, IgG2c, and IgG3 production (Figure 3.3 A-H). IgM levels did

not follow this pattern and were significantly higher in DR1 mice on days 14 and 21, perhaps reflecting the high frequency of IgM ASCs in the spleen on day 14 [268]. NC-specific serum Ig levels, which provide a measure of all antibodies with virus neutralizing potential, were significantly higher in B10 compared with DR1 mice on day 8 and similar at later sampling times [268]. Overall, ELISA measurements of NC-specific serum antibodies were consistent with the pattern of ASC generation in lymphoid tissues.

In a surprising contrast to the pattern of NC-specific serum antibody levels in DR1 and B10 mice demonstrated by ELISA, the trend was for higher early virus neutralization titers in DR1 mice [268]. This difference was particularly striking on day 14. HAI titers in DR1 and B10 mice closely paralleled the neutralization titers [268]. Since virus neutralization in vitro and inhibition of viral hemagglutination is mediated by antibodies specific for the viral HA molecule, an early antibody response in DR1 mice characterized by higher virus neutralization and HAI titers, but not higher ELISA titers of antiviral antibodies, raised the possibility of a stronger HA-specific antibody response and/or generation of higher affinity HA-specific antibodies. The production of virus-specific antibodies with higher binding affinity in DR1 mice would be consistent with the stronger germinal center response.

Anti-HA and anti-NP analysis

Following NC infection in the DR1 mice, there is a stronger germinal center B response, with stronger virus neutralization and HAI titers, compared to NC infection in B10 mice. In addition, the CD4+ T cell repertoire following infection in the DR1 mice was exceptionally broad and included multiple strong epitopes in the four viral proteins analyzed: HA, NA, NP, and nonstructural protein 1 (NS1), in comparison to B10 mice which had restricted epitopes in HA [256]. Therefore, the levels of anti-HA and anti-NP Abs were measured in the sera derived from DR1 and B10 mice infected with NC. In addition, Ab affinity assays were carried out, in order to assess differences in binding

affinity in DR1 and B10 mice. On day 10 post-NC infection, the pattern of anti-HA and anti-NP Abs in the serum paralleled the trend observed with virus-specific Abs differences observed between B10 and DR1 mice (Figure 3.4 A). In contrast, on day 14 post-NC infection, the anti-NP Abs in B10 and DR1 still paralleled the trend observed on day 10, but the anti-HA Abs in the DR1 mice did not follow the day 10 trend, while the anti-HA Abs in the B10 mice followed the same trend as day 10 (Figure 3.4 B). The affinity ELISA on day 14 sera did not reveal any differences between B10 and DR1 mice (Figure 3.4 C).

The virus-specific B cell response in DR1 mice is substantially modulated by the nature of the infecting virus

Total serum levels of IgM and the IgG isotypes were not significantly different between DR1 and B10 mice (data not shown), suggesting that in general, the predominance of IgG1 in the response of DR1 mice to NC infection did not reflect an intrinsic bias impacting B cell responses. We therefore compared B cell responses in DR1 and B10 mice after infection with other influenza viruses (PR8 and X31), or with a non-influenza virus (MHV68) that replicates in the lung. Infection of DR1 mice with PR8, X31, or MHV68 generated a virus-specific B cell response in the MedLN that, in many respects, was more comparable to the response in B10 mice than was the case following NC infection (Figure 3.5). Most notably, the kinetics of the IgG response was similar in DR1 and B10 mice, and the IgG1 bias of the response of DR1 mice to NC infection was no longer present. Interestingly, there was a markedly stronger IgM ASC response in DR1 compared with B10 mice after PR8, X31, and MHV68 infection, a trend that was also evident, but much less pronounced, after NC infection.

The response to PR8 infection in DR1 and B10 mice was evaluated in greater detail. Virus titers in the lungs ($TCID_{50}$/ml ± SD) were similar in both mouse strains on day 6 ($4.4 \times 10^6 \pm 3.9 \times 10^6$ for DR1 and $9.5 \times 10^5 \pm 7.9 \times 10^5$ for B10) and day 8 ($1.3 \times 10^6 \pm 9.4 \times 10^5$ for DR1 and $8.5 \times 10^5 \pm 4.9 \times 10^5$ for B10), indicating comparable

replication and Ag load. Flow cytometric analysis of cell populations in the MedLN on day 8 after PR8 infection showed similar percentages of $B220^+$ B cells (mean ± SD) in DR1 and B10 mice (50.99 ± 3.599 and 46.79 ± 8.762, respectively). In marked contrast to the situation after NC infection, the proportion of $B220^{int}$ $CD138^+$ was higher in DR1 compared with B10 mice (Figure 3.2 C, D), reflecting the vigor of the early PR8-specific IgM response in DR1 mice measured by ELISPOT assay. The proportion of germinal center cells (PNA^+ Fas^+) in the $B220^+$ cell population was significantly higher in DR1 compared with B10 mice (Figure 3.6 C, E), as was also the case after NC infection, suggesting an inherent tendency towards a stronger germinal center response in DR1 mice regardless of the infecting virus. The PR8-specific response in DR1 mice was evaluated after CD4 T cell depletion, since high frequencies of IgM and, to a lesser degree; IgG3 ASCs raised the possibility of T-independent antibody production. CD4 T cell depletion largely prevented PR8-specific ASC formation in the MedLN of DR1 mice on day 8 (Figure 3.2 F), indicating a dependence of the early and strong IgM and IgG3 ASC response on T cell help. Our findings indicate that PR8 infection, but not NC infection, generated a vigorous early extrafollicular B cell response in DR1 mice. Unlike the situation in DR1 mice, the kinetics of ASC generation in B10 mice was not obviously increased after PR8 compared with NC infection (Figure 3.2 D), emphasizing the influence of host factors on the extent that different viruses modulate the B cell response.

Serum levels of virus-specific antibody were consistent with comparable B cell responses in DR1 and B10 mice after PR8 infection. Although there was a trend towards higher neutralization titers in DR1 compared with B10 mice on day 10 [128], reflecting the pattern seen after NC infection, the difference was not significant. Overall, our experiments using PR8, X31, and MHV68, in comparison to the results after NC infection, demonstrated that the kinetics and quality of the B cell response to respiratory tract infection in DR1 mice was dependent on the nature of the infecting virus.

Contrasting B cell responses to NC and PR8 in DR1 mice relates to CD4 T cell cytokine production

The extrafollicular and germinal center pathways of B cell differentiation are T cell-dependent processes [12]. In addition, cytokines produced by T cells during cognate interactions with B cells play a key role in directing the expression of particular Ig isotypes [257]. We therefore investigated the relationship between the B cell response in DR1 and B10 mice following infection with NC or PR8 and the characteristics of the virus-specific CD4 T cell response, in particular the pattern of cytokine production. To evaluate the CD4 T cell response, purified CD4 T cells from the MedLN and spleen on day 10 after infection were tested for their ability to produce cytokines after stimulation with peptides corresponding to previously defined epitopes. Peptide-reactive CD4 T cells stimulated to secrete IL-2, IFN-g, or IL-4 during in vitro culture were quantified by ELISPOT assay.

Following NC infection, in the MedLN on day 10, there was a difference between DR1 and B10 mice in the pattern of cytokine production by peptide-specific CD4 T cells. This pattern was largely independent of peptide specificity and generally reflected the mouse strain. Peptide-reactive CD4 T cells in the MedLN of DR1 mice consisted of similar numbers of IL-2, IFN-γ-secreting cells and IL-4-secreting cells (Figure 3.7). In contrast, in the MedLN of B10 mice, very few IL-4-secreting cells, some IL-2-secreting cells were observed and IFN-γ-secreting cells predominated (Figure 3.8). The results described above were essentially the same in an analysis of CD4 T cells in the MedLN on day 13 after NC infection (data not shown). The prevalence of virus-specific IL-4-secreting CD4 T cells in DR1 but not B10 mice suggested a basis for the IgG1 bias of the NC-specific response, since IL-4 has been shown to promote switching to IgG1 and negatively regulate switching to other IgG isotypes [258-259].

An analysis of the CD4 T cell response was also performed on day 10 after PR8 infection of DR1 and B10 mice. As described above, the PR8-specific B cell response in DR1 and B10 mice featured similarly strong early extrafollicular B cell responses. In addition, the IgG1 bias in DR1 mice after NC infection was absent after PR8 infection.

Supporting the B cell response, the pattern of cytokines secreted by peptide-reactive CD4 T cells after PR8 infection in DR1 largely differed from the pattern after NC infection (Figure 3.9, 3.10). Interestingly, this pattern of cytokine production was also different from B10 mice infected with PR8. Most notable was the higher proportion of IL-4-secreting CD4 T cells in DR1 mice (Figure 3.9) compared to B10 mice (Figure 3.10). Apparently, the IgG1 bias of the NC-specific B cell response in DR1 mice was driven by the high prevalence of IL-4-secreting CD4 T cells. Our findings suggest that the nature of the extrafollicular B cell response is dependent of the pattern of cytokines secreted by virus-specific CD4 T cells.

The virus-specific B cell response in DR1 mice is substantially modulated by non-specific factors associated with infection

We hypothesized that the markedly different B cell responses in DR1 mice following infection with NC compared with PR8 (and other viruses tested) reflected differences in early innate responses to lung infection. This idea was tested in a co-infection experiment using NC and MHV68. We had shown that the MHV68-specific B cell response in DR1 and B10 mice followed similar kinetics and featured IgG2c predominance among switched antibody isotypes. IgG or IgA ASCs were not detected when cells from mice infected with NC or MHV68 alone were incubated on ELISPOT plates coated with the heterologous virus, indicating an absence of cross-reactivity between NC and MHV68 at the B cell level (Data not shown).

Cohorts of DR1 and B10 mice were infected with NC plus MHV68, or with NC only, and the B cell response on days 8 and 10 was assessed by ELISPOT assay using plates coated with NC or MHV68 (Figure 3.11). The NC-specific response in DR1 mice infected with NC alone was dramatically modified by concurrent MHV68 infection and closely resembled the response in B10 mice infected with NC alone. Importantly, the NC-specific IgG response in co-infected DR1 mice was not delayed relative to the response in B10 mice and the predominant IgG isotype was IgG2c, not IgG1. Serum

levels of NC-specific IgG and Ig on day 8 were also consistent with a more rapid NC-specific response in co-infected DR1 mice compared with those infected with NC alone (Figure 3.11 E, F). Our findings establish that non-specific factors associated with infection of the lung by some viruses have the potential to substantially modulate the isotype switching and isotype bias of a virus-specific B cell response. Our interpretation is that this influence is primarily on the extrafollicular pathway of B cell differentiation.

Discussion

Effective generation of B cell response to viruses is largely dependent on CD4+ T cell help and it is unclear how these interactions best achieve effective generation of neutralizing antibodies. Generation of effective B cell response is central for vaccine design and protection against re-infection. Following infection, the antigen engaged B cells receive cognate help from CD4+ T cells and undergo either of the following pathways of B cell differentiation. 1. Migration to extra follicular foci in the spleen or in the medullary cords of draining lymph nodes, initiating the extra-follicular pathway of B cell differentiation [19], that generates low affinity and rapid Abs. 2. B cell proliferation in follicles leading to germinal center (GC) formation and generation of delayed, but high affinity Abs [12]. Although several mechanisms have been proposed that delineate the choice between these pathways of differentiation [13-15], it is still largely unclear, especially in the context of virus infection, host and viral factors regulating extra follicular or GC pathway of B cell differentiation. Our analysis identifies HLA-DR1 transgenic mice as a model for the investigation of the addressed issues, providing insight into the host and viral factors that modulate the characteristics of B cell response to influenza infection.

Following NC infection in DR1 mice, there is a delay in the generation of virus-specific isotype-switching, compared to NC infection in B10 mice. Rapid isotype switching response in the B10 mice is characteristic of an extra-follicular B cell response, and therefore there seems to be a lack of isotype switching along this

pathway in the DR1 mice. The nature of extra follicular pathway of B cell differentiation is regulated by the induction of non-specific factors in the lungs, as indicated by the co-infection studies with MHV-68 and NC. Manipulation of these factors by MHV-68 and also the fact that PR8 infection generates a rapid B cell response in these mice emphasize the point that lack of isotype-switching towards extra follicular B cell differentiation following NC infection in DR1 mice is not an inherent feature of these mice, but rather seems to be regulated by viral factors. There may also be an interplay of host factors as well, indicated by our comparative preliminary innate cytokine and chemokine analysis in the lung (data not shown). These studies indicate that the DR1 mice have a delayed or much lower generation of certain cytokines and chemokines which may be critical for the initiation of a down stream rapid isotype switching. An elaborate analysis of these innate factors following PR8 or MHV-68 infection in the DR1 mice will identify virus induced host factors that may provide mechanistic insights into these processes. Although the early B cell response is of low affinity, our studies indicate that these extra- follicular generated B cells may perhaps contribute to virus clearance as indicated by delayed virus clearance pattern associated with DR1 mice.

Cytokines secreted by CD4+ T cells during cognate interaction with B cells are critical mediators that induce isotype switching of B cells [253, 257, 260]. Our studies indicate that this rule applies to extrafollicular B cells as well, contrary to a study that demonstrated extra follicular IgG1 class switching unimpaired in the absence of IL-4 [261]. Our analysis indicates that there is a good correlation between the pattern of cytokines produced by CD4+ T cells and the corresponding isotype of Abs. The H1N1 viruses; NC and PR8 tested in this study induced different pattern of CD4+ T cell cytokine in the DR1 mice, but a similar pattern in the B10 mice. Following infection in DR1 mice, NC seems to favor a strong IL-4 induction, while PR8 seems to favor more of IFN-γ, along with IL-4. Interestingly, the PR8-specific Ab isotype pattern is not entirely the same between B10 and DR1 mice, with a bias towards IgG3 and an early strong IgM isotype in the DR1 mice. The IgM and IgG3 Ab phenotype is associated with CD4+ T cell independent mechanisms, and our CD4+ T cell depletion studies indicate that these Abs in the DR1 mice are not generated through this pathway. It is also likely that

some of the non-CD4+ T cell derived factors may be involved in the extra-follicular Ab generation, that are also involved in T cell independent Ab generation. The IgG3 bias may perhaps reflect the combinatorial effects of IL-4 and IFN-γ in the microenvironment. For example, TGF-β1 alone is capable of inducing both IgG2b and IgA class switching. In contrast, TGF-β1 in the presence of IL-21 inhibits TGF-β1 mediated class switching to IgG2b, without influencing IgA class switching [245]. There seems to be a role for non-specific factors in the isotype bias, as co-infection studies with MHV-68 and NC resulted in removal of the IgG1 bias in the DR1 mice.

Although it is not clear what virus dictated mechanisms in these mice induce the Th1 versus Th2 differentiation, it is likely that perhaps the APCs presenting the peptides to the naïve T cells might be differentially modulated by these viruses. For example, dendritic cells (DCs) can be conditioned by NC to polarize naïve T cells to be differentiated towards Th2 cells, while PR8 favoring Th1 cells. Innate signals can drive conditioning of DCs as Th2 polarization is MyD88 signaling independent, while Th1 polarization is MyD88 dependent [262]. In addition, in the absence of IL-12, Th2 polarization is preferred [263]. Along these lines, it would be interesting to characterize the B cell response, perhaps following immunization of DR1 mice with rIL-12 and infect them with NC or alternatively following infection of IL-12-/- mice with NC. Other factors, including enhancement of Notch signaling, up regulation of CD40 [263] and OX40L [264]on APCs are also key determinants favoring Th2 over Th1 differentiation.

There is a stronger GC induction on day 8 following NC or PR8 infection in the DR1 mice, compared to B10 mice. Although, NC infection in the DR1 seem to imply that the extra follicular pathway of B cell differentiation is compromised at the expense of GC reaction, analysis of PR8 infection in the DR1 mice revealed that this might not be the case, as GC and EF were pathways were induced normally. Our studies have demonstrated that the strong GC induced in these mice is completely CD4+ T cell-dependent process (data not shown), as some GC reactions can be generated independent of CD4+ T cells [265]. Therefore, this argues for a CD4+ T cell derived influence on a strong GC reaction. In this direction, one of the players could be the stronger IL-4 component from CD4+ T cells in the DR1 mice, a cytokine pattern

observed in these mice, irrespective of the infecting virus. Indeed, IL-4 has an important role in maintaining GC reactions [26]. Although our studies do not identify the CD4+ T cell subset producing IL-4, one possible candidate is follicular helper T cells (Tfh), which produce IL-4 and also regulate B cell responses in the GC reaction [266-267]. In fact, there is a good correlation between Tfh cells and GC numbers. Another scenario that could explain stronger GC in the DR1 is that these mice may be biased towards IL-21 production, as lack of IL-21 or IL-21R on B cells results in reduced germinal centers, with reduced Bcl-6 expression in germinal center B cells [24-25]. Apart from the importance of IL-21 in germinal center reactions, there is also a role for IL-21 in regulating IgG1 class switching, as the germinal center B cells in mice lacking IL-21R fail to class-switch to IgG1. Other studies have also identified Th17 cells, through IL-21 production, to be important players in inducing a strong GC [27]. In addition, the stronger GC in the DR1 may also be linked to the pattern of innate factors induced in the lung. Therefore, further studies characterizing these different CD4+ T cell subsets in the DR1 mice will be important to address these issues.

NC infection in the DR1 mice also induced stronger neutralizing Abs and HAI titers, compared to B10 mice. Although there was a similar trend following PR8 infection, the titers did not reach statistical significance in the DR1 mice, perhaps reflecting stronger GC proportions on day 10 following NC infection. In contrast, by this time post infection, the GC proportions in the DR1 mice following PR8 infection were similar to B10 mice. Indeed, neutralizing Abs is established in the serum at least 2 weeks post infection. Another possible explanation explored in the current study is that there is perhaps a bias towards the generation of HA-specific Abs in the DR1 mice. This is based on the comparison of CD4+ T cell repertoire to NC infection, which revealed a broad recognition (multiple epitopes recognized in multiple viral proteins including HA). In contrast, the repertoire in B10 mice was narrow (recognition of few epitopes, mostly in NP) [256]. In support of this thinking, on day 14 post NC infection, there was a trend towards higher HA-specific Abs in the DR1 mice. Further studies, contrasting the findings following PR8 infection will be important. The broad repertoire of Abs do not seem to be a factor in influencing the isotype of Abs, as NC infection of B10.D2 mice,

which also have a broad repertoire, similar to DR1 mice did not induce an IgG1 bias (data not shown).

In summary, these studies establish a model for the investigation of host and viral factors that modulate the quality and effectiveness of the B cell response to influenza infection. These studies indicate that the strength of the extrafollicular pathway of rapid antiviral production is modulated by host factors and by the nature of infecting virus. In addition, the regulation of the extrafollicular pathway relates to the induction of non-specifically acting factors in the lung by viral infection and also to the pattern of cytokines produced by virus-specific CD4+ T cells.

APPENDIX

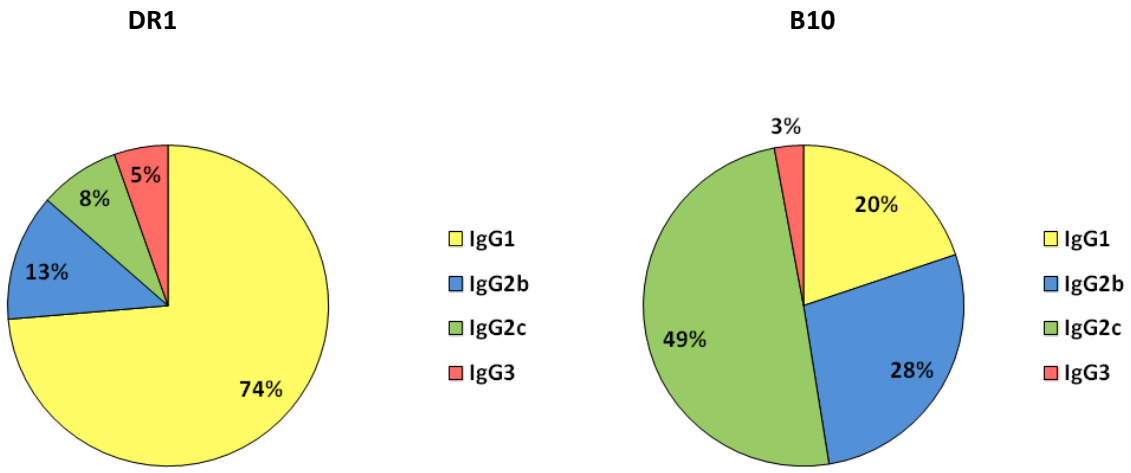

Figure 3.1. The NC-specific ASC response in DR1 mice is biased towards IgG1 production. DR1 and B10 mice were infected intranasally with 40,000 EID50 NC. Virus-specific ASC frequencies in the MedLN were determined by ELISPOT assay on day 14. The IgG isotypes proportions are shown. The proportions were determined for 3-8 individual mice per group.

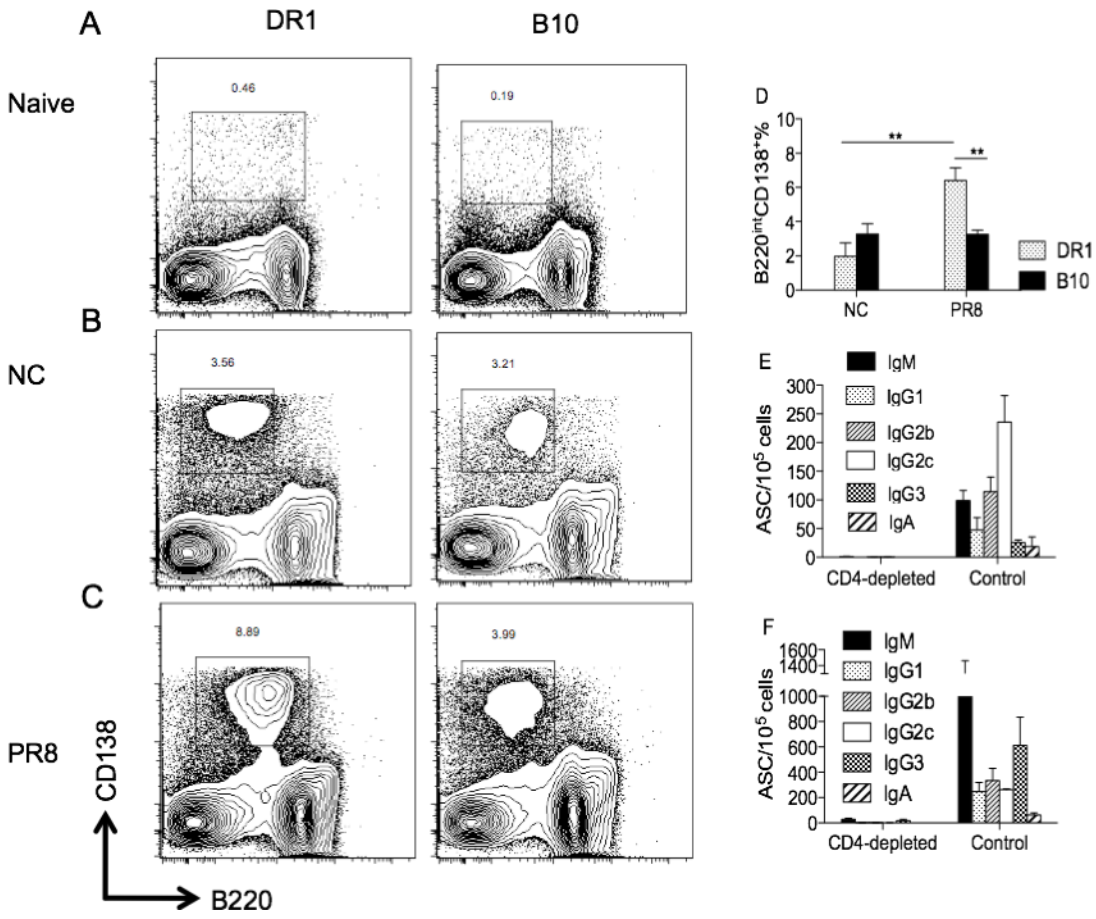

Figure 3.2. Extrafollicular ASC generation in DR1 and B10 mice after NC or PR8 infection. A-D, MedLN cells from DR1 and B10 mice on day 8 after intranasal NC or PR8 infection were analyzed by flow cytometry. Single cell suspensions from individual mice were stained and gated for expression of B220 and CD138 to identify extrafollicular ASCs, defined as a B220int CD138+ population. Representative staining for extrafollicular ASCs is shown for naive mice (A) and on day 8 after infection with NC (B), PR8 (C). Staining is shown as 5% contour plots, with the number indicating the cell frequency in the depicted gate. Mean frequencies of extrafollicular ASCs are compiled in D. Frequencies + SE is shown for 4-8 individual mice in each group. NC-specific ASC frequencies in CD4 T cell-depleted B10 mice and mock-depleted control mice on day 8 after infection is shown (E). PR8-specific ASCs in CD4 T cell depleted DR1 mice and mock-depleted control mice on day 8 after infection is shown (F). The mean + SE is shown for 4 individual mice per group.

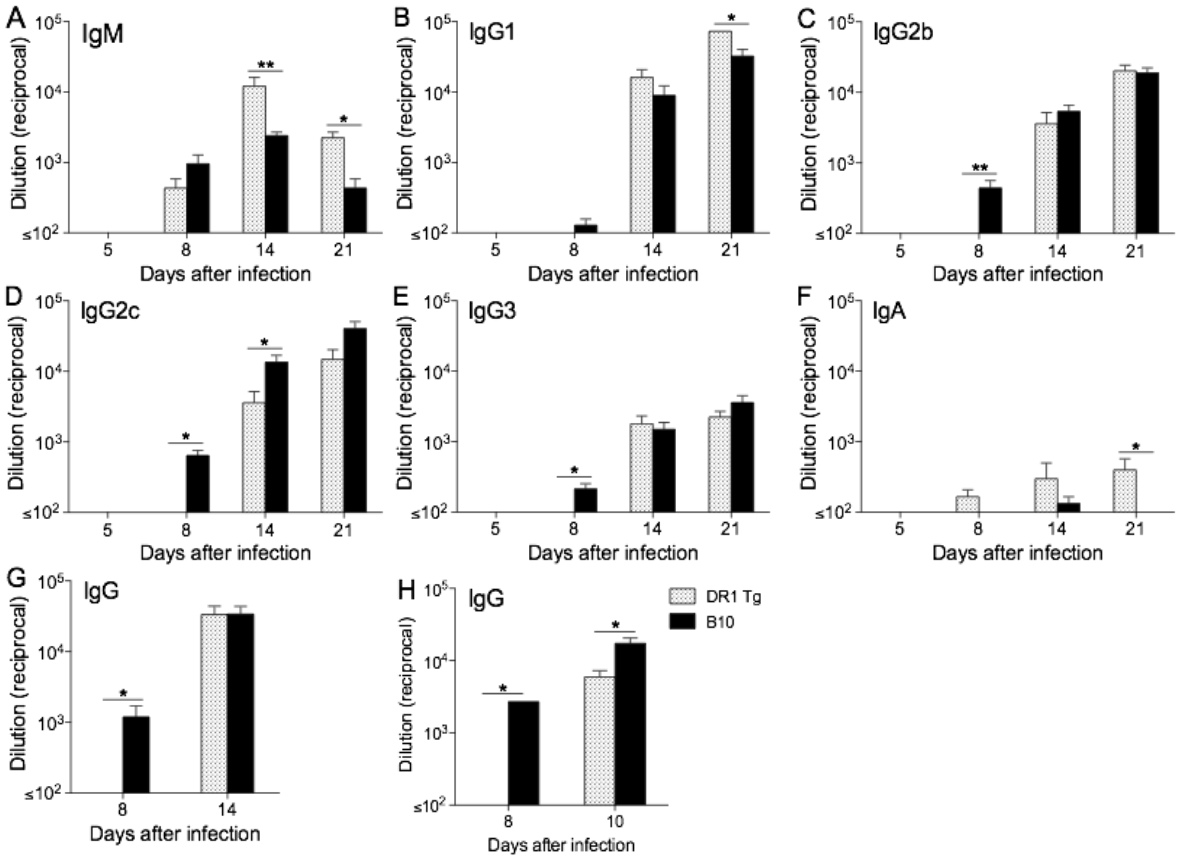

Figure 3.3. Serum levels of NC-specific antibody in DR1 and B10 mice. Different assays were used to determine NC-specific antibody levels in sera collected at intervals after infection. A-H, Antibody titers measured by ELISA. NC-specific IgM (A), IgG1 (B), IgG2b (C), IgG2c (D), IgG3 (E), IgA (F), IgG (G), and Ig (H) titers were determined by endpoint titration on plates coated with disrupted viral particles. Titers are shown as the reciprocal of the highest serum dilution scored as positive relative to naïve control serum. The mean + SE is shown for 4-7 (A-H) individual mice per group.

Figure 3.4. HA (A) and NP (B) - specific Abs and avidity of HA- specific Abs (C) in DR1 and B10 mice following NC infection. The concentrations were determined based on a standard curve using mouse Ig's. Avidity index was calculated as a ratio of concentration of Abs in the presence of NaSCN to the concentration of Abs in the absence of NaSCN. The mean + SE is shown for 3-4 individual mice per group.

A

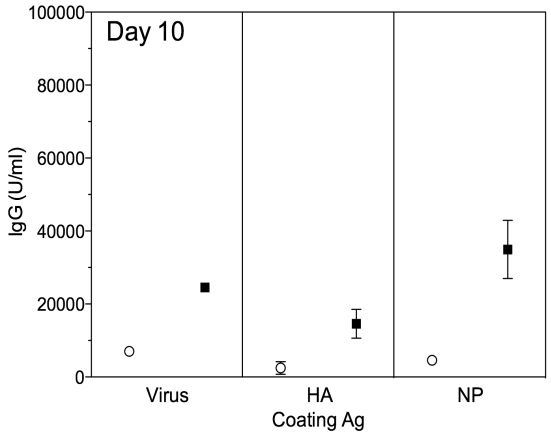
Day 10
IgG (U/ml)
100000
80000
60000
40000
20000
0
Virus
HA
NP
Coating Ag

B

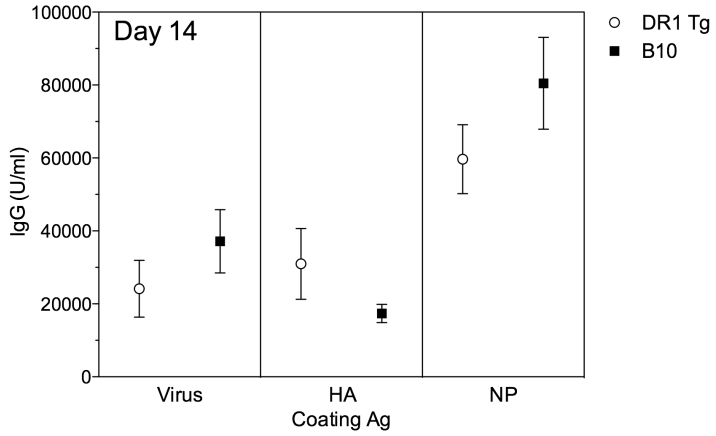
Day 14
IgG (U/ml)
100000
80000
60000
40000
20000
0
Virus
HA
NP
Coating Ag
DR1 Tg
B10

C

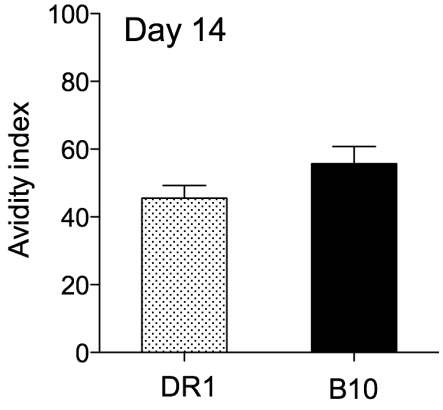
Day 14
Avidity index
100
80
60
40
20
0
DR1
B10

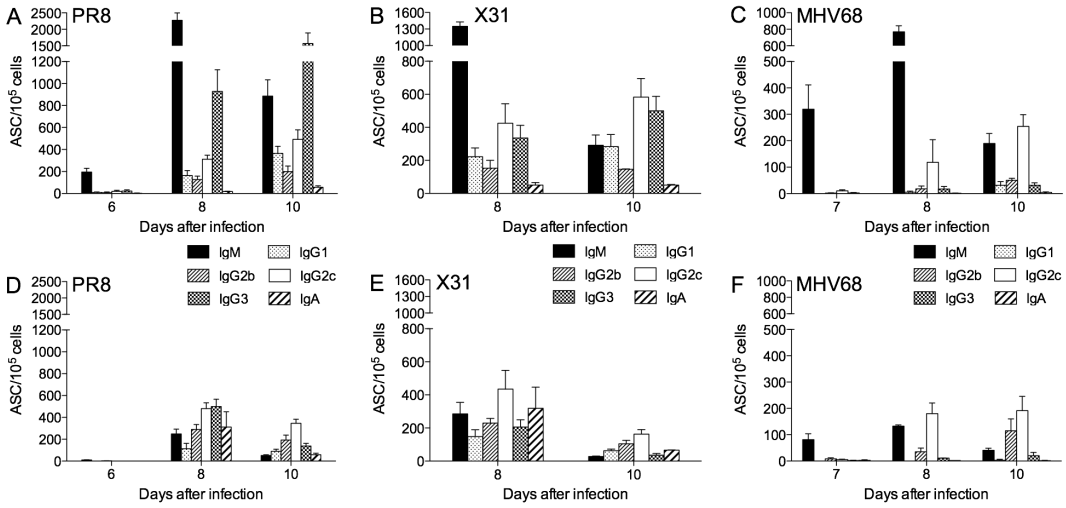

Figure 3.5. The virus-specific ASC response in DR1 and B10 mice following infection with different viruses that replicate in the lung. DR1 (A-C) and B10 (D-F) mice were infected intranasally with the influenza viruses PR8 (A and D) and X31 (B and E), and with the non-influenza virus MHV68 (C and F). Virus-specific ASC frequencies in the MedLN were determined by ELISPOT assay at intervals after infection. The ASC frequency is shown as a proportion of nucleated cells. The mean + SE is shown for 3-8 individual mice per group.

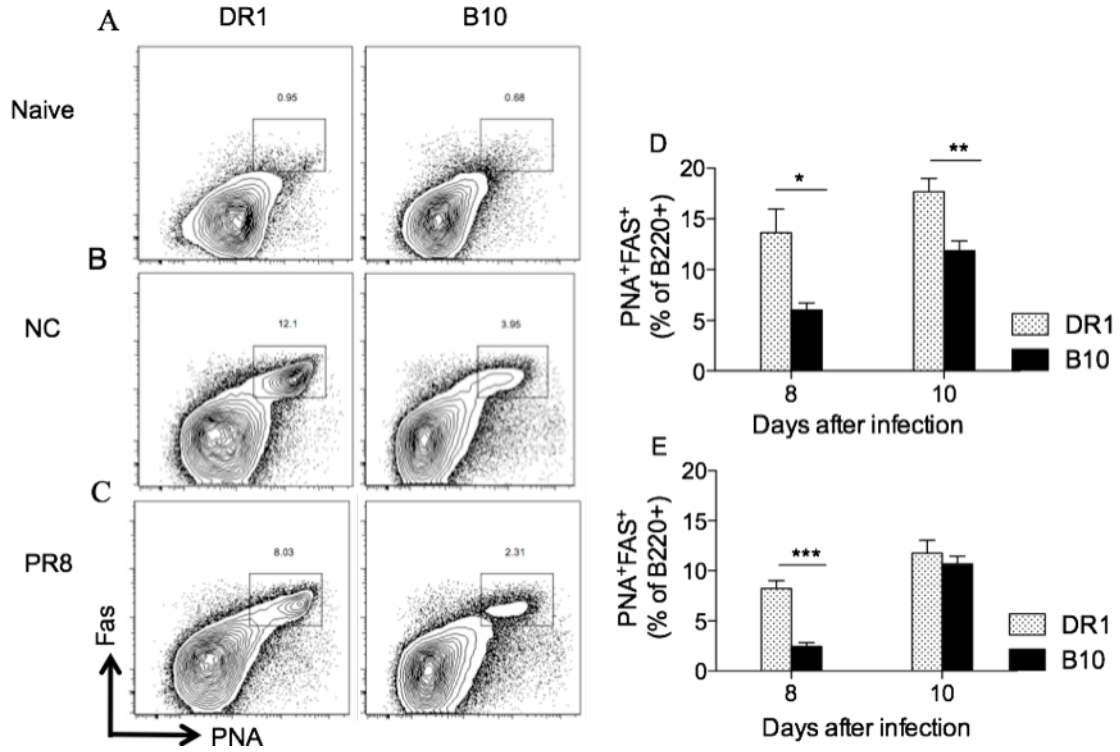

Figure 3.6. Strong germinal center B cell response to NC or PR8 infection in DR1 mice. A-E, MedLN cells from DR1 and B10 mice on day 8 after intranasal PR8 infection were analyzed by flow cytometry by gating on B220+ cells, followed by PNA+FAS+ gating. Representative staining for germinal center B cells is shown in uninfected mice (A) and on day 8 after NC (B) or PR8 (C) infection. Staining is shown as 5% contour plots, with the number indicating the cell frequency in the depicted gate. Mean frequencies of germinal center B cells following NC or PR8 infection are compiled in D and E, respectively. Frequencies + SE are shown for 4-8 individual mice in each group.

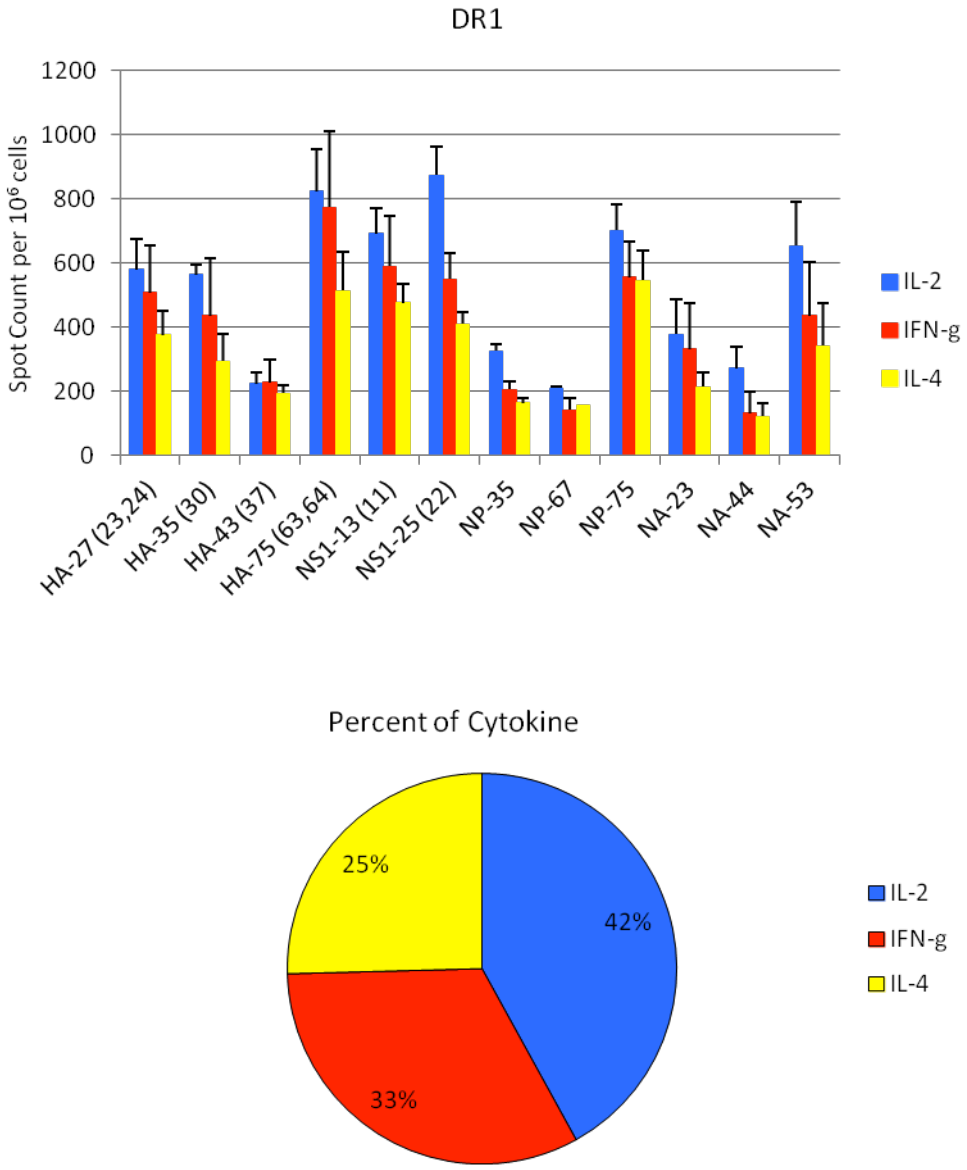

Figure 3.7. Cytokine secretion by influenza-specific CD4 T cells in DR1 mice following NC infection. Enriched CD4+ T cells from MLN were cultured in vitro with APCs and a range of class-II restricted peptide epitopes. Cytokine production was determined by ELISPOT assay after 24 hrs.

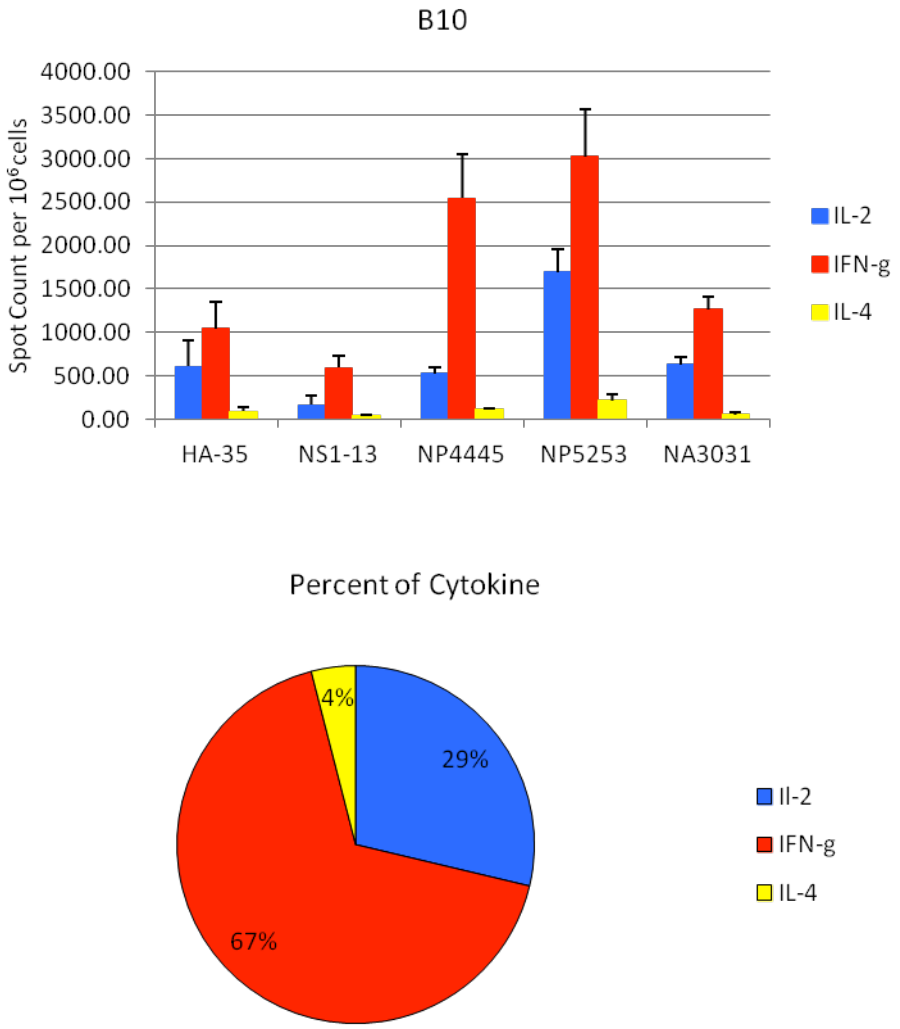

Figure 3.8. Cytokine secretion by influenza-specific CD4 T cells in B10 mice following NC infection. Enriched CD4+ T cells from MLN were cultured in vitro with APCs and a range of class-II restricted peptide epitopes. Cytokine production was determined by ELISPOT assay after 24 hrs.

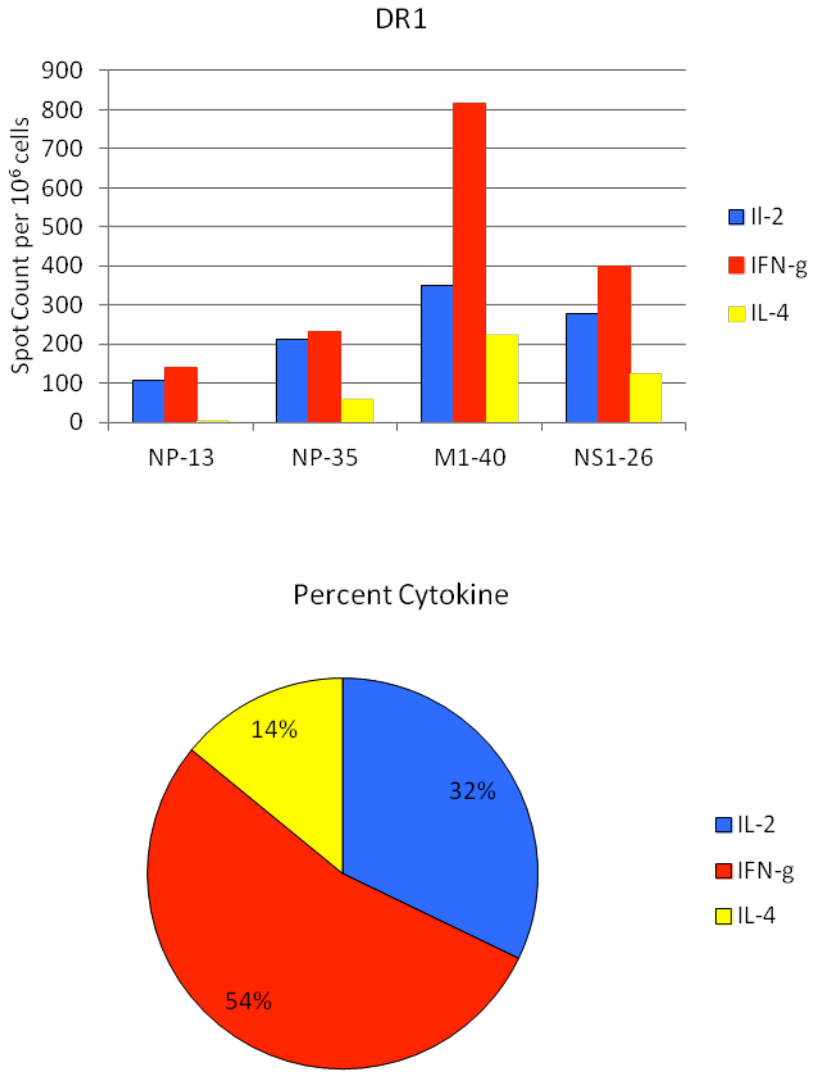

Figure 3.9. Cytokine secretion by influenza-specific CD4 T cells in DR1 mice following PR8 infection. Enriched CD4+ T cells from MLN were cultured in vitro with APCs and a range of class-II restricted peptide epitopes. Cytokine production was determined by ELISPOT assay after 24 hrs.

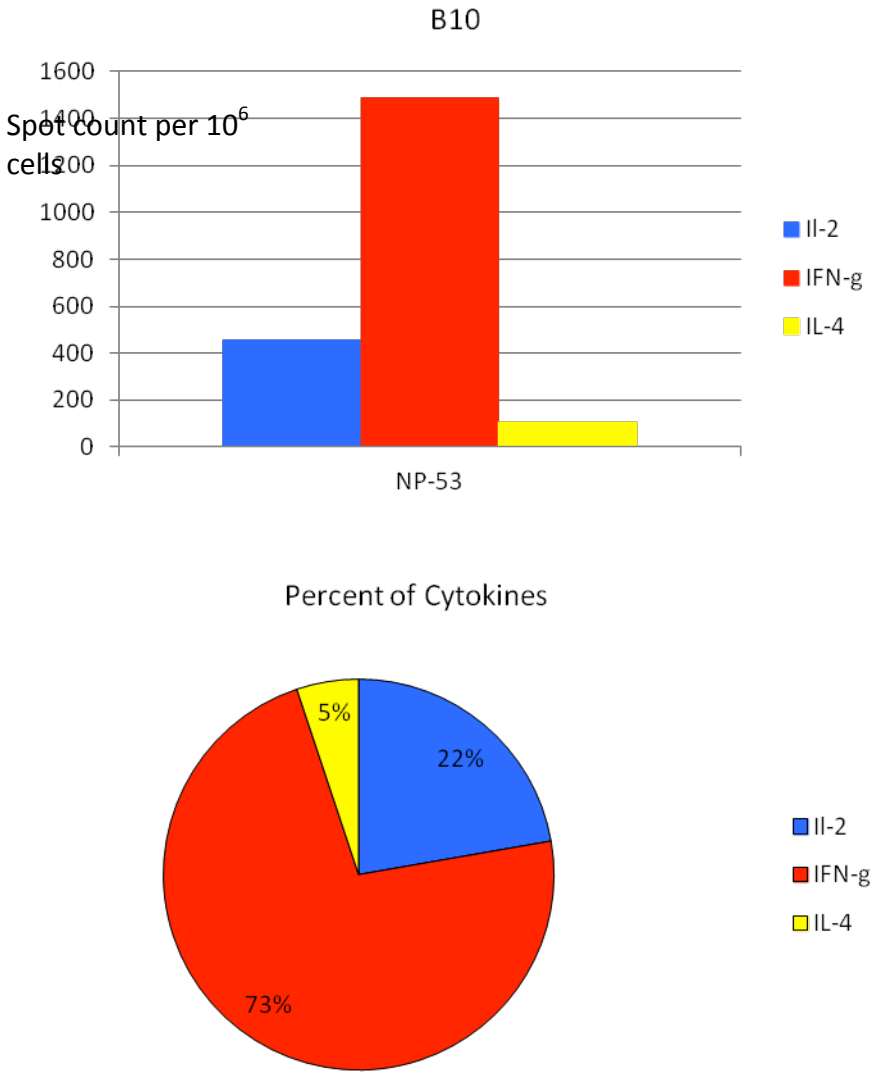

Figure 3.10. Cytokine secretion by influenza-specific CD4 T cells in B10 mice following PR8 infection. Enriched CD4+ T cells from MLN were cultured in vitro with APCs and a range of class-II restricted peptide epitopes. Cytokine production was determined by ELISPOT assay after 24 hrs.

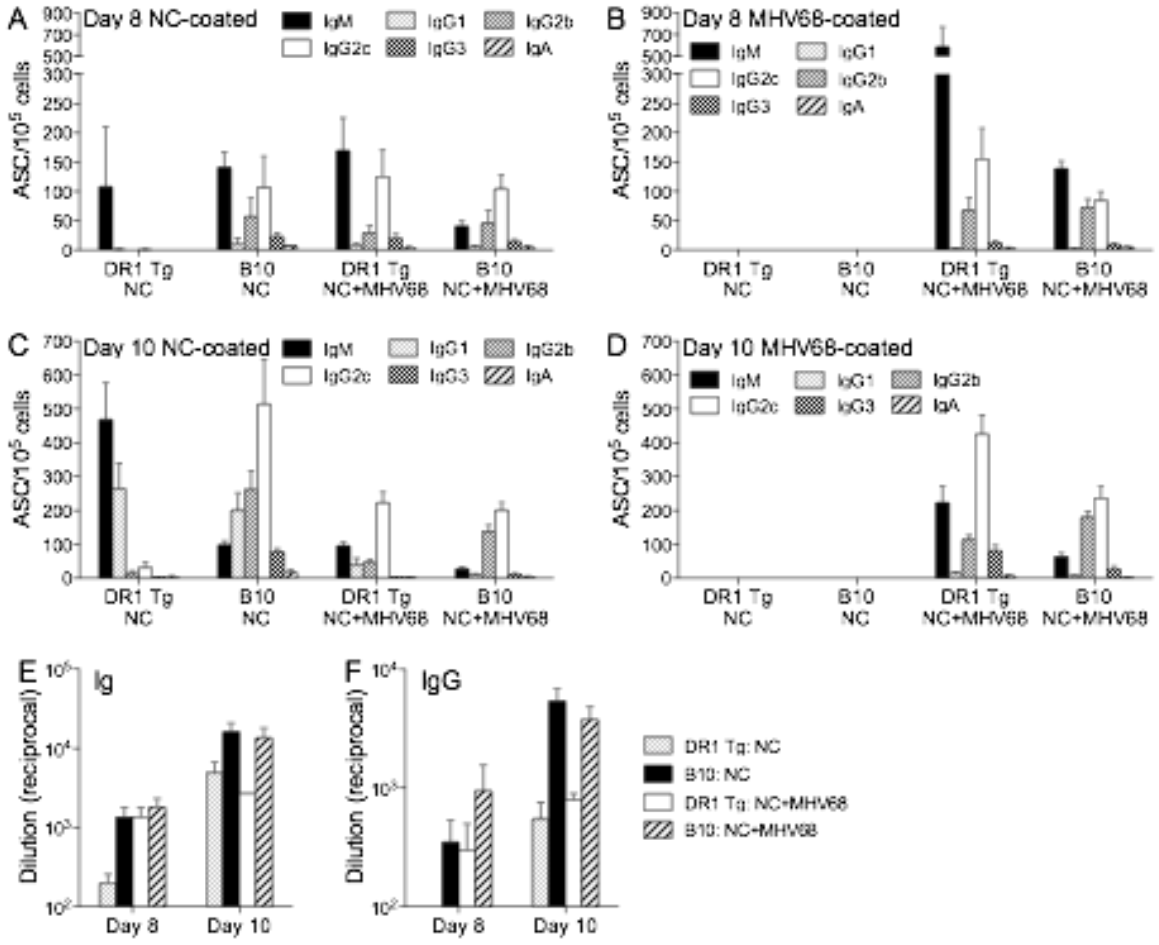

Figure 3.11. The NC-specific B cell response in DR1 mice is modulated by concurrent infection with MHV68. DR1 and B10 mice were infected intranasally with NC only, or with NC and MHV68. ASC frequencies in the MedLN were determined by ELISPOT assay on day 8 (A and B) and day 10 (C and D) after infection. ASCs specific for NC or MHV68 were detected using plates coated with disrupted NC (A and C) and disrupted MHV68 (B and D), respectively. ASC frequencies are shown as a proportion of nucleated cells. E and F, NC-specific serum IgG (E) and Ig (F) levels. Titers were determined by ELISA and are shown as the reciprocal of the highest serum dilution scored as positive relative to naïve control serum. The mean + SE is shown for 6-9 individual mice per group.

OVERALL CONCLUSION FOR DISSERTATION WORK

Innate and adaptive immune mechanisms in the RT play a major role in virus clearance. Generation of virus-specific IgA at mucosal surfaces is important for effective neutralization of viruses at mucosal surfaces, blocking infection and transmission. In addition, establishment of B cell memory, in terms of localization of IgG and IgA ASCs in the upper and lower RT, along with effective generation of B_{Mem} frequencies is important. Although several studies have highlighted the regulation of IgA class switching in the gut, currently, it is unclear what mechanisms (similar or different) regulate induction of IgA response in the RT. In addition, trafficking mechanisms of ASCs and B_{Mem} to the upper and lower RT over long-term post infection is not clear. More specifically, are there differential factors regulating IgG Vs IgA ASCs trafficking to the upper Vs lower RT? Most importantly, how are these features modulated following virus infection? The studies described in Chapter 2 provide insight into these aspects. The interplay between CD4+ T cells and B cells lead to the generation of high-affinity neutralizing Abs and regulating isotype-switch mechanisms. In addition, the cognate interaction between these cells also regulates B cell differentiation towards germinal center pathway (high affinity) or extrafollicular pathway (rapid, low-affinity). What factors regulate these pathways; especially in the context of virus infection in the RT is currently not clear. These aspects are addressed in the chapter 3 of the current dissertation, along with CD4+ T cell mediated regulation of B cell isotype class switching and differentiation.

LIST OF REFERENCES

1. *Cyster, J.G., B cell follicles and antigen encounters of the third kind. Nat Immunol, 2010. 11(11): p. 989-96.*
2. *Phan, T.G., et al., Immune complex relay by subcapsular sinus macrophages and noncognate B cells drives antibody affinity maturation. Nat Immunol, 2009. 10(7): p. 786-93.*
3. *Carrasco, Y.R. and F.D. Batista, B cells acquire particulate antigen in a macrophage-rich area at the boundary between the follicle and the subcapsular sinus of the lymph node. Immunity, 2007. 27(1): p. 160-71.*
4. *Junt, T., et al., Subcapsular sinus macrophages in lymph nodes clear lymph-borne viruses and present them to antiviral B cells. Nature, 2007. 450(7166): p. 110-4.*
5. *Gonzalez, S.F., et al., Capture of influenza by medullary dendritic cells via SIGN-R1 is essential for humoral immunity in draining lymph nodes. Nat Immunol, 2010. 11(5): p. 427-34.*
6. *Iannacone, M., et al., Subcapsular sinus macrophages prevent CNS invasion on peripheral infection with a neurotropic virus. Nature, 2010. 465(7301): p. 1079-83.*
7. *Coro, E.S., W.L. Chang, and N. Baumgarth, Type I IFN receptor signals directly stimulate local B cells early following influenza virus infection. J Immunol, 2006. 176(7): p. 4343-51.*
8. *Suzuki, K., et al., Visualizing B cell capture of cognate antigen from follicular dendritic cells. J Exp Med, 2009. 206(7): p. 1485-93.*
9. *Lindquist, R.L., et al., Visualizing dendritic cell networks in vivo. Nat Immunol, 2004. 5(12): p. 1243-50.*
10. *Kiyono, H. and S. Fukuyama, NALT- versus Peyer's-patch-mediated mucosal immunity. Nat Rev Immunol, 2004. 4(9): p. 699-710.*
11. *Porgador, A., et al., Intranasal immunization with cytotoxic T-lymphocyte epitope peptide and mucosal adjuvant cholera toxin: selective augmentation of peptide-presenting dendritic cells in nasal mucosa-associated lymphoid tissue. Infect Immun, 1998. 66(12): p. 5876-81.*

12. *Vinuesa, C.G., et al., T cells and follicular dendritic cells in germinal center B-cell formation and selection. Immunol Rev, 2010. 237(1): p. 72-89.*
13. *Paus, D., et al., Antigen recognition strength regulates the choice between extrafollicular plasma cell and germinal center B cell differentiation. J Exp Med, 2006. 203(4): p. 1081-91.*
14. *Chan, T.D., et al., Antigen affinity controls rapid T-dependent antibody production by driving the expansion rather than the differentiation or extrafollicular migration of early plasmablasts. J Immunol, 2009. 183(5): p. 3139-49.*
15. *Anderson, S.M., et al., Taking advantage: high-affinity B cells in the germinal center have lower death rates, but similar rates of division, compared to low-affinity cells. J Immunol, 2009. 183(11): p. 7314-25.*
16. *Jacob, J. and G. Kelsoe, In situ studies of the primary immune response to (4-hydroxy-3-nitrophenyl)acetyl. II. A common clonal origin for periarteriolar lymphoid sheath-associated foci and germinal centers. J Exp Med, 1992. 176(3): p. 679-87.*
17. *Eckl-Dorna, J. and F.D. Batista, BCR-mediated uptake of antigen linked to TLR9 ligand stimulates B-cell proliferation and antigen-specific plasma cell formation. Blood, 2009. 113(17): p. 3969-77.*
18. *Cannons, J.L., et al., Optimal germinal center responses require a multistage T cell:B cell adhesion process involving integrins, SLAM-associated protein, and CD84. Immunity, 2010. 32(2): p. 253-65.*
19. *MacLennan, I.C., et al., Extrafollicular antibody responses. Immunol Rev, 2003. 194: p. 8-18.*
20. *Lu, R., Interferon regulatory factor 4 and 8 in B-cell development. Trends Immunol, 2008. 29(10): p. 487-92.*
21. *Pereira, J.P., et al., EBI2 mediates B cell segregation between the outer and centre follicle. Nature, 2009. 460(7259): p. 1122-6.*

22. *Gatto, D., et al., Guidance of B cells by the orphan G protein-coupled receptor EBI2 shapes humoral immune responses. Immunity, 2009. 31(2): p. 259-69.*
23. *Vogelzang, A., et al., A fundamental role for interleukin-21 in the generation of T follicular helper cells. Immunity, 2008. 29(1): p. 127-37.*
24. *Zotos, D., et al., IL-21 regulates germinal center B cell differentiation and proliferation through a B cell-intrinsic mechanism. J Exp Med, 2010. 207(2): p. 365-78.*
25. *Linterman, M.A., et al., IL-21 acts directly on B cells to regulate Bcl-6 expression and germinal center responses. J Exp Med, 2010. 207(2): p. 353-63.*
26. *Cunningham, A.F., et al., Pinpointing IL-4-independent acquisition and IL-4-influenced maintenance of Th2 activity by CD4 T cells. Eur J Immunol, 2004. 34(3): p. 686-94.*
27. *Mitsdoerffer, M., et al., Proinflammatory T helper type 17 cells are effective B-cell helpers. Proc Natl Acad Sci U S A, 2010. 107(32): p. 14292-7.*
28. *Okada, T., et al., Chemokine requirements for B cell entry to lymph nodes and Peyer's patches. J Exp Med, 2002. 196(1): p. 65-75.*
29. *Cyster, J.G., et al., Follicular stromal cells and lymphocyte homing to follicles. Immunol Rev, 2000. 176: p. 181-93.*
30. *Kunkel, E.J. and E.C. Butcher, Plasma-cell homing. Nat Rev Immunol, 2003. 3(10): p. 822-9.*
31. *Hargreaves, D.C., et al., A coordinated change in chemokine responsiveness guides plasma cell movements. J Exp Med, 2001. 194(1): p. 45-56.*
32. *Agace, W.W., et al., Constitutive expression of stromal derived factor-1 by mucosal epithelia and its role in HIV transmission and propagation. Curr Biol, 2000. 10(6): p. 325-8.*

33. *Hauser, A.E., et al., Chemotactic responsiveness toward ligands for CXCR3 and CXCR4 is regulated on plasma blasts during the time course of a memory immune response. J Immunol, 2002. 169(3): p. 1277-82.*
34. *Pan, J., et al., A novel chemokine ligand for CCR10 and CCR3 expressed by epithelial cells in mucosal tissues. J Immunol, 2000. 165(6): p. 2943-9.*
35. *Wang, W., et al., Identification of a novel chemokine (CCL28), which binds CCR10 (GPR2). J Biol Chem, 2000. 275(29): p. 22313-23.*
36. *Roy, M.P., C.H. Kim, and E.C. Butcher, Cytokine control of memory B cell homing machinery. J Immunol, 2002. 169(4): p. 1676-82.*
37. *Kunkel, E.J., et al., CCR10 expression is a common feature of circulating and mucosal epithelial tissue IgA Ab-secreting cells. J Clin Invest, 2003. 111(7): p. 1001-10.*
38. *Crotty, S., et al., SAP is required for generating long-term humoral immunity. Nature, 2003. 421(6920): p. 282-7.*
39. *Qi, H., et al., SAP-controlled T-B cell interactions underlie germinal centre formation. Nature, 2008. 455(7214): p. 764-9.*
40. *Smith, K.G., et al., bcl-2 transgene expression inhibits apoptosis in the germinal center and reveals differences in the selection of memory B cells and bone marrow antibody-forming cells. J Exp Med, 2000. 191(3): p. 475-84.*
41. *Yoshida, T., et al., Memory B and memory plasma cells. Immunol Rev, 2010. 237(1): p. 117-39.*
42. *Quemeneur, L., et al., SWAP-70 deficiency causes high-affinity plasma cell generation despite impaired germinal center formation. Blood, 2008. 111(5): p. 2714-24.*
43. *Matsumoto, M., et al., Lymphotoxin-alpha-deficient and TNF receptor-I-deficient mice define developmental and functional characteristics of germinal centers. Immunol Rev, 1997. 156: p. 137-44.*

44. *Karrer, U., et al., Antiviral B cell memory in the absence of mature follicular dendritic cell networks and classical germinal centers in TNFR1-/- mice. J Immunol, 2000. 164(2): p. 768-78.*
45. *Rauch, M., et al., Crucial role for BAFF-BAFF-R signaling in the survival and maintenance of mature B cells. PLoS One, 2009. 4(5): p. e5456.*
46. *Joo, H.M., Y. He, and M.Y. Sangster, Broad dispersion and lung localization of virus-specific memory B cells induced by influenza pneumonia. Proc Natl Acad Sci U S A, 2008. 105(9): p. 3485-90.*
47. *Moyron-Quiroz, J.E., et al., Persistence and responsiveness of immunologic memory in the absence of secondary lymphoid organs. Immunity, 2006. 25(4): p. 643-54.*
48. *Huard, B., et al., APRIL secreted by neutrophils binds to heparan sulfate proteoglycans to create plasma cell niches in human mucosa. J Clin Invest, 2008. 118(8): p. 2887-95.*
49. *Weck, K.E., et al., Macrophages are the major reservoir of latent murine gammaherpesvirus 68 in peritoneal cells. J Virol, 1999. 73(4): p. 3273-83.*
50. *Stavnezer, J., Antibody class switching. Adv Immunol, 1996. 61: p. 79-146.*
51. *Vitetta, E.S., et al., Serological, biochemical, and functional identity of B cell-stimulatory factor 1 and B cell differentiation factor for IgG1. J Exp Med, 1985. 162(5): p. 1726-31.*
52. *Sideras, P., S. Bergstedt-Lindqvist, and E. Severinson, Partial biochemical characterization of IgG1-inducing factor. Eur J Immunol, 1985. 15(6): p. 593-8.*
53. *Snapper, C.M. and W.E. Paul, Interferon-gamma and B cell stimulatory factor-1 reciprocally regulate Ig isotype production. Science, 1987. 236(4804): p. 944-7.*
54. *Mount, B.M. and L.C. Stevens, The early natural history of murine germinal testicular tumors. J Urol, 1971. 105(6): p. 812-6.*
55. *Kaplan, H.S., On the natural history of the murine leukemias: presidential address. Cancer Res, 1967. 27(8): p. 1325-40.*

56. *Nash, A.A., et al., Natural history of murine gamma-herpesvirus infection. Philos Trans R Soc Lond B Biol Sci, 2001. 356(1408): p. 569-79.*
57. *Flano, E., et al., Latent murine gamma-herpesvirus infection is established in activated B cells, dendritic cells, and macrophages. J Immunol, 2000. 165(2): p. 1074-81.*
58. *Cerutti, A., The regulation of IgA class switching. Nat Rev Immunol, 2008. 8(6): p. 421-34.*
59. *Sunil-Chandra, N.P., S. Efstathiou, and A.A. Nash, Murine gammaherpesvirus 68 establishes a latent infection in mouse B lymphocytes in vivo. J Gen Virol, 1992. 73 (Pt 12): p. 3275-9.*
60. *Dedeoglu, F., et al., Induction of activation-induced cytidine deaminase gene expression by IL-4 and CD40 ligation is dependent on STAT6 and NFkappaB. Int Immunol, 2004. 16(3): p. 395-404.*
61. *Stavnezer, J., Regulation of antibody production and class switching by TGF-beta. J Immunol, 1995. 155(4): p. 1647-51.*
62. *Coffman, R.L., D.A. Lebman, and B. Shrader, Transforming growth factor beta specifically enhances IgA production by lipopolysaccharide-stimulated murine B lymphocytes. J Exp Med, 1989. 170(3): p. 1039-44.*
63. *Litinskiy, M.B., et al., DCs induce CD40-independent immunoglobulin class switching through BLyS and APRIL. Nat Immunol, 2002. 3(9): p. 822-9.*
64. *Kuper, C.F., et al., The role of nasopharyngeal lymphoid tissue. Immunol Today, 1992. 13(6): p. 219-24.*
65. *Kuper, C.F., et al., Lymphoid and non-lymphoid cells in nasal-associated lymphoid tissue (NALT) in the rat. An immuno- and enzyme-histochemical study. Cell Tissue Res, 1990. 259(2): p. 371-7.*
66. *Zuercher, A.W., et al., Nasal-associated lymphoid tissue is a mucosal inductive site for virus-specific humoral and cellular immune responses. J Immunol, 2002. 168(4): p. 1796-803.*

67. *Hiroi, T., et al., Nasal immune system: distinctive Th0 and Th1/Th2 type environments in murine nasal-associated lymphoid tissues and nasal passage, respectively. Eur J Immunol, 1998. 28(10): p. 3346-53.*
68. *Shimoda, M., et al., Isotype-specific selection of high affinity memory B cells in nasal-associated lymphoid tissue. J Exp Med, 2001. 194(11): p. 1597-607.*
69. *Bienenstock, J. and M.R. McDermott, Bronchus- and nasal-associated lymphoid tissues. Immunol Rev, 2005. 206: p. 22-31.*
70. *Asanuma, H., et al., Isolation and characterization of mouse nasal-associated lymphoid tissue. J Immunol Methods, 1997. 202(2): p. 123-31.*
71. *Shikina, T., et al., IgA class switch occurs in the organized nasopharynx- and gut-associated lymphoid tissue, but not in the diffuse lamina propria of airways and gut. J Immunol, 2004. 172(10): p. 6259-64.*
72. *Liang, B., L. Hyland, and S. Hou, Nasal-associated lymphoid tissue is a site of long-term virus-specific antibody production following respiratory virus infection of mice. J Virol, 2001. 75(11): p. 5416-20.*
73. *Tamura, S., et al., Antibody-forming cells in the nasal-associated lymphoid tissue during primary influenza virus infection. J Gen Virol, 1998. 79 (Pt 2): p. 291-9.*
74. *Blaskovic, D., et al., Isolation of five strains of herpesviruses from two species of free living small rodents. Acta Virol, 1980. 24(6): p. 468.*
75. *Efstathiou, S., Y.M. Ho, and A.C. Minson, Cloning and molecular characterization of the murine herpesvirus 68 genome. J Gen Virol, 1990. 71 (Pt 6): p. 1355-64.*
76. *Gompels, U.A., M.A. Craxton, and R.W. Honess, Conservation of gene organization in the lymphotropic herpesviruses herpesvirus Saimiri and Epstein-Barr virus. J Virol, 1988. 62(3): p. 757-67.*
77. *Greensill, J., et al., Two distinct gamma-2 herpesviruses in African green monkeys: a second gamma-2 herpesvirus lineage among old world primates? J Virol, 2000. 74(3): p. 1572-7.*

78. *Li, H., et al., Newly recognized herpesvirus causing malignant catarrhal fever in white-tailed deer (Odocoileus virginianus). J Clin Microbiol, 2000. 38(4): p. 1313-8.*
79. *Li, H., et al., Transmission of ovine herpesvirus 2 among adult sheep. Vet Microbiol, 2000. 71(1-2): p. 27-35.*
80. *Ensser, A., R. Pflanz, and B. Fleckenstein, Primary structure of the alcelaphine herpesvirus 1 genome. J Virol, 1997. 71(9): p. 6517-25.*
81. *Ehlers, B., S. Ulrich, and M. Goltz, Detection of two novel porcine herpesviruses with high similarity to gammaherpesviruses. J Gen Virol, 1999. 80 (Pt 4): p. 971-8.*
82. *Holloway, S.A., et al., Identification, sequence analysis and characterisation of equine herpesvirus 5 glycoprotein B. Arch Virol, 1999. 144(2): p. 287-307.*
83. *Alexander, L., et al., The primary sequence of rhesus monkey rhadinovirus isolate 26-95: sequence similarities to Kaposi's sarcoma-associated herpesvirus and rhesus monkey rhadinovirus isolate 17577. J Virol, 2000. 74(7): p. 3388-98.*
84. *Moore, P.S., et al., Primary characterization of a herpesvirus agent associated with Kaposi's sarcomae. J Virol, 1996. 70(1): p. 549-58.*
85. *Flano, E., D.L. Woodland, and M.A. Blackman, A mouse model for infectious mononucleosis. Immunol Res, 2002. 25(3): p. 201-17.*
86. *Nash, A.A. and N.P. Sunil-Chandra, Interactions of the murine gammaherpesvirus with the immune system. Curr Opin Immunol, 1994. 6(4): p. 560-3.*
87. *Simas, J.P. and S. Efstathiou, Murine gammaherpesvirus 68: a model for the study of gammaherpesvirus pathogenesis. Trends Microbiol, 1998. 6(7): p. 276-82.*
88. *Speck, S.H. and H.W. Virgin, Host and viral genetics of chronic infection: a mouse model of gamma-herpesvirus pathogenesis. Curr Opin Microbiol, 1999. 2(4): p. 403-9.*

89. *Virgin, H.W.t., et al., Complete sequence and genomic analysis of murine gammaherpesvirus 68. J Virol, 1997. 71(8): p. 5894-904.*
90. *Blasdell, K., et al., The wood mouse is a natural host for Murid herpesvirus 4. J Gen Virol, 2003. 84(Pt 1): p. 111-3.*
91. *Chastel, C., et al., A herpesvirus from an European shrew (Crocidura russula). Acta Virol, 1994. 38(5): p. 309.*
92. *Mistrikova, J., et al., [New findings on the ecology and epidemiology of murine herpes virus isolated in Slovakia]. Bratisl Lek Listy, 2000. 101(3): p. 157-62.*
93. *Henle, G., W. Henle, and V. Diehl, Relation of Burkitt's tumor-associated herpes-ytpe virus to infectious mononucleosis. Proc Natl Acad Sci U S A, 1968. 59(1): p. 94-101.*
94. *Burkitt, D., A sarcoma involving the jaws in African children. Br J Surg, 1958. 46(197): p. 218-23.*
95. *O'Conor, G.T., Malignant lymphoma in African children. II. A pathological entity. Cancer, 1961. 14: p. 270-83.*
96. *Henle, G. and W. Henle, Immunofluorescence in cells derived from Burkitt's lymphoma. J Bacteriol, 1966. 91(3): p. 1248-56.*
97. *Chang, Y., et al., Identification of herpesvirus-like DNA sequences in AIDS-associated Kaposi's sarcoma. Science, 1994. 266(5192): p. 1865-9.*
98. *Cesarman, E., et al., Kaposi's sarcoma-associated herpesvirus in non-AIDS related lymphomas occurring in body cavities. Am J Pathol, 1996. 149(1): p. 53-7.*
99. *Corbellino, M., et al., The role of human herpesvirus 8 and Epstein-Barr virus in the pathogenesis of giant lymph node hyperplasia (Castleman's disease). Clin Infect Dis, 1996. 22(6): p. 1120-1.*
100. *Castleman, B., L. Iverson, and V.P. Menendez, Localized mediastinal lymphnode hyperplasia resembling thymoma. Cancer, 1956. 9(4): p. 822-30.*
101. *Andreoni, M., et al., Primary human herpesvirus 8 infection in immunocompetent children. JAMA, 2002. 287(10): p. 1295-300.*

102. Luppi, M., et al., Severe pancytopenia and hemophagocytosis after HHV-8 primary infection in a renal transplant patient successfully treated with foscarnet. Transplantation, 2002. 74(1): p. 131-2.

103. Barozzi, P., et al., Post-transplant Kaposi sarcoma originates from the seeding of donor-derived progenitors. Nat Med, 2003. 9(5): p. 554-61.

104. Di Alberti, L., et al., Human herpesvirus 8 variants in sarcoid tissues. Lancet, 1997. 350(9092): p. 1655-61.

105. Rettig, M.B., et al., Kaposi's sarcoma-associated herpesvirus infection of bone marrow dendritic cells from multiple myeloma patients. Science, 1997. 276(5320): p. 1851-4.

106. Cool, C.D., et al., Expression of human herpesvirus 8 in primary pulmonary hypertension. N Engl J Med, 2003. 349(12): p. 1113-22.

107. Eichberg, J.W., et al., Clinical, virological, and pathological features of herpesvirus SA8 infection in conventional and gnotobiotic infant baboons (Papio cynocephalus). Arch Virol, 1976. 50(4): p. 255-70.

108. Ebrahimi, B., et al., Transcriptome profile of murine gammaherpesvirus-68 lytic infection. J Gen Virol, 2003. 84(Pt 1): p. 99-109.

109. Rochford, R., et al., Kinetics of murine gammaherpesvirus 68 gene expression following infection of murine cells in culture and in mice. J Virol, 2001. 75(11): p. 4955-63.

110. Peacock, J.W. and K.L. Bost, Infection of intestinal epithelial cells and development of systemic disease following gastric instillation of murine gammaherpesvirus-68. J Gen Virol, 2000. 81(Pt 2): p. 421-9.

111. Milho, R., et al., In vivo imaging of murid herpesvirus-4 infection. J Gen Virol, 2009. 90(Pt 1): p. 21-32.

112. Jacoby, M.A., H.W.t. Virgin, and S.H. Speck, Disruption of the M2 gene of murine gammaherpesvirus 68 alters splenic latency following intranasal, but not intraperitoneal, inoculation. J Virol, 2002. 76(4): p. 1790-801.

113. Gangappa, S., et al., Identification of the in vivo role of a viral bcl-2. J Exp Med, 2002. 195(7): p. 931-40.

114. *Hwang, S., et al., Persistent gammaherpesvirus replication and dynamic interaction with the host in vivo. J Virol, 2008. 82(24): p. 12498-509.*
115. *Cardin, R.D., et al., Progressive loss of CD8+ T cell-mediated control of a gamma-herpesvirus in the absence of CD4+ T cells. J Exp Med, 1996. 184(3): p. 863-71.*
116. *Sunil-Chandra, N.P., et al., Virological and pathological features of mice infected with murine gamma-herpesvirus 68. J Gen Virol, 1992. 73 (Pt 9): p. 2347-56.*
117. *Gill, M.B., et al., Murid herpesvirus-4 lacking thymidine kinase reveals route-dependent requirements for host colonization. J Gen Virol, 2009. 90(Pt 6): p. 1461-70.*
118. *Coleman, H.M., et al., Murine gammaherpesvirus 68 lacking thymidine kinase shows severe attenuation of lytic cycle replication in vivo but still establishes latency. J Virol, 2003. 77(4): p. 2410-7.*
119. *May, J.S., et al., The murine gammaherpesvirus 68 ORF27 gene product contributes to intercellular viral spread. J Virol, 2005. 79(8): p. 5059-68.*
120. *Gill, M.B., et al., Important role for the murid herpesvirus 4 ribonucleotide reductase large subunit in host colonization via the respiratory tract. J Virol, 2010. 84(20): p. 10937-42.*
121. *Macrae, A.I., et al., Analysis of a novel strain of murine gammaherpesvirus reveals a genomic locus important for acute pathogenesis. J Virol, 2001. 75(11): p. 5315-27.*
122. *Tripp, R.A., et al., Pathogenesis of an infectious mononucleosis-like disease induced by a murine gamma-herpesvirus: role for a viral superantigen? J Exp Med, 1997. 185(9): p. 1641-50.*
123. *Flano, E., et al., Differential gamma-herpesvirus distribution in distinct anatomical locations and cell subsets during persistent infection in mice. J Immunol, 2003. 170(7): p. 3828-34.*
124. *Stewart, J.P., et al., Lung epithelial cells are a major site of murine gammaherpesvirus persistence. J Exp Med, 1998. 187(12): p. 1941-51.*

125. *Flano, E., et al., Gamma-herpesvirus latency is preferentially maintained in splenic germinal center and memory B cells. J Exp Med, 2002. 196(10): p. 1363-72.*
126. *Laichalk, L.L., et al., The dispersal of mucosal memory B cells: evidence from persistent EBV infection. Immunity, 2002. 16(5): p. 745-54.*
127. *Babcock, G.J., et al., EBV persistence in memory B cells in vivo. Immunity, 1998. 9(3): p. 395-404.*
128. *Weck, K.E., et al., Murine gamma-herpesvirus 68 causes severe large-vessel arteritis in mice lacking interferon-gamma responsiveness: a new model for virus-induced vascular disease. Nat Med, 1997. 3(12): p. 1346-53.*
129. *Stevenson, P.G., et al., A gamma-herpesvirus sneaks through a CD8(+) T cell response primed to a lytic-phase epitope. Proc Natl Acad Sci U S A, 1999. 96(16): p. 9281-6.*
130. *Clambey, E.T., H.W.t. Virgin, and S.H. Speck, Disruption of the murine gammaherpesvirus 68 M1 open reading frame leads to enhanced reactivation from latency. J Virol, 2000. 74(4): p. 1973-84.*
131. *Thorley-Lawson, D.A., Epstein-Barr virus: exploiting the immune system. Nat Rev Immunol, 2001. 1(1): p. 75-82.*
132. *Grundhoff, A. and D. Ganem, Inefficient establishment of KSHV latency suggests an additional role for continued lytic replication in Kaposi sarcoma pathogenesis. J Clin Invest, 2004. 113(1): p. 124-36.*
133. *Wu, T.T., et al., Rta of murine gammaherpesvirus 68 reactivates the complete lytic cycle from latency. J Virol, 2000. 74(8): p. 3659-67.*
134. *Gargano, L.M., J.C. Forrest, and S.H. Speck, Signaling through Toll-like receptors induces murine gammaherpesvirus 68 reactivation in vivo. J Virol, 2009. 83(3): p. 1474-82.*
135. *Gargano, L.M., J.M. Moser, and S.H. Speck, Role for MyD88 signaling in murine gammaherpesvirus 68 latency. J Virol, 2008. 82(8): p. 3853-63.*

136. *Krug, L.T., et al., Inhibition of NF-kappaB activation in vivo impairs establishment of gammaherpesvirus latency. PLoS Pathog, 2007. 3(1): p. e11.*
137. *Brown, H.J., et al., NF-kappaB inhibits gammaherpesvirus lytic replication. J Virol, 2003. 77(15): p. 8532-40.*
138. *Rickabaugh, T.M., et al., Generation of a latency-deficient gammaherpesvirus that is protective against secondary infection. J Virol, 2004. 78(17): p. 9215-23.*
139. *Liang, X., et al., Gammaherpesvirus-driven plasma cell differentiation regulates virus reactivation from latently infected B lymphocytes. PLoS Pathog, 2009. 5(11): p. e1000677.*
140. *Usherwood, E.J., et al., Latent antigen vaccination in a model gammaherpesvirus infection. J Virol, 2001. 75(17): p. 8283-8.*
141. *Woodland, D.L., et al., Vaccination against murine gamma-herpesvirus infection. Viral Immunol, 2001. 14(3): p. 217-26.*
142. *Apcher, S., R. Fahraeus, and B. Manoury, Epstein-Barr virus: exploiting the immune system by interfering with defective ribosomal products. Microbes Infect, 2004. 6(13): p. 1212-8.*
143. *Boname, J.M., et al., Protection against wild-type murine gammaherpesvirus-68 latency by a latency-deficient mutant. J Gen Virol, 2004. 85(Pt 1): p. 131-5.*
144. *Jia, Q., et al., Induction of protective immunity against murine gammaherpesvirus 68 infection in the absence of viral latency. J Virol, 2010. 84(5): p. 2453-65.*
145. *Fowler, P. and S. Efstathiou, Vaccine potential of a murine gammaherpesvirus-68 mutant deficient for ORF73. J Gen Virol, 2004. 85(Pt 3): p. 609-13.*
146. *Dutia, B.M., et al., Type I interferons and IRF-1 play a critical role in the control of a gammaherpesvirus infection. Virology, 1999. 261(2): p. 173-9.*

147. *Sarawar, S.R., et al., Cytokine production in the immune response to murine gammaherpesvirus 68. J Virol, 1996. 70(5): p. 3264-8.*
148. *Weinberg, J.B., et al., Mouse strain differences in the chemokine response to acute lung infection with a murine gammaherpesvirus. Viral Immunol, 2004. 17(1): p. 69-77.*
149. *Sarawar, S.R., et al., Pathogenesis of murine gammaherpesvirus-68 infection in interleukin-6-deficient mice. Virology, 1998. 249(2): p. 359-66.*
150. *Siegel, A.M., J.H. Herskowitz, and S.H. Speck, The MHV68 M2 protein drives IL-10 dependent B cell proliferation and differentiation. PLoS Pathog, 2008. 4(4): p. e1000039.*
151. *Sarawar, S.R., et al., Chemokine induction and leukocyte trafficking to the lungs during murine gammaherpesvirus 68 (MHV-68) infection. Virology, 2002. 293(1): p. 54-62.*
152. *Weinberg, J.B., et al., Elevated chemokine responses are maintained in lungs after clearance of viral infection. J Virol, 2002. 76(20): p. 10518-23.*
153. *Lee, B.J., et al., Role of CXCR3 in the immune response to murine gammaherpesvirus 68. J Virol, 2005. 79(14): p. 9351-5.*
154. *Wakeling, M.N., et al., Characterization of the murine gammaherpesvirus 68 ORF74 product: a novel oncogenic G protein-coupled receptor. J Gen Virol, 2001. 82(Pt 5): p. 1187-97.*
155. *van Berkel, V., et al., Identification of a gammaherpesvirus selective chemokine binding protein that inhibits chemokine action. J Virol, 2000. 74(15): p. 6741-7.*
156. *Ehtisham, S., N.P. Sunil-Chandra, and A.A. Nash, Pathogenesis of murine gammaherpesvirus infection in mice deficient in CD4 and CD8 T cells. J Virol, 1993. 67(9): p. 5247-52.*
157. *Tarakanova, V.L., et al., Murine gammaherpesvirus 68 infection is associated with lymphoproliferative disease and lymphoma in BALB beta2 microglobulin-deficient mice. J Virol, 2005. 79(23): p. 14668-79.*

158. *Thomsen, A.R., et al., Exhaustion of CTL memory and recrudescence of viremia in lymphocytic choriomeningitis virus-infected MHC class II-deficient mice and B cell-deficient mice. J Immunol, 1996. 157(7): p. 3074-80.*
159. *Belz, G.T., et al., Absence of a functional defect in CD8+ T cells during primary murine gammaherpesvirus-68 infection of I-A(b-/-) mice. J Gen Virol, 2003. 84(Pt 2): p. 337-41.*
160. *Stevenson, P.G., et al., Immunological control of a murine gammaherpesvirus independent of CD8+ T cells. J Gen Virol, 1999. 80 (Pt 2): p. 477-83.*
161. *Boname, J.M., et al., Viral degradation of the MHC class I peptide loading complex. Immunity, 2004. 20(3): p. 305-17.*
162. *Lybarger, L., et al., Virus subversion of the MHC class I peptide-loading complex. Immunity, 2003. 18(1): p. 121-30.*
163. *Mount, A.M., et al., Interference with dendritic cell populations limits early antigen presentation in chronic gamma-herpesvirus-68 infection. J Immunol, 2010. 185(6): p. 3669-76.*
164. *Rice, J., et al., A gamma-herpesvirus immune evasion gene allows tumor cells in vivo to escape attack by cytotoxic T cells specific for a tumor epitope. Eur J Immunol, 2002. 32(12): p. 3481-7.*
165. *Stevenson, P.G., et al., Changing patterns of dominance in the CD8+ T cell response during acute and persistent murine gamma-herpesvirus infection. Eur J Immunol, 1999. 29(4): p. 1059-67.*
166. *Stevenson, P.G. and P.C. Doherty, Kinetic analysis of the specific host response to a murine gammaherpesvirus. J Virol, 1998. 72(2): p. 943-9.*
167. *Hardy, C.L., et al., Murine gamma-herpesvirus infection causes V(beta)4-specific CDR3-restricted clonal expansions within CD8(+) peripheral blood T lymphocytes. Int Immunol, 2000. 12(8): p. 1193-204.*

168. *Brooks, J.W., et al., Requirement for CD40 ligand, CD4(+) T cells, and B cells in an infectious mononucleosis-like syndrome. J Virol, 1999. 73(11): p. 9650-4.*
169. *Gasper-Smith, N., I. Marriott, and K.L. Bost, Murine gamma-herpesvirus 68 limits naturally occurring CD4+CD25+ T regulatory cell activity following infection. J Immunol, 2006. 177(7): p. 4670-8.*
170. *Christensen, J.P., et al., CD4(+) T cell-mediated control of a gamma-herpesvirus in B cell-deficient mice is mediated by IFN-gamma. Proc Natl Acad Sci U S A, 1999. 96(9): p. 5135-40.*
171. *Sparks-Thissen, R.L., et al., CD4 T cell control of acute and latent murine gammaherpesvirus infection requires IFNgamma. Virology, 2005. 338(2): p. 201-8.*
172. *Stevenson, P.G. and P.C. Doherty, Non-antigen-specific B-cell activation following murine gammaherpesvirus infection is CD4 independent in vitro but CD4 dependent in vivo. J Virol, 1999. 73(2): p. 1075-9.*
173. *Topham, D.J. and P.C. Doherty, Clearance of an influenza A virus by CD4+ T cells is inefficient in the absence of B cells. J Virol, 1998. 72(1): p. 882-5.*
174. *Usherwood, E.J., et al., Murine gammaherpesvirus-induced splenomegaly: a critical role for CD4 T cells. J Gen Virol, 1996. 77 (Pt 4): p. 627-30.*
175. *Tibbetts, S.A., et al., Effective vaccination against long-term gammaherpesvirus latency. J Virol, 2003. 77(4): p. 2522-9.*
176. *Dutia, B.M., et al., Pathological changes in the spleens of gamma interferon receptor-deficient mice infected with murine gammaherpesvirus: a role for CD8 T cells. J Virol, 1997. 71(6): p. 4278-83.*
177. *Christensen, J.P. and P.C. Doherty, Quantitative analysis of the acute and long-term CD4(+) T-cell response to a persistent gammaherpesvirus. J Virol, 1999. 73(5): p. 4279-83.*
178. *Ewing, C., D.J. Topham, and P.C. Doherty, Prevalence and activation phenotype of Sendai virus-specific CD4+ T cells. Virology, 1995. 210(1): p. 179-85.*

179. *Gangappa, S., et al., Antibody to a lytic cycle viral protein decreases gammaherpesvirus latency in B-cell-deficient mice. J Virol, 2002. 76(22): p. 11460-8.*
180. *Wright, D.E., et al., Antibody limits in vivo murid herpesvirus-4 replication by IgG Fc receptor-dependent functions. J Gen Virol, 2009. 90(Pt 11): p. 2592-603.*
181. *de Lima, B.D., J.S. May, and P.G. Stevenson, Murine gammaherpesvirus 68 lacking gp150 shows defective virion release but establishes normal latency in vivo. J Virol, 2004. 78(10): p. 5103-12.*
182. *Gillet, L., et al., The murine gammaherpesvirus-68 gp150 acts as an immunogenic decoy to limit virion neutralization. PLoS One, 2007. 2(1): p. e705.*
183. *Sangster, M.Y., et al., Analysis of the virus-specific and nonspecific B cell response to a persistent B-lymphotropic gammaherpesvirus. J Immunol, 2000. 164(4): p. 1820-8.*
184. *Portela, A., et al., Replication of orthomyxoviruses. Adv Virus Res, 1999. 54: p. 319-48.*
185. *Julkunen, I., et al., Molecular pathogenesis of influenza A virus infection and virus-induced regulation of cytokine gene expression. Cytokine Growth Factor Rev, 2001. 12(2-3): p. 171-80.*
186. *Schmolke, M. and A. Garcia-Sastre, Evasion of innate and adaptive immune responses by influenza A virus. Cell Microbiol, 2010. 12(7): p. 873-80.*
187. *Julkunen, I., et al., Inflammatory responses in influenza A virus infection. Vaccine, 2000. 19 Suppl 1: p. S32-7.*
188. *Kohlmeier, J.E. and D.L. Woodland, Immunity to respiratory viruses. Annu Rev Immunol, 2009. 27: p. 61-82.*
189. *Iwasaki, A. and R. Medzhitov, Toll-like receptor control of the adaptive immune responses. Nat Immunol, 2004. 5(10): p. 987-95.*

190. *Le Goffic, R., et al., Detrimental contribution of the Toll-like receptor (TLR)3 to influenza A virus-induced acute pneumonia. PLoS Pathog, 2006. 2(6): p. e53.*
191. *Lund, J.M., et al., Recognition of single-stranded RNA viruses by Toll-like receptor 7. Proc Natl Acad Sci U S A, 2004. 101(15): p. 5598-603.*
192. *Thomas, P.G., et al., The intracellular sensor NLRP3 mediates key innate and healing responses to influenza A virus via the regulation of caspase-1. Immunity, 2009. 30(4): p. 566-75.*
193. *Kozak, W., et al., Thermal and behavioral effects of lipopolysaccharide and influenza in interleukin-1 beta-deficient mice. Am J Physiol, 1995. 269(5 Pt 2): p. R969-77.*
194. *Schmitz, N., et al., Interleukin-1 is responsible for acute lung immunopathology but increases survival of respiratory influenza virus infection. J Virol, 2005. 79(10): p. 6441-8.*
195. *Hale, B.G., et al., The multifunctional NS1 protein of influenza A viruses. J Gen Virol, 2008. 89(Pt 10): p. 2359-76.*
196. *Pirhonen, J., et al., Virus infection activates IL-1 beta and IL-18 production in human macrophages by a caspase-1-dependent pathway. J Immunol, 1999. 162(12): p. 7322-9.*
197. *Chan, M.C., et al., Proinflammatory cytokine responses induced by influenza A (H5N1) viruses in primary human alveolar and bronchial epithelial cells. Respir Res, 2005. 6: p. 135.*
198. *Legge, K.L. and T.J. Braciale, Accelerated migration of respiratory dendritic cells to the regional lymph nodes is limited to the early phase of pulmonary infection. Immunity, 2003. 18(2): p. 265-77.*
199. *Belz, G.T., et al., Distinct migrating and nonmigrating dendritic cell populations are involved in MHC class I-restricted antigen presentation after lung infection with virus. Proc Natl Acad Sci U S A, 2004. 101(23): p. 8670-5.*

200. Topham, D.J., R.A. Tripp, and P.C. Doherty, CD8+ T cells clear influenza virus by perforin or Fas-dependent processes. J Immunol, 1997. 159(11): p. 5197-200.

201. Wareing, M.D., et al., Chemokine expression during the development and resolution of a pulmonary leukocyte response to influenza A virus infection in mice. J Leukoc Biol, 2004. 76(4): p. 886-95.

202. Carding, S.R., et al., Activation of cytokine genes in T cells during primary and secondary murine influenza pneumonia. J Exp Med, 1993. 177(2): p. 475-82.

203. Xu, L., et al., Cutting edge: pulmonary immunopathology mediated by antigen-specific expression of TNF-alpha by antiviral CD8+ T cells. J Immunol, 2004. 173(2): p. 721-5.

204. Bender, B.S., et al., Transgenic mice lacking class I major histocompatibility complex-restricted T cells have delayed viral clearance and increased mortality after influenza virus challenge. J Exp Med, 1992. 175(4): p. 1143-5.

205. Gerhard, W., The role of the antibody response in influenza virus infection. Curr Top Microbiol Immunol, 2001. 260: p. 171-90.

206. Kopf, M., F. Brombacher, and M.F. Bachmann, Role of IgM antibodies versus B cells in influenza virus-specific immunity. Eur J Immunol, 2002. 32(8): p. 2229-36.

207. Palladino, G., et al., Virus-neutralizing antibodies of immunoglobulin G (IgG) but not of IgM or IgA isotypes can cure influenza virus pneumonia in SCID mice. J Virol, 1995. 69(4): p. 2075-81.

208. Bishop, G.A. and B.S. Hostager, B lymphocyte activation by contact-mediated interactions with T lymphocytes. Curr Opin Immunol, 2001. 13(3): p. 278-85.

209. Sangster, M.Y., et al., An early CD4+ T cell-dependent immunoglobulin A response to influenza infection in the absence of key cognate T-B interactions. J Exp Med, 2003. 198(7): p. 1011-21.

210. Lee, B.O., et al., CD4 T cell-independent antibody response promotes resolution of primary influenza infection and helps to prevent reinfection. J Immunol, 2005. 175(9): p. 5827-38.

211. Lee, B.O., et al., CD40, but not CD154, expression on B cells is necessary for optimal primary B cell responses. J Immunol, 2003. 171(11): p. 5707-17.

212. Doherty, P.C., et al., Effector CD4+ and CD8+ T-cell mechanisms in the control of respiratory virus infections. Immunol Rev, 1997. 159: p. 105-17.

213. Stevenson, P.G. and S. Efstathiou, Immune mechanisms in murine gammaherpesvirus-68 infection. Viral Immunol, 2005. 18(3): p. 445-56.

214. Evans, A.G., et al., A gammaherpesvirus-secreted activator of Vbeta4+ CD8+ T cells regulates chronic infection and immunopathology. J Exp Med, 2008. 205(3): p. 669-84.

215. Rodrigues, L., et al., Activation of Vav by the gammaherpesvirus M2 protein contributes to the establishment of viral latency in B lymphocytes. J Virol, 2006. 80(12): p. 6123-35.

216. Simas, J.P., et al., The M2 gene product of murine gammaherpesvirus 68 is required for efficient colonization of splenic follicles but is not necessary for expansion of latently infected germinal centre B cells. J Gen Virol, 2004. 85(Pt 10): p. 2789-97.

217. Parry, C.M., et al., A broad spectrum secreted chemokine binding protein encoded by a herpesvirus. J Exp Med, 2000. 191(3): p. 573-8.

218. Bridgeman, A., et al., A secreted chemokine binding protein encoded by murine gammaherpesvirus-68 is necessary for the establishment of a normal latent load. J Exp Med, 2001. 194(3): p. 301-12.

219. Geere, H.M., et al., The M4 gene of murine gammaherpesvirus 68 modulates latent infection. J Gen Virol, 2006. 87(Pt 4): p. 803-7.

220. Renegar, K.B., Influenza virus infections and immunity: a review of human and animal models. Lab Anim Sci, 1992. 42(3): p. 222-32.

221. Bender, B.S. and P.A. Small, Jr., Influenza: pathogenesis and host defense. Semin Respir Infect, 1992. 7(1): p. 38-45.

222. van der Ven, I. and T. Sminia, The development and structure of mouse nasal-associated lymphoid tissue: an immuno- and enzyme-histochemical study. Reg Immunol, 1993. 5(2): p. 69-75.
223. Bradford, M.M., A rapid and sensitive method for the quantitation of microgram quantities of protein utilizing the principle of protein-dye binding. Anal Biochem, 1976. 72: p. 248-54.
224. Nedrud, J.G., et al., Combined oral/nasal immunization protects mice from Sendai virus infection. J Immunol, 1987. 139(10): p. 3484-92.
225. Topham, D.J. and P.C. Doherty, Longitudinal analysis of the acute Sendai virus-specific CD4+ T cell response and memory. J Immunol, 1998. 161(9): p. 4530-5.
226. Joo, H.M., et al., Quantitative analysis of influenza virus-specific B cell memory generated by different routes of inactivated virus vaccination. Vaccine, 2010. 28(10): p. 2186-94.
227. Clambey, E.T., H.W.t. Virgin, and S.H. Speck, Characterization of a spontaneous 9.5-kilobase-deletion mutant of murine gammaherpesvirus 68 reveals tissue-specific genetic requirements for latency. J Virol, 2002. 76(13): p. 6532-44.
228. Simas, J.P., et al., Analysis of murine gammaherpesvirus-68 transcription during lytic and latent infection. J Gen Virol, 1999. 80 (Pt 1): p. 75-82.
229. Townsley, A.C., B.M. Dutia, and A.A. Nash, The m4 gene of murine gammaherpesvirus modulates productive and latent infection in vivo. J Virol, 2004. 78(2): p. 758-67.
230. Usherwood, E.J., et al., Control of gammaherpesvirus latency by latent antigen-specific CD8(+) T cells. J Exp Med, 2000. 192(7): p. 943-52.
231. Bowden, R.J., et al., Murine gammaherpesvirus 68 encodes tRNA-like sequences which are expressed during latency. J Gen Virol, 1997. 78 (Pt 7): p. 1675-87.
232. Gajewski, T.F. and F.W. Fitch, Anti-proliferative effect of IFN-gamma in immune regulation. I. IFN-gamma inhibits the proliferation of Th2 but not

Th1 murine helper T lymphocyte clones. J Immunol, 1988. 140(12): p. 4245-52.

233. *Mora, A.L., et al., Lung infection with gamma-herpesvirus induces progressive pulmonary fibrosis in Th2-biased mice. Am J Physiol Lung Cell Mol Physiol, 2005. 289(5): p. L711-21.*
234. *Cazac, B.B. and J. Roes, TGF-beta receptor controls B cell responsiveness and induction of IgA in vivo. Immunity, 2000. 13(4): p. 443-51.*
235. *Borsutzky, S., et al., TGF-beta receptor signaling is critical for mucosal IgA responses. J Immunol, 2004. 173(5): p. 3305-9.*
236. *Sonoda, E., et al., Transforming growth factor beta induces IgA production and acts additively with interleukin 5 for IgA production. J Exp Med, 1989. 170(4): p. 1415-20.*
237. *Sangster, M.Y., et al., Matching antibody class with pathogen type and portal of entry: cognate mechanisms regulate local isotype expression patterns in lymph nodes draining the respiratory tract of mice inoculated with respiratory viruses, according to virus replication competence and site of inoculation. J Immunol, 1997. 159(4): p. 1893-902.*
238. *Mega, J., J.R. McGhee, and H. Kiyono, Cytokine- and Ig-producing T cells in mucosal effector tissues: analysis of IL-5- and IFN-gamma-producing T cells, T cell receptor expression, and IgA plasma cells from mouse salivary gland-associated tissues. J Immunol, 1992. 148(7): p. 2030-9.*
239. *Mo, X.Y., S.R. Sarawar, and P.C. Doherty, Induction of cytokines in mice with parainfluenza pneumonia. J Virol, 1995. 69(2): p. 1288-91.*
240. *Quezada, S.A., et al., CD40/CD154 interactions at the interface of tolerance and immunity. Annu Rev Immunol, 2004. 22: p. 307-28.*
241. *Chaudhuri, J. and F.W. Alt, Class-switch recombination: interplay of transcription, DNA deamination and DNA repair. Nat Rev Immunol, 2004. 4(7): p. 541-52.*
242. *Rubtsov, Y.P. and A.Y. Rudensky, TGFbeta signalling in control of T-cell-mediated self-reactivity. Nat Rev Immunol, 2007. 7(6): p. 443-53.*

243. Zan, H., et al., CD40 engagement triggers switching to IgA1 and IgA2 in human B cells through induction of endogenous TGF-beta: evidence for TGF-beta but not IL-10-dependent direct S mu-->S alpha and sequential S mu-->S gamma, S gamma-->S alpha DNA recombination. J Immunol, 1998. 161(10): p. 5217-25.

244. Ulloa, L., J. Doody, and J. Massague, Inhibition of transforming growth factor-beta/SMAD signalling by the interferon-gamma/STAT pathway. Nature, 1999. 397(6721): p. 710-3.

245. Seo, G.Y., J. Youn, and P.H. Kim, IL-21 ensures TGF-beta 1-induced IgA isotype expression in mouse Peyer's patches. J Leukoc Biol, 2009. 85(5): p. 744-50.

246. Muehlinghaus, G., et al., Regulation of CXCR3 and CXCR4 expression during terminal differentiation of memory B cells into plasma cells. Blood, 2005. 105(10): p. 3965-71.

247. Woodland, D.L. and T.D. Randall, Anatomical features of anti-viral immunity in the respiratory tract. Semin Immunol, 2004. 16(3): p. 163-70.

248. Kocks, J.R., et al., Chemokine receptor CCR7 contributes to a rapid and efficient clearance of lytic murine gamma-herpes virus 68 from the lung, whereas bronchus-associated lymphoid tissue harbors virus during latency. J Immunol, 2009. 182(11): p. 6861-9.

249. McDermott, M.R., D.A. Clark, and J. Bienenstock, Evidence for a common mucosal immunologic system. II. Influence of the estrous cycle on B immunoblast migration into genital and intestinal tissues. J Immunol, 1980. 124(6): p. 2536-9.

250. Flynn, K.J., et al., In vivo proliferation of naive and memory influenza-specific CD8(+) T cells. Proc Natl Acad Sci U S A, 1999. 96(15): p. 8597-602.

251. Graham, M.B. and T.J. Braciale, Resistance to and recovery from lethal influenza virus infection in B lymphocyte-deficient mice. J Exp Med, 1997. 186(12): p. 2063-8.

252. *Noelle, R.J., et al., A 39-kDa protein on activated helper T cells binds CD40 and transduces the signal for cognate activation of B cells. Proc Natl Acad Sci U S A, 1992. 89(14): p. 6550-4.*
253. *Brink, R., et al., Visualizing the effects of antigen affinity on T-dependent B-cell differentiation. Immunol Cell Biol, 2008. 86(1): p. 31-9.*
254. *Johnston, R.J., et al., Bcl6 and Blimp-1 are reciprocal and antagonistic regulators of T follicular helper cell differentiation. Science, 2009. 325(5943): p. 1006-10.*
255. *Woods, A., et al., Human major histocompatibility complex class II-restricted T cell responses in transgenic mice. J Exp Med, 1994. 180(1): p. 173-81.*
256. *Richards, K.A., et al., Direct ex vivo analyses of HLA-DR1 transgenic mice reveal an exceptionally broad pattern of immunodominance in the primary HLA-DR1-restricted CD4 T-cell response to influenza virus hemagglutinin. J Virol, 2007. 81(14): p. 7608-19.*
257. *Toellner, K.M., et al., T helper 1 (Th1) and Th2 characteristics start to develop during T cell priming and are associated with an immediate ability to induce immunoglobulin class switching. J Exp Med, 1998. 187(8): p. 1193-204.*
258. *Moon, H.B., et al., Regulation of IgG1 and IgE synthesis by interleukin 4 in mouse B cells. Scand J Immunol, 1989. 30(3): p. 355-61.*
259. *Snapper, C.M., F.D. Finkelman, and W.E. Paul, Differential regulation of IgG1 and IgE synthesis by interleukin 4. J Exp Med, 1988. 167(1): p. 183-96.*
260. *Stavnezer, J., J.E. Guikema, and C.E. Schrader, Mechanism and regulation of class switch recombination. Annu Rev Immunol, 2008. 26: p. 261-92.*
261. *Cunningham, A.F., et al., Th2 activities induced during virgin T cell priming in the absence of IL-4, IL-13, and B cells. J Immunol, 2002. 169(6): p. 2900-6.*
262. *Sun, J., et al., TLR ligands can activate dendritic cells to provide a MyD88-dependent negative signal for Th2 cell development. J Immunol, 2005. 174(2): p. 742-51.*

263. Koch, F., et al., High level IL-12 production by murine dendritic cells: upregulation via MHC class II and CD40 molecules and downregulation by IL-4 and IL-10. J Exp Med, 1996. 184(2): p. 741-6.

264. Jenkins, S.J., et al., Dendritic cell expression of OX40 ligand acts as a costimulatory, not polarizing, signal for optimal Th2 priming and memory induction in vivo. J Immunol, 2007. 179(6): p. 3515-23.

265. de Vinuesa, C.G., et al., Germinal centers without T cells. J Exp Med, 2000. 191(3): p. 485-94.

266. Yusuf, I., et al., Germinal center T follicular helper cell IL-4 production is dependent on signaling lymphocytic activation molecule receptor (CD150). J Immunol, 2010. 185(1): p. 190-202.

267. King, I.L. and M. Mohrs, IL-4-producing CD4+ T cells in reactive lymph nodes during helminth infection are T follicular helper cells. J Exp Med, 2009. 206(5): p. 1001-7.

268. Huan, Lifang, "Influenza-specific B cell responses in HLA-DR1 transgenic mice". Master's thesis, University of Tennessee, 2010.

VITA

Aarthi Sundararajan was born in Srirangam, India. She was awarded with a Bachelor in Science (BSc) degree in 2004, at St. Ann's Degree College, affiliated with Osmania University, Hyderabad, India. Her BSc specialization was in the subjects; Microbiology, Chemistry and Botany. She was awarded with a Master in Science (MSc) degree in Biochemistry in the year 2006 at Osmania University, Hyderabad, India. She began her graduate studies at the Department of Microbiology, University of Tennessee in the fall, 2006. During the fall 2010-summer 2011, she was appointed as a visiting graduate student in residence at David Smith Center for Vaccine and Immunobiology, University of Rochester, Rochester, New York. She graduated with a Doctor of Philosophy in Microbiology from the University of Tennessee in the summer of 2011.